

THESIS

ASSESSMENT OF DIGITAL LAND COVER MAPS FOR HYDROLOGICAL
MODELING OF THE YAMPA RIVER BASIN, COLORADO, USA

Submitted by

Julie Mae Repass

Department of Forest, Rangeland, and Watershed Science

In partial fulfillment of the requirements

For the Degree of Master of Science

Colorado State University

Fort Collins, Colorado

Summer 2005

COLORADO STATE UNIVERSITY

June 24, 2005

WE HEREBY RECOMMEND THAT THE THESIS PREPARED UNDER OUR SUPERVISION BY JULIE REPASS ENTITLED ASSESSMENT OF DIGITAL LAND COVER MAPS FOR HYDROLOGICAL MODELING OF THE YAMPA RIVER BASIN, COLORADO, USA BE ACCEPTED AS FULFILLING IN PART REQUIREMENTS FOR THE DEGREE OF MASTER OF SCIENCE.

Committee on Graduate Work

Advisor _____

Department Head _____

ABSTRACT OF THESIS

ASSESSMENT OF DIGITAL LAND COVER MAPS FOR HYDROLOGICAL MODELING OF THE YAMPA RIVER BASIN, COLORADO, USA

In order to produce satisfactory results from hydrologic models, it is imperative to use good input data. Today there is a multitude of different land cover maps available, and determining which input data map for the model can be unclear. The goal of this study was to quantify the differences between several readily available land cover maps to determine their relative suitability for hydrological modeling of the Yampa River Basin, Colorado. The land cover maps compared in this study are derived from Advanced Very High Resolution Radiometer (AVHRR), Landsat Thematic Mapper (TM), and Moderate Resolution Imaging Spectroradiometer (MODIS) imagery. These maps were compared to a 30-m land cover map modeled from ground data, Landsat imagery, and MODIS imagery, all collected in 2004. This map was regarded as “truth” in this study due to its fine resolution and use of recent ground data and imagery, and was used to rank the public domain land cover data sets. In order to compare the different land cover data sets, all data were first degraded to a common spatial resolution (~30-m) and a common species resolution. Once this was accomplished, the maps were assessed on four levels. The four assessments were based on: (i) the relative agreement of the total aggregated land class percentages after the data had been cross-walked with respect to the reference map; (ii) pixel accuracy; (iii) scene accuracy; and (iv) cumulative streamflow model output from the United States Geological Survey (USGS) Precipitation-Runoff

Modeling System (PRMS) in relation to observed cumulative streamflow. The results showed that the pixel and scene accuracies did not correlate with model performance within the Yampa River Basin using the PRMS model. The qualitative comparison of the total aggregated land class percentages helped explain the general trends in the simulation results. It was found that maps with the correct proportion of forested and non-forested areas generally had simulated cumulative streamflow that matched closest to observed cumulative streamflow. Overall, the MODIS-derived land cover maps performed the best in terms of hydrological modeling using PRMS in the Yampa River Basin. However, the model was not found to be particularly sensitive to accurate land cover conditions. As a result, the scene and pixel accuracy results would not necessarily correlate with the model results.

Julie Mae Repass
Forest, Rangeland, and Watershed Stewardship Department
Colorado State University
Fort Collins, CO 80523
Summer 2005

ACKNOWLEDGEMENTS

Special appreciation goes to Douglas M. Hultstrand who volunteered help and support with the field data collection, and to David K. Wright for his technical support. In addition, Red Hen Systems, Inc. provided the iPIX® camera, Mediamapper® software, and training to map digital stills; and Rocky Coleman provided the GPS unit. I would also like to acknowledge Steven Fassnacht, Robin Reich, and Greg Butters, who as committee members provided invaluable direction and insight. Special appreciation also goes to the USGS EROS Data Center and EOS Data Gateway for providing the public domain land cover maps, as well as David Theobald and others for making the Colorado Vegetation Model (CVM) map available to the public.

TABLE OF CONTENTS

LIST OF FIGURES	ix
LIST OF TABLES	xi
LIST OF ABBREVIATIONS	xiii
<i>CHAPTER I: INTRODUCTION</i>	1
<i>CHAPTER II: BACKGROUND</i>	4
II.i. LAND COVER EFFECTS ON THE HYDROLOGY OF SNOWMELT-DOMINATED BASINS	4
II.i.i. SNOW ACCUMULATION	4
II.i.ii. SNOWMELT	5
II.ii. DIGITAL LAND COVER MAPS IN HYDROLOGIC MODELING	5
II.ii.i. SPECIFICATIONS OF THE USGS PRMS MODEL	6
II.iii. PUBLIC DOMAIN DIGITAL LAND COVER MAPS	9
II.iii.i. AVHRR LAND COVER PRODUCTS	9
II.iii.i.i. <i>Global Land Cover Characteristics (GLCC) Data Base</i>	10
II.iii.ii. MODIS LAND COVER PRODUCTS	11
II.iii.iii. LANDSAT TM LAND COVER PRODUCTS	12
II.iv. DIGITAL MAP ASSESSMENT	13
<i>CHAPTER III: STUDY AREA</i>	16
<i>CHAPTER IV: MATERIALS AND METHODS</i>	18
IV.i. DIGITAL LAND COVER PRODUCTS	18
IV.i.i. AVHRR-DERIVED LAND COVER PRODUCTS	18
IV.i.ii. MODIS-DERIVED LAND COVER PRODUCTS	20
IV.i.iii. LANDSAT TM-DERIVED LAND COVER PRODUCTS	21
IV.ii. MODELED VEGETATION MAP (MVM)	21
IV.ii.i. SPATIAL DATA AND IMAGE PROCESSING	21
IV.ii.ii. SAMPLING DESIGN	22
IV.ii.iii. FIELD DATA	25
IV.ii.iv. REFERENCE MAP GENERATION	25
IV.iii. ASSESSMENT OF DIGITAL LAND COVER MAPS	26
IV.iii.i. DATA PREPARATION	27
IV.iii.i.i. <i>Data Reprojection</i>	27
IV.iii.i.ii. <i>Data Cross-Walk</i>	27
IV.iii.i.iii. <i>Grid Resampling</i>	28
IV.iii.ii. TOTAL AGGREGATED LAND CLASS PERCENTAGES	28
IV.iii.iii. SCENE ACCURACY	28
IV.iii.iv. PIXEL ACCURACY	29
IV.iii.iv.i. <i>Raw Error Matrices</i>	29
IV.iii.iv.ii. <i>Normalized Error Matrices</i>	32
IV.iv. HYDROLOGICAL MODELING COMPARISON	33

IV.iv.i. STREAMFLOW SIMULATIONS	33
IV.iv.i.i. PRMS Runs	34
IV.iv.i.ii. Model Parameterization	35
IV.iv.i.iii. Preparing and Distributing the Meteorological Data	36
IV.iv.i.iii.i. Preparing the Precipitation Data	41
IV.iv.i.iii.ii. Preparing the Temperature Data	42
CHAPTER V: RESULTS	43
V.i. MODELED VEGETATION MAP	43
V.i.i. BINARY REGRESSION RESULTS FOR THE LANDSAT-DERIVED LAND COVER MAP	43
V.i.ii. BINARY REGRESSION RESULTS FOR THE MODIS-DERIVED LAND COVER MAP	47
V.ii. COMPARISON RESULTS FOR THE DIGITAL LAND COVER MAPS	50
V.ii.i. DATA CROSS-WALK	50
V.ii.ii. AGGREGATED LAND CLASS PERCENTAGES	53
V.ii.iii. SCENE ACCURACY	57
V.ii.iv. PIXEL ACCURACY	59
V.ii.v. SIMULATED STREAMFLOW RESULTS USING THE PRMS MODEL	63
V.ii.v.i. Data Preparation	63
V.ii.v.ii. PRMS Runs	65
V.ii.v.ii.i. Cumulative Streamflow Results	65
V.ii.v.ii.i.i. Effect of Using Landsat-Derived Land Cover Parameters in the PRMS Runs	69
V.ii.v.ii.i.ii. Effect of Using MODIS-Derived Land Cover Parameters in the PRMS Runs	70
V.ii.v.ii.i.iii. Effect of Using AVHRR-Derived Land Cover Parameters in the PRMS Runs	70
V.ii.v.ii.ii. Daily Discharge Results	72
V.ii.vi. OVERALL ACCURACY RESULTS FOR THE LAND COVER DATA SETS	73
CHAPTER VI: DISCUSSION	76
VI.i. MODELED VEGETATION MAP	76
VI.ii. METHODS FOR ASSESSMENT OF THE DIGITAL LAND COVER MAPS	76
VI.ii.i. DATA CROSS-WALK	76
VI.ii.ii. AGGREGATED LAND CLASS PERCENTAGES	77
VI.ii.iii. SCENE ACCURACY	77
VI.ii.iv. PIXEL ACCURACY	78
VI.ii.v. PRMS RUNS	79
VI.iii. OVERALL ASSESSMENT OF DIGITAL LAND COVER MAPS	80
VI.iii.i. LANDSAT-DERIVED LAND COVER MAPS	82
VI.iii.i.i. National Land Cover Dataset (NLCD)	82
VI.iii.i.ii. Colorado Vegetation Model (CVM)	83
VI.iii.ii. MODIS-DERIVED LAND COVER MAPS	84
VI.iii.ii.i. International Geosphere Biosphere Programme (IGBP)	84

<i>VI.iii.ii.ii. University of Maryland Modified IGBP (UMD)</i>	85
<i>VI.iii.ii.iii. Leaf Area Index / fraction of Photosynthetically Active Radiation (LAI/fPAR) Biome Scheme</i>	86
VI.iii.iii. AVHRR-DERIVED LAND COVER MAPS	87
<i>VI.iii.iii.i. Vegetation Lifeforms (RUN)</i>	87
<i>VI.iii.iii.ii. USGS Land Use / Land Cover (LULC)</i>	88
<i>VI.iii.iii.iii. Global Ecosystems (OGE)</i>	89
<i>VI.iii.iii.iv. Biosphere-Atmosphere Transfer Scheme (BATS)</i>	89
<i>VI.iii.iii.v. Simple Biosphere Model (SiB)</i>	89
<i>VI.iii.iii.vi. Simple Biosphere 2 Model (SiB2)</i>	90
<i>VI.iii.iii.vii. International Geosphere Biosphere Programme (IGBP)</i>	90
<i>VI.iii.iii.viii. Seasonal Land Cover Regions (SLCR)</i>	91
VI.iv. DISCUSSION	91
VI.iv.i. OVERALL DIFFERENCES AMONG THE PUBLIC DOMAIN LAND COVER DATASETS	92
VI.iv.ii. IMPLICATIONS OF THE ASSESSMENT ON MODELING CONSIDERATIONS	93
CHAPTER VII: CONCLUSIONS	96
REFERENCES	99
APPENDIX A: MODIS-DERIVED REGRESSION TREES	104
APPENDIX B: DATA CROSSWALK TO LOWEST COMMON CLASSIFICATION SCHEME	107
APPENDIX C: DATA CROSSWALK TO LOWEST USFS/USGS COMPOSITE CLASSIFICATION SCHEME	116
APPENDIX D: RAW ERROR MATRICES	134
APPENDIX E: NORMALIZED ERROR MATRICES USING MARGFIT	142
APPENDIX F: CLASS ACCURACIES DERIVED FROM ERROR MATRIX DATA	150
APPENDIX G: REGRESSION RESULTS FOR THE PRECIPITATION AND TEMPERATURE STATIONS	155
APPENDIX H: MODELED ANNUAL WATER BALANCE SUMMARY FOR EACH OF THE PRMS RUNS	161
APPENDIX I: PREDICTED VERSUS OBSERVED DISCHARGE FOR THE YAMPA RIVER BASIN AT MAYBELL FROM WATER YEARS 1987 TO 2002 USING PRMS ...	169

LIST OF FIGURES

FIGURE 2.1. The general schematic for the conceptual watershed system used to determine the basic inputs for the PRMS model.....	8
FIGURE 3.1. Site map showing the location of the Yampa River Basin.....	16
FIGURE 4.1. Approximate boundaries of private property, BLM land, and National Forest Land.....	23
FIGURE 4.2. 2004 Landsat image of the Yampa River Basin depicting the locations of the final sample points.....	24
FIGURE 4.3. Locations of the meteorological stations used to populate the data file.....	37
FIGURE 4.4. Thiessen polygons generated for the precipitation stations.....	39
FIGURE 4.5. Thiessen polygons generated for the temperature stations.....	40
FIGURE 5.1. Regression tree where 0 represents the non-forest land class and 1 represents the forest land class.....	44
FIGURE 5.2. Regression tree used to develop the decision rules for the coniferous forest and the deciduous forest land classes.....	45
FIGURE 5.3. Regression tree used to develop the decision rules for the shrubland, grassland or herbaceous, agricultural, and barren or sparsely vegetated land classes.....	46
FIGURE 5.4. Map highlighting the original unclassified area while showing the effect of under-laying the MODIS-derived land cover map.....	48
FIGURE 5.5. Classification accuracy for each class using only the MODIS data compared to the classification accuracy for each class using both LANDSAT and MODIS Data.....	49
FIGURE 5.6. Effect of cross-walking the land cover classes with respect to the species resolution of the different land cover maps.....	52

FIGURE 5.7. Histograms comparing the percentage of each land class present in the Yampa River Basin for each land cover map to the percentage present when using the MVM.....58

FIGURE 5.8. Predicted cumulative streamflow for each of the test runs and the observed cumulative streamflow.....66

FIGURE 5.9. Figure 5.9 shows the predicted cumulative streamflow for each of the model runs minus the observed cumulative streamflow.....68

FIGURE 5.10. Comparison chart where the overall rank based on scene and pixel accuracy is shown on the x-axis, and the rank based on model performance is shown on the y-axis.....74

LIST OF TABLES

TABLE 2.1. Average LAI by biome.....	5
TABLE 2.2. List of the thematic maps produced through the GLCC project.....	10
TABLE 4.1. Projection, resolution, classification, and source information for the different land cover products used in the map assessment.....	19
TABLE 4.2. Map abbreviations and their corresponding map names.....	20
TABLE 4.3. Land cover categories for the reference map, and the number of sample points (if applicable) used to develop the decision rules for each category.....	26
TABLE 4.4. Summary of the spatial parameters that were derived from the land cover grid.....	36
TABLE 4.5. The average annual precipitation and the average number of days that precipitation was observed for each station for water years 1987 through 2001.....	38
TABLE 5.1. Classification accuracy results when running a single regression versus running multiple regressions.....	43
TABLE 5.2. Classification error matrix where the sample points are the reference data.....	47
TABLE 5.3. Error matrix for the MODIS-derived classification.....	50
TABLE 5.4. Percentage of pixels assigned to each land cover category for the different land cover datasets after cross-walk to the lowest common classification scheme.....	54
TABLE 5.5. Percentage of pixels assigned to each land cover category for the different land cover datasets after cross-walk to the USFS/USGS composite classification scheme.....	55
TABLE 5.6. Scene accuracy computed for each land cover map.....	57
TABLE 5.7. Summary of the producer's accuracy, user's accuracy, and overall accuracy for each of the land cover maps.....	60

TABLE 5.8. The calculated KAPPA value, variance, Z statistic, and rank of agreement with respect to the MVM for each land cover map.....	62
TABLE 5.9. Results of the error matrix analysis for each map.....	63
TABLE 5.10. Percentage of the total missing precipitation values for each station and percent corrected by each method.....	64
TABLE 5.11. Percent of missing or erroneous temperature values for each station and the percent corrected by each method.....	65
Table 5.12. Summary of the mean absolute error (MAE) for simulated cumulative streamflow compared to observed cumulative streamflow over the 15-year modeling period using the test datasets.....	67
TABLE 5.13. Summary of the total cumulative predicted streamflow minus observed streamflow ($P - O$), and the mean absolute error (MAE) for simulated cumulative streamflow compared to observed cumulative streamflow over the 15-year modeling period using each of the land cover maps to derive the land cover parameters.....	69
TABLE 5.14. Ranks for each land cover dataset determined from the quantitative assessment methods as compared to the MVM.....	73

LIST OF ABBREVIATIONS

AML: Arc Macro Language

AVHRR: Advanced Very High Resolution Radiometer

BGC: Bio-Geochemical Cycle

COOP: Cooperative Observation Program

CSU: Colorado State University

CVM: Colorado Vegetation Model

DAAC: Distributed Active Archive Center

DEM: Digital Elevation Model

EDC: Earth Resources Observation System Data Center

EOS: Earth Observing System

EROS: Earth Resources Observation System

ET: Evapotranspiration

GEWEX: Global Energy and Water Experiment

GLCC: Global Land Cover Characteristics Data Base

HRU: Hydrologic Response Unit

IGBP: International Geosphere Biosphere Programme

ISIN: Integerized Sinusoidal Grid

LAC: Local Area Coverage

LAI/FPAR: Leaf Area Index/ Fraction of Photosynthetically Active Radiation Biome Scheme

MAE: Mean Absolute Error

MAGS: Mackenzie basin GEWEX Study

MISR: Multiangle Imaging Spectroradiometer

MODIS: Moderate Resolution Imaging Spectroradiometer

MRLC: Multi-Resolution Land Characterization Consortium

MVM: Modeled Vegetation Map

NAD83: North American Datum 1983

NOAA: National Oceanic and Atmospheric Administration

NLCD: National Land Cover Data

OGE: Olson Global Ecosystems

PRMS: Precipitation-Runoff Modeling System

QA/QC: Quality Assurance/Quality Control

SIB: Simple Biosphere Model

SIB2: Simple Biosphere 2 Model

SLCR: Seasonal Land Cover Regions

SNOTEL: Snow Telemetry

STATSGO: State Soils Geographic

TM: Landsat Thematic Mapper

UMD: University of Maryland Modified International Geosphere Biosphere Programme

US: United States

USDA: United States Department of Agriculture

USEPA: United States Environmental Protection Agency

USFS: United States Forest Service

USGS: United States Geological Survey

UTM: Universal Transverse Mercator

CHAPTER I: INTRODUCTION

Satellite-derived land cover maps are often used as input data for hydrologic models. A land cover map identifies the different types of vegetation present in the watershed of interest, and each type of vegetation has a different effect on the cycling of water through the watershed. For example, canopy interception is strongly influenced by vegetation type, stage of growth, and vegetation density (Fassnacht and Soulis, 2002). However, there is a multitude of land cover maps and land classification schemes being utilized today, and there are no definitive rules that govern which map a researcher should use since the choice is dependent upon the research application. For the purposes of this study, the research application will be restricted to modeling streamflow for the water years 1987 through 2001.

This research project has two main objectives where one is to evaluate the differences among publicly available land cover maps for the Yampa region using several different comparison methods. In order to compare these publicly-available land cover products, a 30-meter land cover map that was derived from 2004 field data, TM, and MODIS imagery will be regarded as “ground truth” in this investigation. This determination is based on the fact that all data used to model the map are current, the classification will be specific to the vegetation present within the Yampa River Basin, and the resolution is significantly higher than the 1-km data. The other objective is to assess the performance of the different land cover maps for deriving land cover parameters for predicting streamflow in the Yampa River Basin using the USGS

Precipitation-Runoff Modeling System (PRMS) model developed by Leavesley et al. (1983). This will be accomplished by using the various land cover maps as input for the PRMS model and comparing streamflow predictions to observed streamflow values.

Historically, the high temporal resolution, data volume, cost, and sensitivity to vegetation have made 1-km Advanced Very High Resolution Radiometer (AVHRR) data useful for studies featuring large-scale study areas (Zhu and Evans, 1992). However, since most publicly-available AVHRR-based land cover maps are based on data collected more than 10 years ago, any land cover change that occurred after the dates of data acquisition will not be considered in the hydrological model. With the launch of the Terra Earth Observing System (EOS) in 1999 and Aqua EOS in 2002, the Moderate Resolution Imaging Spectroradiometer (MODIS) instruments onboard each satellite collect more recent remotely sensed data that can be used to derive land cover maps.

The United States Geological Survey (USGS)/United States Environmental Protection Agency (USEPA) National Land Cover Data (NLCD) product derived from Landsat Thematic Mapper (TM) imagery also collected during 1992 has a higher spatial resolution (~30-m) than both the AVHRR and MODIS land cover products, but there is a tradeoff with a lower species classification resolution and a higher data volume. The TM-based map is also based on data collected more than 10 years ago, so it does not reflect any land cover change that occurred since 1992. In addition to the NLCD, Theobald et al. (2004) at Colorado State University (CSU) have modified the NLCD land cover product to create a Colorado land cover map with a higher species resolution. Ancillary spatial data and ecological expertise were used to break down the general

NLCD classes into subclasses to increase the species resolution from 21 land categories to 47 land categories (Theobald et al., 2004).

Each of the maps used in this study vary by classification resolution, spatial resolution, source imagery, and/or date of creation. Ultimately, this comparison assesses the differences among several public domain land cover datasets and how or if the differences affect streamflow simulations, as well as provide specific answers for the optimal spatial and classification resolution for modeling basins of this size.

CHAPTER II: BACKGROUND

II.i. LAND COVER EFFECTS ON THE HYDROLOGY OF SNOWMELT-DOMINATED BASINS

In cold regions, land cover is an important hydrologic control since it influences both the water and energy balance across the land surface (Pietroniro and Soulis, 2001). The following is an overview of the major interactions between climate and land cover that affect the winter water budget in snow-melt dominated basins.

II.i.i. SNOW ACCUMULATION

Before spring melt, snow accumulation in forested areas is a balance of precipitation as snow, canopy storage of snow via interception, and loss of canopy storage through sublimation, melt, and canopy unloading (Buttle et al., 2000). Snow accumulation is significantly different between forested and open areas attributed to processes such as canopy interception, sublimation, and wind redistribution (Pomeroy et al., 2002).

Generally the vegetation extent, or the degree of leaf-cover over a certain area, has an inverse relationship with the amount of snow accumulation on the ground surface (Storck, 2000) primarily due to interception by the canopy. The vegetation extent is often represented as leaf-area index (LAI), which is the leaf area per unit ground area. Table 2.1 shows an average LAI by biome derived from Scurlock et al. (2001). Intercepted snow has a higher sublimation rate than snow on the ground due to greater exposure to short-wave radiation and turbulent energy fluxes in the canopy. This is supported by a

Table 2.1. Average LAI by biome derived from Scurlock et al. (2001).

Biome	Average LAI
Crops	3.6
Desert	1.3
Grassland	1.7
Shrub	2.1
Wetlands	6.3
Tundra	1.9
Coniferous Forest	5.5
Deciduous Forest	5.1

study by Lundberg and Halldin (2001) that observed up to 40 percent reductions in snow accumulation in forested areas compared to open areas, which was attributed to sublimation of snow in the forest canopy.

II.i.ii. SNOWMELT

An increase in evapotranspiration (ET), which can be caused by forest regrowth after a fire for example, can reduce runoff potential (Waring and Running, 1998). Conversely, a decrease in ET can result in increased soil moisture which raises the degree of saturation in the soil surface leading to increased runoff during snowmelt (VanShaar et al., 2002). In open areas, the relatively large snowpacks that accumulate can melt faster than the snowpacks under the forest canopy due to a greater heat transfer caused by more direct exposure to the sun into the pack and greater incident short-wave radiation during the spring (VanShaar et al., 2002).

II.ii. DIGITAL LAND COVER MAPS IN HYDROLOGIC MODELING

Satellite-derived land cover maps are often used as input data for hydrologic models.

Usually the raw data files will require a degree of pre-processing to meet the spatial

specifications of the model, which can be accomplished through use of a geographic information system (GIS). For example, the pre-processing may involve extraction of data that only fall within the area of interest, or data reprojection into a required spatial reference scheme. A GIS can be used to assimilate the raw spatial data into a common framework in terms of spatial reference, scale, and format (Stocks and Wise, 2000).

Even before the data are pre-processed, the user needs to decide which land cover product to use as input. A preliminary study conducted by Fassnacht et al. (2000) explored whether or not there is any difference among the different available land cover maps for the purpose of modeling streamflow in the Salt Basin in Arizona. The results showed different estimates of cumulative streamflow using the United States Geological Survey (USGS) Precipitation-Runoff Modeling System (PRMS) model when different land cover sources were used as input. The simulations also showed differences in both the timing and magnitude of basin runoff compared to observed values.

II.ii.i. SPECIFICATIONS OF THE USGS PRMS MODEL

The USGS PRMS is a physically-based model with a modular design and distributed parameters. It was designed for watersheds where the majority of precipitation comes in the form of snow, and the majority of the annual streamflow is supplied by runoff from snowmelt. The model was developed by the Water Resources Division of the USGS, and the model simulates mean daily streamflow from snowmelt (Singh and Singh, 2001). The model predictions can then be for flood control, irrigation, and water supply projects, as well as for predicting effects of land-use changes (Leavesley, 1973).

Discharge is predicted using a water balance that determines the path of precipitation within the watershed. Equation 2.1 shows the general water balance equation used to derive discharge:

$$Q = P - ET - \Delta S \quad \text{Equation 2.1}$$

where Q is discharge, P is precipitation within the watershed, ET is the amount of water lost through evaporation within the watershed, and ΔS is the change in the amount of water stored in the watershed. In this case, change in storage includes changes in ground water storage and changes in soil moisture (Bossong et al., 2003).

Figure 2.1 provides the general schematic for the conceptual watershed system used to determine the basic inputs for the PRMS model. The figure was adapted from the schematic in Leavesley et al. (1983). For the air temperature and precipitation inputs, data is derived from observations at meteorological stations in the vicinity of the study area. The remaining user inputs are derived using the USGS GIS Weasel program. The GIS Weasel is a GIS interface that delineates and characterizes a watershed specific to the requirements of certain models (Leavesley et al., 2002). The spatial parameter estimation methods are applied through Arc Macro Language (AML) scripts driven by the GIS Weasel. In order to derive the spatial parameters for the PRMS model in the USA, the digital database inputs include a USGS digital elevation model (DEM), a State Soils Geographic (STATSGO) grid of soils data (US Department of Agriculture, 1994), a Forest Service grid of vegetation type and density data (US Department of Agriculture, 1992), and a USGS grid of land use/land cover (LULC) data (Anderson et al., 1976). The parameters are distributed to hydrologic response units (HRUs) which are assumed to be homogenous in terms of the hydrologic response and parameter values. A water balance

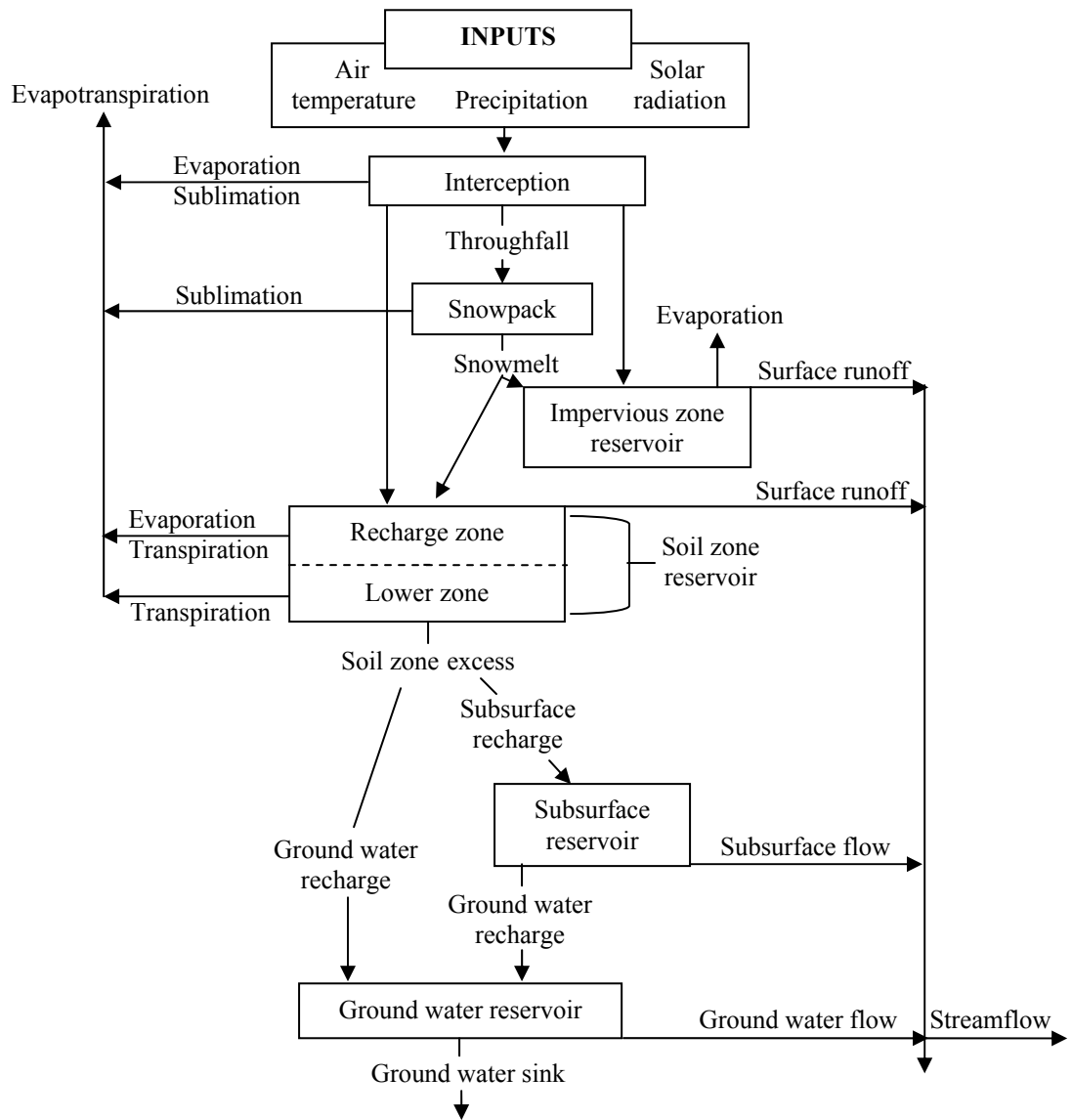


Figure 2.1. The general schematic for the conceptual watershed system used to determine the basic inputs for the PRMS model. The figure was adapted from the schematic found in Leavesley et al. (1983).

and energy balance are calculated for each HRU on a daily time step. The hydrologic response is summed for all the HRUs to determine the daily hydrologic response of the watershed (Leavesley et al., 2002).

II.iii. PUBLIC DOMAIN DIGITAL LAND COVER MAPS

Currently, there is a variety of land cover products available to the public at little or no cost. The majority of the available land cover maps are derived from National Oceanic and Atmospheric Administration (NOAA) Local Area Coverage (LAC) data, and many can be obtained from the Earth Resources Observation System (EROS) Data Center (EDC) Distributed Active Archive Center (DAAC) (Pietroniro and Soulis, 2001). The majority of the public domain land cover datasets are derived from Landsat, Moderate Resolution Imaging Spectroradiometer (MODIS), or Advanced Very High Resolution Radiometer (AVHRR) imagery.

II.iii.i. AVHRR LAND COVER PRODUCTS

The first global land cover map derived from remote sensing data was developed by Defries and Townshend (1994) using monthly composites of AVHRR Normalized Difference Vegetation Index (NDVI) data (Friedl et al, 2002). The NDVI is a greenness index that is calculated from a ratio of reflectances measured by satellites in the visible and near infrared regions of the electromagnetic spectrum. The map has a 100-km spatial resolution, and was derived using a maximum likelihood classification algorithm.

Defries et al. (1998) followed with an AVHRR-derived global land cover map available at 8-km resolution using a decision tree classification algorithm. The spatial resolutions of these maps, however, are very coarse compared to the global land cover characteristics (GLCC) data base product.

II.iii.i.i. Global Land Cover Characteristics (GLCC) Data Base

The United States Geological Survey's EROS Data Center, the University of Nebraska-Lincoln (UNL), and the Joint Research Centre of the European Commission have generated the GLCC data base derived from AVHRR 1-km imagery for use in a variety of environmental research applications (Loveland et al., 2000). The GLCC data set includes land cover products derived from 1-km NDVI composites of AVHRR data collected between April 1992 and March 1993 (Global Land Cover Characteristics Data Base, 2003). Although AVHRR imagery has moderate spatial resolution compared to Landsat imagery, AVHRR data have a higher temporal resolution where almost the entire earth is imaged twice daily compared to every 16 days for Landsat (Loveland et al., 1991; Williams, 2004). The high temporal resolution of AVHRR increases the probability of cloud-free acquisitions since both AVHRR and Landsat collect visible spectrum imagery, and permits monitoring of dynamic land cover conditions over short periods (Loveland et al., 1991). Table 2.2 provides a list of the thematic maps produced through the GLCC project.

Table 2.2. List of the thematic maps produced through the GLCC project.

Thematic Map	Classification Source
Seasonal Land Cover Regions	Global Land Cover Characteristics Data Base
Global Ecosystems	Olson; 1994a, 1994b
International Geosphere Biosphere Programme Land Cover Classification	Belward, 1996
USGS Land Use/Land Cover System	Anderson et al., 1976
Simple Biosphere Model	Sellers et al., 1986
Simple Biosphere 2 Model	Sellers et al., 1996
Biosphere-Atmosphere Transfer Scheme	Dickinson et al., 1986
Vegetation Lifeforms	Running et al., 1994

II.iii.ii. MODIS LAND COVER PRODUCTS

Compared to AVHRR data, MODIS data have a higher spectral, spatial, radiometric, and geometric quality, and the map algorithms provide a narrower temporal window between data collection and map production. Also, the 1-km resolution MODIS land cover product is based on data collected since 1999, so it is based on more recent data than the AVHRR GLCC product. The MODIS instrument has seven spectral bands designed especially for measuring land characteristics (Friedl et al., 2002). However, since the design of MODIS was a conciliation of the requirements of different disciplines, some of the bands represent a compromise between the needs of both land and oceans research applications. The Terra satellite MODIS sensor has a daily repeat coverage for areas north of approximately 30° latitude, and a 2-day repeat coverage for areas south of 30° latitude. (Justice et al., 2002).

Currently, there are 44 standard MODIS data products distributed via the EDC DAAC that are available for different research applications, and the MODIS 12 product specifically addresses land cover and land cover change (MODARCH, 2005). Currently the MODIS land cover product is available in the International Geosphere Biosphere Program (IGBP) classification scheme (Belward et al., 1999; Scepan, 1999), the University of Maryland (UMD) scheme (Hansen et al, 2000), the Bio-Geochemical Cycle (BGC) Biome scheme (Running et al., 1994), and the Leaf Area Index/ Fraction of Photosynthetically Active Radiation (LAI/fPAR) Biome scheme (Myneni et al, 1997).

The MODIS land cover product is compiled using the MODIS land cover classification algorithm (MLCCA) that includes two major components. The first component involves use of training sites representative of each land cover class, and the

second component involves supervised classification algorithms to classify the MODIS data. The land cover product is updated quarterly, which are effectively revisions to the existing map. After continued database development, it is anticipated that updates will occur on an annual or semiannual basis (Friedl et al., 2002).

II.iii.iii. LANDSAT TM LAND COVER PRODUCTS

The United States Geological Survey (USGS) and the United States Environmental Protection Agency (USEPA) have developed the National Land Cover Data (NLCD) product derived from 1992 Landsat Thematic Mapper (TM) imagery. It has a higher spatial resolution (~30-m) than both the AVHRR and MODIS land cover products, but there is a tradeoff with a lower species classification resolution, a smaller coverage area, and a higher data volume. The classification scheme is a modified Anderson land use and land cover classification system (Anderson et al., 1976), and the NLCD covers the conterminous U.S. rather than the entire globe. The LULC classification system was engineered around the needs of government agencies to provide a current overview of land cover throughout the U.S. The categories are organized into levels where the first and second levels contain more generalized categories, and the third and fourth levels are left open-ended so government agencies can develop more detailed land categories to suit their specific needs and goals (Anderson et al., 1976).

The primary data source for the NLCD is TM images capturing both leaf-on and leaf-off conditions, which was collected by the Multiresolution Land Characterization (MRLC) Consortium in 1992. An unsupervised classification was used to separate the data into clusters which were then labeled using aerial photographs. If a cluster

represented more than one land class, the cluster was split using spatial modeling of ancillary data sets such as elevation or population census data (Vogelmann et al., 1998).

In addition to the NLCD, Colorado State University (CSU) has modified the NLCD product to create a Colorado land cover map with a higher species resolution. Ancillary spatial data and ecological expertise were used to break down the general NLCD classes into subclasses to increase the species resolution from 21 land categories to 47 land categories (Theobald et al., 2004).

II.iv. DIGITAL MAP ASSESSMENT

A map is simply a representation usually on a two-dimensional surface of a portion or all of the earth (Merriam-Webster, 1995). Since by definition a map is a representation, a map will always have errors. There is a large variety of land cover maps available today, and selecting a suitable map to use in a particular application is an important decision. The decision should be based on several characteristics that may involve quantitative accuracy, dates of acquisition, spatial resolution, temporal resolution, cost, or classification resolution considerations. Smits et al. (1999) expressed that “the user of land-cover maps needs to know how *accurate* the product is in order to use the data efficiently” (qtd in Gebelein and Estes, 2000).

An accuracy assessment procedure can be conducted to determine the quality of a land cover product. The purpose of a quantitative assessment is to determine the errors associated with a map by comparing areas on the map to reference data that are assumed to be correct (Congalton and Green, 1999). Reference data include, but are not limited

to, aerial photography, ground-truth data (information collected on the physical earth) (Congalton and Green, 1999), and/or other land cover maps (Pietroniro and Soulis, 2001).

Even a highly accurate map with respect to what is observed on the ground may not be the most suitable map for the end user. One also needs to consider the dates of data acquisition and the dates of the accuracy assessment procedure. In other words, a map that was accurate ten years ago will almost certainly be less accurate than it would be today.

Given a map is current and accurate, there are additional factors to consider. The end user should assess the needs of the intended research application such as the size of the study area, model capabilities and scale, budgetary restraints, and the importance of capturing certain land classes. For example, most classification schemes are useful for only a narrow scope of applications (Loveland et al., 1991), so it is imperative to choose a classification scheme that suits the end application. Considering all factors together will provide the end user with a qualitative assessment specific to the needs of the respective application.

Pietroniro and Soulis (2001) provide an excellent example of assessing maps based on a desired application. The objective was to compare global medium-resolution land-cover datasets derived from AVHRR data to assess their relative suitability for modeling applications within the Mackenzie River basin Global Energy and Water Experiment (GEWEX) Study (MAGS). This region was the geographical focus of part of the GEWEX Program Science Plan to concentrate Canada's research focus on characteristics of cold regions. In order to compare several land cover maps, it was necessary to create a common framework in terms of spatial resolution and classification

resolution. The authors found that the process of aggregating land-cover categories was highly subjective, as there are no present standards for interpreting land class definitions. Although the authors found it difficult to compare the maps for the study region, the most effective method to determine an overall accuracy was to compare the maps to Landsat-derived maps which had a significantly higher spatial resolution (30-m vs. 1-km). Also, the Landsat maps were developed by researchers working within the respective map regions, and the maps represented the dominant land classes present in the Mackenzie basin. Overall the authors found that the comparison allowed for a ranking of the AVHRR-derived land cover maps, which aided in the selection of the most suitable dataset with respect to the objectives of the MAGS program.

CHAPTER III: STUDY AREA

The Yampa River Basin, along with the White River Basin, drains the northwest corner of Colorado. The study area is located in northwestern Colorado and encompasses an approximate area of 8,758 square kilometers. Figure 3.1 is a site map showing the location of the Yampa River Basin delineated using a seamless 30-meter Digital Elevation Model (DEM) and the USGS GIS Weasel.

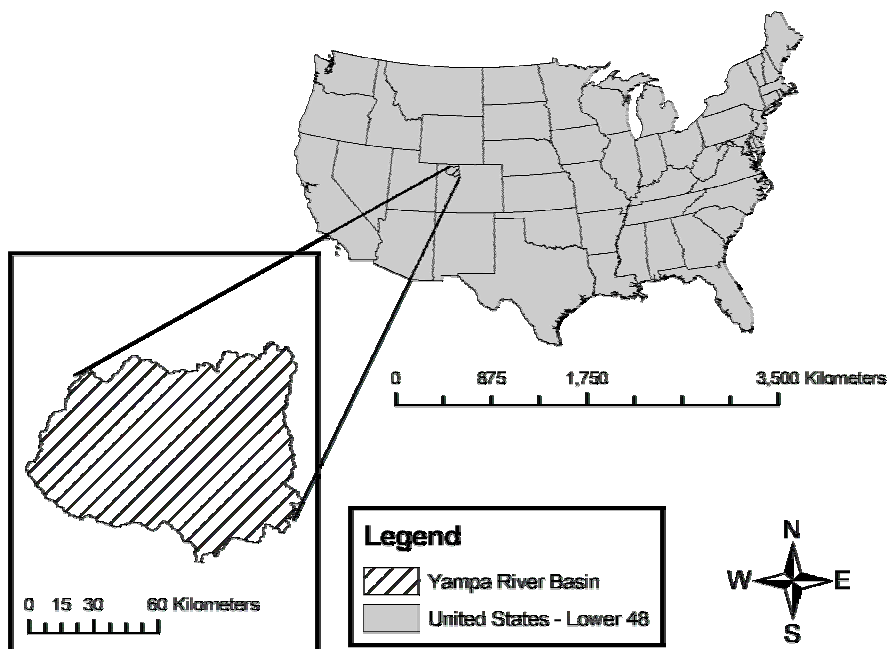


Figure 3.1. Site map showing the location of the Yampa River Basin delineated using a seamless 30-meter Digital Elevation Model (DEM) and the USGS GIS Weasel. Data were obtained from USGS and ESRI, and the map is presented in the Universal Transverse Mercator (UTM) Zone 13 projection North American Datum 1983 (NAD83).

Precipitation varies between less than 9 inches annually along the semiarid lower region to greater than 50 inches along the upper western regions where the majority of

annual precipitation occurs as snow. The majority of runoff is attributed to melting of the winter snowpack in higher elevation areas around the continental divide.

(Smith et al., 1998). This basin was chosen because it is largely unregulated, representative of a variety of land cover types, and is of adequate size for comparing 1-km data.

CHAPTER IV: MATERIALS AND METHODS

IV.i. DIGITAL LAND COVER PRODUCTS

Thirteen land cover products were chosen for this study that were widely available and well-documented. Table 4.1 summarizes the projection, resolution, classification, and source information for the different land cover products used in the map assessment. Table 4.2 lists the map abbreviations and their corresponding map names for ease of reference.

IV.i.i. AVHRR-DERIVED LAND COVER PRODUCTS

The majority of the AVHRR-derived data sets used in this study were obtained from the United States Geological Survey Bureau (USGS) Earth Resources Observing Systems (EROS) Data Center (EDC) Global Land Cover Characterization database (GLCC). The land cover data sets were produced from multitemporal AVHRR data compiled over a 12-month period from April 1992 to March 1993. This product is available in 8 different classification schemes for ease of use in different applications.

Another publicly-available map utilized in this study was developed by the United States Department of Agriculture (USDA) Forest Service (USFS). This map was derived from AVHRR scenes of the 1991 growing season.

Table 4.1. Summary of land cover datasets including projection, resolution, classification, and source information.

Original Projection	Resolution	Classification System	Land Classes	Data Source	Classification Source
USFS Forest Land Distribution Data					
Lambert Azimuthal Equal Area	1-km	USFS Classification	29	NOAA-AVHRR (1991)	USFS/USGS, 2002
National Land Cover Data (NLCD) v. 09-09-2000					
Albers Conical Equal Area	30-m	NLCD Classification	21	MRLC-Landsat TM (1992)	Anderson et al., 1976
DAAC Global Land Cover (North America) v. 2.0					
Lambert Azimuthal Equal Area	1-km	Global Ecosystems	96	NOAA AVHRR (1992-1993)	Olson, 1994a; 1994b
		International Geosphere Biosphere Programme (IGBP)	17		Belward, 1996
		USGS Land Use/Land Cover (LULC) System (Modified Level II)	24		Anderson et al., 1976
		Seasonal Land Cover Regions (SLCR)	202		
		Simple Biosphere Model (SiB)	16		Sellers et al., 1986
		Simple Biosphere 2 Model (SiB2)	11		Sellers et al., 1996
		Biosphere-Atmosphere Transfer Scheme (BATS)	20		Dickinson et al., 1986
		Vegetation Lifeforms	8		Running et al., 1994
DAAC MODIS/Terra Land Cover Type 96-Day L3 Global 1km					
Integerized Sinusoidal (ISIN)	1-km	University of Maryland (UMD) Modified IGBP	14	MODIS/Terra (2000-2001)	Hansen et al., 2000
		Leaf Area Index/fraction of Photosynthetically Active Radiation (LAI/fPAR) Biome scheme	9		Myneni et al., 1997
		IGBP	17		
CSU Colorado Vegetation Model (CVM) v. 8					
Universal Transverse Mercator	30-m	CVM (Modified NLCD)	47	Landsat (1992)	Theobald et al., 2004
Modeled Vegetation Map (MVM)					
Universal Transverse Mercator	30-m	Based on field data	9	MODIS/Landsat TM (2004)	

Table 4.2. Map abbreviations and their corresponding map names for ease of reference. Thirteen of the maps were public domain, but the remaining map (MVM) was modeled specifically for this study so it is not currently public domain.

Abbreviation	Land Cover Map
NLCD	National Land Cover Data
OGE	Global Ecosystems
IGBP (AVHRR)	International Geosphere Biosphere Programme based on Advanced Very High Resolution Radiometer data
LULC	Land Use/Land Cover
SLCR	Seasonal Land Cover Regions
SIB	Simple Biosphere Model
SIB2	Simple Biosphere 2 Model
BATS	Biosphere-Atmosphere Transfer Scheme
RUN	Vegetation Lifeforms
UMD	University of Maryland Modified International Geosphere Biosphere Programme
LAI/FPAR	Leaf Area Index/fraction of Photosynthetically Active Radiation Biome Scheme
IGBP (MODIS)	International Geosphere Biosphere Programme based on Moderate Imaging Spectroradiometer data
CVM	Colorado Vegetation Model
MVM	Modeled Vegetation Map

IV.i.ii. MODIS-DERIVED LAND COVER PRODUCTS

The MODIS Land Cover Classification product, MOD12Q1 version 003, was obtained from the EDC DAAC and is based on MODIS imagery obtained from 15 October 2000 through 15 October 2001. This product is available in four different classification schemes for ease of use in different research applications (Hodges, 2002). However, one of the four products, the Biogeochemical Biome Scheme land cover grid, was not used in this study because it was unavailable.

IV.i.iii. LANDSAT TM-DERIVED LAND COVER PRODUCTS

The National Land Cover Dataset (NLCD) is the result of a cooperative effort between the USGS and the United USEPA to create a land cover data set for the United States (US) based on 30-meter TM data. The TM data were obtained by the MRLC Consortium, and the NLCD product used in this study is derived from TM data collected in 1992.

Also included in the study was a refined NLCD map unique to the state of Colorado that was created by Theobald et al. (2004). Species resolution was increased from 21 land cover categories present in the original NLCD map to 47 land cover categories by using ancillary spatial data and ecological expertise to further subdivide the original classes (Theobald et al., 2004).

IV.ii. MODELED VEGETATION MAP (MVM)

The production of the Modeled Vegetation Map (MVM) was based on field data and supervised classification of training sites. Six decision trees were employed to model the vegetation distribution within the study basin using several independent variables derived from ancillary data sources. An advantage of this map is that it was created in-house, so the classification errors associated with the map are known.

IV.ii.i. SPATIAL DATA AND IMAGE PROCESSING

MODIS and Landsat imagery used to develop the vegetation map were purchased by CSU. The MODIS imagery acquired in 2004 were resampled to 30m x 30m using a nearest neighbor resampling method and an average of a 250m x 250m window. The

imagery consists of 7 spectral bands, and was projected in the Universal Transverse Mercator (UTM) projection. The Landsat (TM 7) imagery was collected in the summer of 2004, and includes bands 1 through 6 and 8.

IV.ii.ii. SAMPLING DESIGN

The field data were collected according to a stratified random sampling design. In order to capture the spectral variability of the study area, an unsupervised classification procedure was performed on the MODIS imagery using the CLASSIFICATION command in ERDAS IMAGINE[®] version 8.5 (ERDAS, 2001). This is based on the ISODATA algorithm by Tou and Gonzalez (1974). The CVM had the highest species resolution with 41 land cover classes in the Yampa region, so 50 spectral classes were isolated to ensure adequate sampling of the spectral variability within the basin.

For the initial sampling plan, random coordinates were generated to sample two points within each spectral class for a total of 100 points using the ACCURACY ASSESSMENT command in IMAGINE[®] (ERDAS, 2001). As per Joy et al. (2003), only the center of 3 x 3 pixel (90-m x 90-m) blocks of uniform spectral class assignment were selected from as sample coordinates because the points were based on geographically referenced pixels. An additional 100 sample points were distributed randomly in order to account for additional vegetative variability within the basin.

In practice, however, the sampling plan required adjustment due to several extraneous factors. The biggest issue involved sampling around private property, especially when it prohibited access to National Forest land and Bureau of Land

Management (BLM) land. Figure 4.1 shows the approximate boundaries of private property, BLM land, and National Forest land.

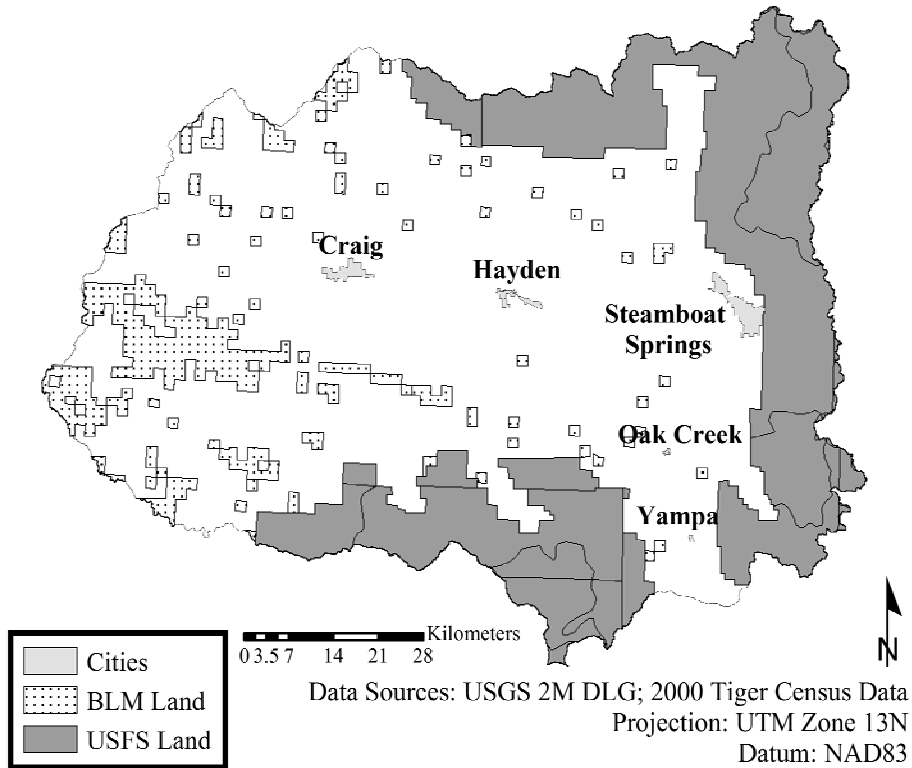


Figure 4.1. Approximate boundaries of private property, BLM land, and National Forest land. Approximately 61.7 percent of the total study area is designated as private property, approximately 30.2 percent is designated as National Forest land, and approximately 8.1 percent is designated as BLM land.

Approximately 61.7 percent of the total study area is designated as private property, approximately 30.2 percent is designated as National Forest land, and approximately 8.1 percent is designated as BLM land.

Also, due to the large size of the study basin, sample points were often located 8-16 kilometers apart which inhibited sampling efficiency, especially due to budgetary and time considerations. In order to collect an adequate amount of points in a reasonable

amount of time, 400 additional points were added (8 per spectral class) with the assumption that a large portion of these points would be inaccessible.

Joy et al. (2003) has recommended at least 200 sample points for complex data sets when utilizing decision trees. By the end of the sampling period, there were 114 total sample points where 72 were collected from the stratified random sample, 20 were collected from the random sample, and 20 were collected subjectively as representatives of important land cover classes. Figure 4.2 is a 2004 Landsat image of the Yampa River Basin depicting the locations of the final sample points.

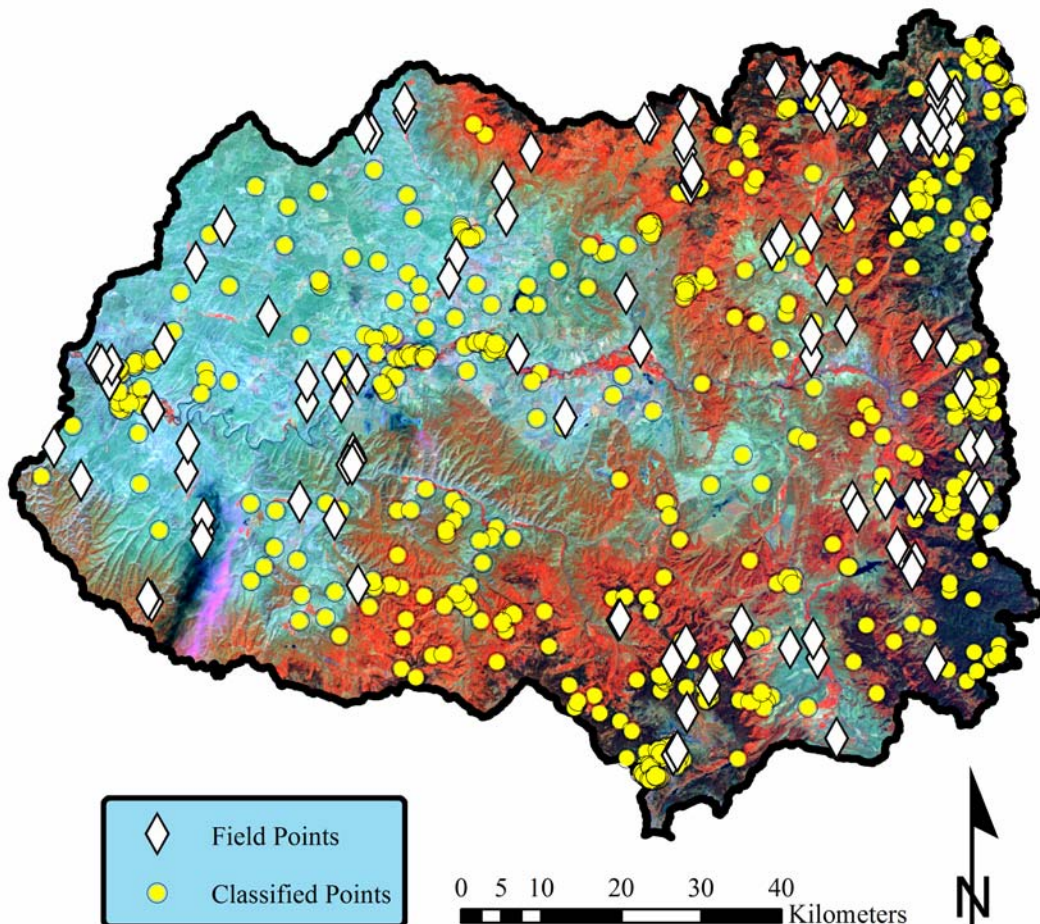


Figure 4.2. 2004 Landsat image of the Yampa River Basin depicting the locations of the final sample points. Band 4 is shown in red, band 5 is shown in green, and band 3 is shown in blue.

In order to increase the number of sample points, additional points were added through supervised classification using Landsat imagery, aerial photographs, field photographs, and *a priori* knowledge from field visits of the vegetation distribution in the Yampa River basin. Combining sample points and training sites, there was a total of 635 points available to create the decision tree.

IV.ii.iii. FIELD DATA

The field data were collected from July to September 2004. Vegetation type and canopy closure data were collected at each point. Canopy closure was measured with a concave, spherical densiometer (Lemmon, 1956, 1957). Photographs were taken using a 360-degree panoramic iPIX[®] camera and an Olympus[®] digital camera at each sample point as part of the Quality Assurance/Quality Control (QA/QC) component. In addition, these photographs became invaluable descriptors of land characteristics when delineating supervised training sites.

IV.ii.iv. REFERENCE MAP GENERATION

The reference map was generated from binary regressions using the 635 sample points as dependent variables. The field points comprised 114 of these sample points, and supervised classification points comprised the remaining 521 sample points. The predictor variables were elevation, aspect, slope, MODIS bands 1-7, Landsat bands 1-6 and 8, and forest density. In order to ensure the reference map had a high accuracy, sample points in addition to the field points were necessary to increase sample size, but the classification categories had to be generalized to maintain confidence in the accuracy

of the supervised classification points. The urban, water, and snow and ice land categories were manually digitized from 2004 Landsat imagery and aerial photographs since the categories had very distinct spectral signatures and were easily verified by the aerial photographs. Table 4.3 lists the land cover categories for the reference map, and the number of sample points (if applicable) used to develop the decision rules for each category.

Table 4.3. Land cover categories for the reference map, and the number of sample points (if applicable) used to develop the decision rules for each category. The categories that were not derived from sample points were manually delineated using 2004 Landsat imagery and aerial photography.

Land Cover Category	Number of Sample Points
Coniferous Forest (2)	41
Deciduous Forest (3)	62
Shrubland (5)	60
Grassland/Herbaceous (6)	65
Agricultural Land (7)	61
Barren/Sparse Vegetated (8)	68
Water (9)	N/A
Urban (11)	N/A
Snow and Ice (12)	N/A

IV.iii. ASSESSMENT OF DIGITAL LAND COVER MAPS

Once all the data were compiled into a common framework, the land cover maps were assessed by four comparison methods. The comparisons were based on: (i) the relative agreement of the total aggregated land class percentages present after the data have been cross-walked (resampled to the same classification scheme); (ii) pixel accuracy; (iii) scene accuracy; and (iv) cumulative streamflow simulated from the USGS Precipitation-Runoff Modeling System (PRMS) hydrological model in relation to cumulative observed streamflow.

IV.iii.i. DATA PREPARATION

Before comparison, all data were registered to a common projection, land classification scheme, and spatial resolution. Once this was accomplished, each land cover map was clipped to the Yampa River Basin watershed using a polygon of the delineated watershed boundary. Figure 4.3 provides an overview of the preliminary data processing steps for the land cover data sets to create a common framework for comparison.

IV.iii.i.i. Data Reprojection

All data sets were reprojected to the UTM Zone 13 grid system. The advantages of this projection over the geographic coordinate system is that every grid block has the same size and shape, and linear values can be used to identify points rather than angular values (Pearson, 1990). The North American Datum 1983 (NAD83) was chosen as the common datum. Transformation from the North American Datum 1927 to the NAD83 datum was performed using the NADCON transformation method in ArcToolbox 8.3 (ESRI[®], 2003).

IV.iii.i.ii. Data Cross-Walk

The term “cross-walk” refers to the process of reclassifying a map’s categories so that they coincide with the categories of another map. In this case, the creation of a common land classification scheme was subjective since there was no standard for the definition of land cover categories across the different classification schemes (Pietroniro and Soulis, 2001). The aggregation of the original land cover categories to the lowest common classification scheme, or “cross-walking”, was guided by available land cover class

definitions and how others have aggregated land cover classes in the past (Pietroniro and Soulis, 2001; Theobald et al., 2004). Each land cover class was reclassified to a consistent value across all data sets.

IV.iii.i.iii. Grid Resampling

Where applicable, the land cover maps were resampled to a common spatial resolution, specifically to 30-m using the nearest neighbor interpolation method in ArcGIS® 8.3 (ESRI®, 2003). Since 30 meters is not a multiple of 1000 and the grid values are categorical data types, the nearest neighbor interpolation method works best because it handles edge values by taking on the closest original cell value rather than changing actual cell values.

IV.iii.ii. TOTAL AGGREGATED LAND CLASS PERCENTAGES

The first comparison involved calculating the total aggregated land class percentage present after the data had been cross-walked to qualitatively assess the differences between the land cover data sets. This is an exploratory comparison to determine the effect of cross-walking the land cover classes for each map.

IV.iii.iii. SCENE ACCURACY

Scene accuracy refers to the proportion of the image that was properly classified, irrespective of location. (Pietroniro and Soulis, 2001). The 1-km data were compared for the Yampa River Basin region, as well as for the relative agreement with the MVM. The scene accuracy was calculated through a histogram comparing total land cover

percentages for each map. The scene accuracy was only assessed for those categories that were present in the MVM.

IV.iii.iv. PIXEL ACCURACY

Pixel accuracy refers to a normalized average of class accuracy for each land cover category based on the percentage of MVM pixels for that class (Pietroniro and Soulis, 2001). Due to the high spatial resolution of the MVM and its development based on the specifics of the Yampa River Basin, the MVM map was regarded as “truth” in this comparison.

In order to calculate pixel accuracy, error matrices were constructed for each land cover map using the MVM for the reference points. An error matrix is a numeric array that relates the number of units, i.e., pixels, defined as a specific class in one image to the number of units defined as a specific class in another image, where one image is typically considered to be correct (Congalton and Green, 1999).

IV.iii.iv.i. Raw Error Matrices

The matrices were populated after multiplying each land class by a multiple of 100 based on land cover type in each of the cross-walked land cover maps and adding each raster image to the MVM raster image using the SPATIAL ANALYST map algebra in ArcGIS[®] 9.0 (ESRI[®], 2004). For example, a value of 202 in the output map would mean the pixel was classified as coniferous in the MVM as well as in the land cover map being compared. A value of 302 in the output map would mean the pixel was classified as coniferous in the MVM and as deciduous in the land cover map being compared.

Once the raw error matrices were constructed, they could be evaluated to identify the errors of inclusion and the errors of exclusion. Errors of inclusion, or commission errors, are pixels that are assigned to a particular category but according to the reference data do not belong in that category. Conversely, errors of exclusion, or omission errors, are pixels that were omitted from their correct category according to the reference data. (Congalton and Green, 1999).

In addition to evaluating commission and omission errors, the error matrices were used to calculate overall accuracy, producer's accuracy, and user's accuracy. Overall accuracy is calculated by summing the major diagonal, or the correctly classified pixels, and dividing by the total number of pixels in the error matrix (Congalton and Green, 1999). Both the producer's and user's accuracies are measures that represent individual category accuracies rather than simply the overall classification accuracy. Producer's accuracy is computed by dividing the number of correct pixels in a particular category by the total number of pixels assigned to the category in the reference data (Congalton and Green, 1999). User's accuracy is computed by dividing the number of correct pixels in a particular category by the total number of pixels assigned to the category in the image that is not considered the reference image (Congalton and Green, 1999).

The error matrices were also evaluated based on the Kappa statistic, which measures the proportion of correctly classified pixels between two maps after the probability of chance agreement has been accounted for (Congalton, 1991). Kappa values can range from +1 to -1 where positive values indicate positive correlation, 0 values indicate no correlation (random), and negative values indicate negative correlation between the classification and the reference data (Congalton and Green, 1999).

Following the notation of Congalton and Green (1999), the Kappa statistic is calculated through the following equation:

$$\hat{K} = \frac{n \sum_{i=1}^k n_{ii} - \sum_{i=1}^k n_{i+} n_{+i}}{n^2 - \sum_{i=1}^k n_{i+} n_{+i}} \quad \text{Equation 4.1}$$

where n is the total number of pixel values, n_{ii} is the main diagonal value of row/column i , n_{i+} is the marginal total for row i , and n_{+i} is the marginal total for column i .

The approximate large sample variance of the Kappa value was computed using the Delta method following the notation of Congalton and Green (1999):

$$\hat{\text{var}}(\hat{K}) = \frac{1}{n} \left\{ \frac{\theta_1(1-\theta_1)}{(1-\theta_2)^2} + \frac{2(1-\theta_1)(2\theta_1\theta_2 - \theta_3)}{(1-\theta_2)^3} + \frac{(1-\theta_1)^2(\theta_4 - 4\theta_2^2)}{(1-\theta_2)^4} \right\} \quad \text{Equation 4.2}$$

where

$$\theta_1 = \frac{1}{n} \sum_{i=1}^k n_{ii} ;$$

$$\theta_2 = \frac{1}{n^2} \sum_{i=1}^k n_{i+} n_{+i} ;$$

$$\theta_3 = \frac{1}{n^2} \sum_{i=1}^k n_{ii} (n_{i+} + n_{+i}); \text{ and}$$

$$\theta_4 = \frac{1}{n^3} \sum_{i=1}^k \sum_{j=1}^k n_{ij} (n_{j+} + n_{+i})^2 .$$

for the θ_4 term, j denotes the column number.

To test whether the agreement between the map and the reference data is significantly higher than a random classification, the test statistic is given as

$$Z = \frac{\hat{K}_1}{\sqrt{\hat{\text{var}}(\hat{K}_1)}} \quad \text{Equation 4.3}$$

following the notation of Congalton and Green (1999). In addition to measuring the agreement between the particular classification and the reference data, it is also possible to test if two independent Kappa values, or two error matrices, are significantly different using the following equation:

$$Z = \frac{|\hat{K}_1 - \hat{K}_2|}{\sqrt{(\hat{\text{var}}(\hat{K}_1) + \hat{\text{var}}(\hat{K}_2))}} \quad \text{Equation 4.4}$$

where \hat{K}_1 and \hat{K}_2 are the Kappa estimate for the two matrices being compared, and $\hat{\text{var}}(\hat{K}_1)$ and $\hat{\text{var}}(\hat{K}_2)$ are the corresponding variance estimates. In both tests, Z is standardized and normally distributed, so the critical value is 1.96 using a 95% confidence level. (Congalton and Green, 1999).

IV.iii.iv.ii. Normalized Error Matrices

Using a technique known as Margfit, the error matrices were normalized for comparison purposes. The Margfit technique utilizes an iterative proportional fitting method to conform the sum of each row and column in the error matrix to a predetermined value. As a result, sample size differences are eliminated to permit direct comparison between cell values inside the matrix. In addition, a normalized accuracy can be calculated by summing the values of the major diagonal and dividing by the sum of the total values in the normalized error matrix (Congalton and Green, 1999).

The Margfit procedure was used on each raw error matrix through the application of a FORTRAN program modified from the Margfit code provided in Congalton et al. (1981). Besides allowing for direct comparison between cell values, the normalized error matrix also permitted direct comparison of cell values between different matrices. Through the iterative proportional fitting technique, each value in the normalized error matrix was balanced by values both in its respective row and column. As a result, both producer's and user's accuracies were incorporated into the normalized cell value, so the normalized cell value was based on a balanced effect of these two accuracy measures (Congalton and Green, 1999).

In summary, the overall accuracy computed from the raw error matrices will only incorporate the values from the major diagonal and will not include the omission and commission errors described by the off-diagonal values. Normalized accuracy may be a better measure for overall accuracy because it does include the off-diagonal values as a result of the proportional fitting technique. Finally, the Kappa statistic also includes the off-diagonal values, but indirectly through the computations involving products of the row and column marginals (Congalton and Green, 1999). All three measures will be assessed for the error matrices to see whether or not the different accuracy measures will result in different rankings for the land cover maps in this particular case.

IV.iv. HYDROLOGICAL MODELING COMPARISON

IV.iv.i. STREAMFLOW SIMULATIONS

The final comparison used each land cover map as input into the USGS PRMS model, which was chosen because it is specifically designed for hydrological applications within

mountainous terrain in the Rocky Mountain Region. Six test datasets were run initially to assess the overall sensitivity of PRMS to characterization of land cover in the Yampa River Basin. The PRMS comparison was mainly based on cumulative streamflow model output in relation to observed cumulative streamflow for the Yampa River Basin. Peak streamflow was also examined to help interpret the results. This comparison serves to assess the effect of using different land cover maps for streamflow prediction, as well as to determine the land cover maps that match closest to observed streamflow after manual calibration of the adjusted precipitation factor in the parameter file using the MVM as the reference. The adjusted precipitation factor was adjusted so that the *total* cumulative streamflow over the modeling period matched as close as possible to the observed total cumulative streamflow.

IV.iv.i.i. PRMS Runs

In order to assess the differences in the land cover maps with respect to hydrological modeling with PRMS, each land cover map was used as the land cover input to derive certain spatial parameters. All other variables including precipitation, maximum and minimum daily temperature, and topographic parameters were held constant, so changes in predicted streamflow could only be attributed to differences present in the land cover datasets. A 2-km modeling block (HRU) was used, and there were 2339 HRUs. This lattice modeling structure was chosen because the purpose was to compare the effects of using the different land cover maps to parameterize the model, so the large number of HRUs was meant to maintain the heterogeneity of the land cover in the Yampa River Basin.

Before performing the model runs, the MVM was used to manually calibrate the model so predicted cumulative streamflow would match closely with observed cumulative streamflow for an accurate map. Then the model was run with varying land cover parameters for the period 1 October 1986 through 31 August 2002 because this represented the most complete, contiguous data period with respect to the available meteorological data.

IV.iv.i.ii. Model Parameterization

In order to run the PRMS model, the hydrologic response units (HRUs) and the parameter file were derived first through the USGS GIS Weasel program which utilizes ESRI's ArcInfo program as a medium to derive the individual parameters. The HRUs were defined as 2-km lattice cells which was the smallest area allowed with respect to the size of the basin (ArcInfo could only accommodate a certain number of HRUs). The parameter file contains spatial and topographic information such as slope, aspect, elevation, soil moisture, and evapotranspiration. More information on the parameterization process can be found at the GIS Weasel website (www.brr.cr.usgs.gov/projects/SW_precip_runoff/weasel, 2003). There were 23 total parameters calculated by the GIS Weasel where nine were calculated using a grid of land cover. Table 4.4 provides a summary of the spatial parameters that were derived from the land cover grid. The parameters derived from the land cover grid involved soil moisture properties and vegetation canopy properties, i.e., interception, density, and transmissivity. As a result, differences in predicted streamflow observed through use of the different land cover maps can be attributed to changes in predicted soil moisture and

Table 4.4. Summary of the spatial parameters that were derived from the land cover grid. The parameter definitions were taken from the GIS Weasel website (Viger, 2003).

Parameter	Definition
soil_moist_max	Mean maximum soil moisture (inches/inch) for each HRU
soil_rechr_max	Mean soil moisture recharge (inches/inch) for the entire soil depth or the top 18 inches of soil for each HRU
covden_sum	Mean summer vegetation cover density (%) for each HRU
covden_win	Mean winter vegetation cover density (%) for each HRU
rad_trncf	Mean winter canopy transmissivity (%) for each HRU
cov_type	Most common occurring land cover type for each HRU
srain_intcp	Mean interception of rain during summer (inches) for each HRU
wrain_intcp	Mean interception of rain during winter (inches) for each HRU
snow_intcp	Mean interception of winter snow (inches) for each HRU

vegetation canopy properties. The parameter file is important because it contains the only information that changes when using different land cover datasets for the model.

IV.iv.i.iii. Preparing and Distributing the Meteorological Data

In addition to the parameter file, a data file was prepared containing daily runoff, precipitation, maximum temperature (T_{max}), and minimum temperature (T_{min}) for each of the climate stations within the vicinity of the study area. Figure 4.3 is a map showing the locations of the meteorological stations used to populate the data file.

The data file contains meteorological data for climate stations that were distributed to the lattice cells (HRUs) in the parameter file through construction of Thiessen polygons. Table 4.5 shows the average annual precipitation and the average number of days that precipitation was observed for each station for water years 1987 through 2001. The Snow Telemetry (SNOTEL) sites, denoted by a numeric prefix, were located in the higher elevation areas, and they had a significantly higher average annual precipitation (950.0 mm or 37.4 in) as well as a higher average number of days (140

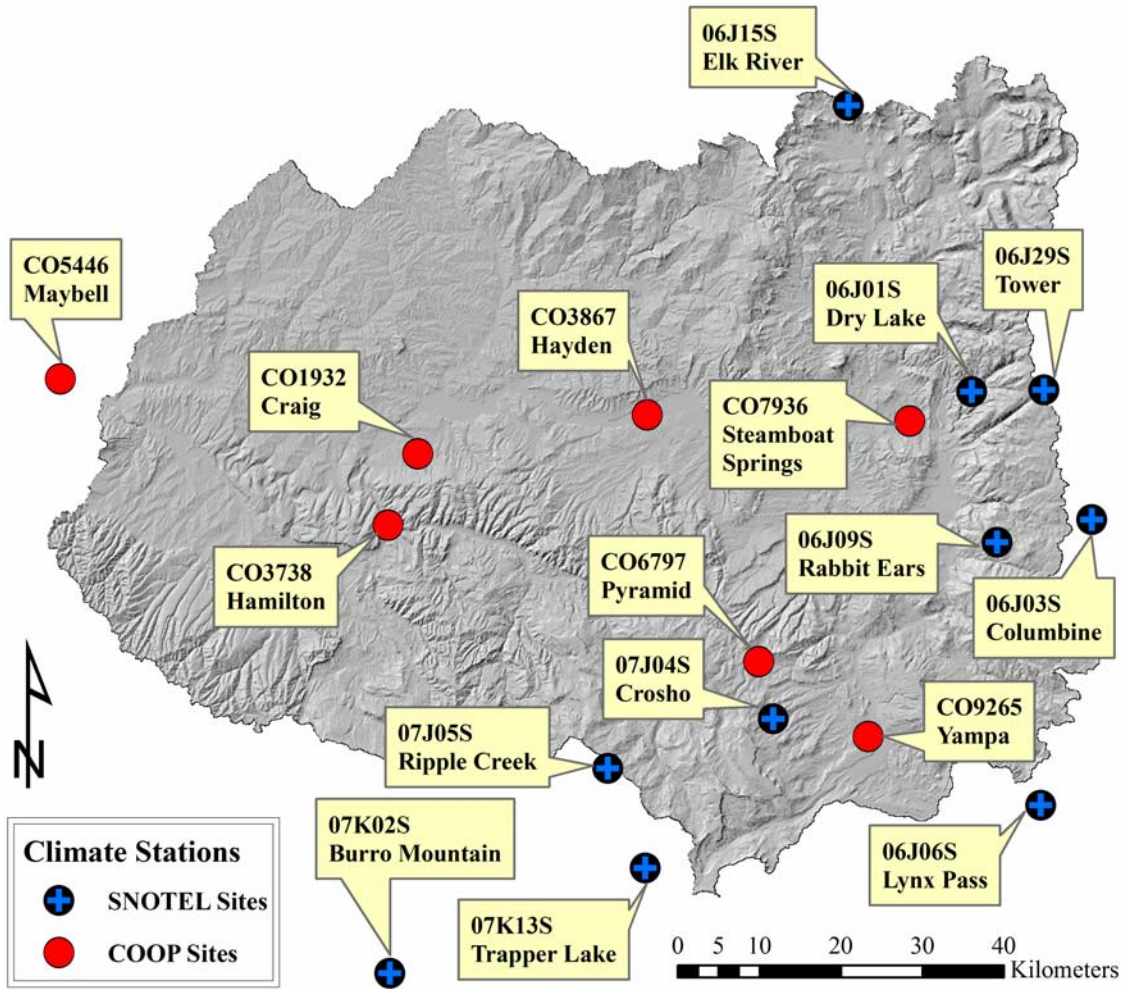


Figure 4.3. Locations of the meteorological stations used to populate the data file. The SNOTEL stations are located in the higher elevation areas while the COOP stations are more prevalent in the lowlands.

days) that observed precipitation (140) than the Cooperative Observer Program (COOP) stations. The COOP stations, denoted by a CO- prefix, are mostly located in the arid lowlands of the basin, so a lower average annual precipitation (475.0 mm or 18.7 in) and a lower average number of days (100 days) of observed precipitation is expected. Since there was a sharp change in land cover and climate between the arid portion and the mountainous portion, the Thiessen polygons were found to be a simple method to distribute climate data over the basin while retaining the climate contrast between the arid

Table 4.5. The average annual precipitation and the average number of days that precipitation was observed for each station for water years 1987 through 2001.

	Average Days Per Year Observing Precipitation	Average Annual Precipitation (mm)
Dry Lake (06J01S)	131	954
Columbine (06J03S)	140	939
Lynx Pass (06J06S)	114	594
Rabbit Ears (06J09S)	147	1168
Elk River (06J15S)	136	796
Tower (06J29S)	161	1451
Croscho (07J04S)	134	712
Ripple Creek (07J05S)	151	1046
Trapper Lake (07K13S)	142	885
Craig (CO1932)	106	461
Hamilton (CO3738)	70	469
Hayden (CO3867)	113	441
Maybell (CO5446)	71	309
Pyramid (CO6797)	94	557
Steamboat Springs (CO7936)	129	639
Yampa (CO9265)	117	460

and mountainous, more temperate, terrain. For example, a station in the arid portion of the basin tended to distribute temperature and precipitation data mostly within the surrounding arid terrain, and a station in the mountainous portion tended to distribute temperature and precipitation data mostly within its surrounding mountainous terrain.

Figure 4.4 is a map showing the Thiessen polygons generated for the precipitation stations where the larger polygons encompass a relatively homogenous area while the smaller polygons encompass a relatively heterogeneous area with respect to land cover.

Figure 4.5 is a map showing the Thiessen polygons generated for the temperature stations where the same trend as for the precipitation stations is observed with respect to a large polygon size and homogeneous land cover.

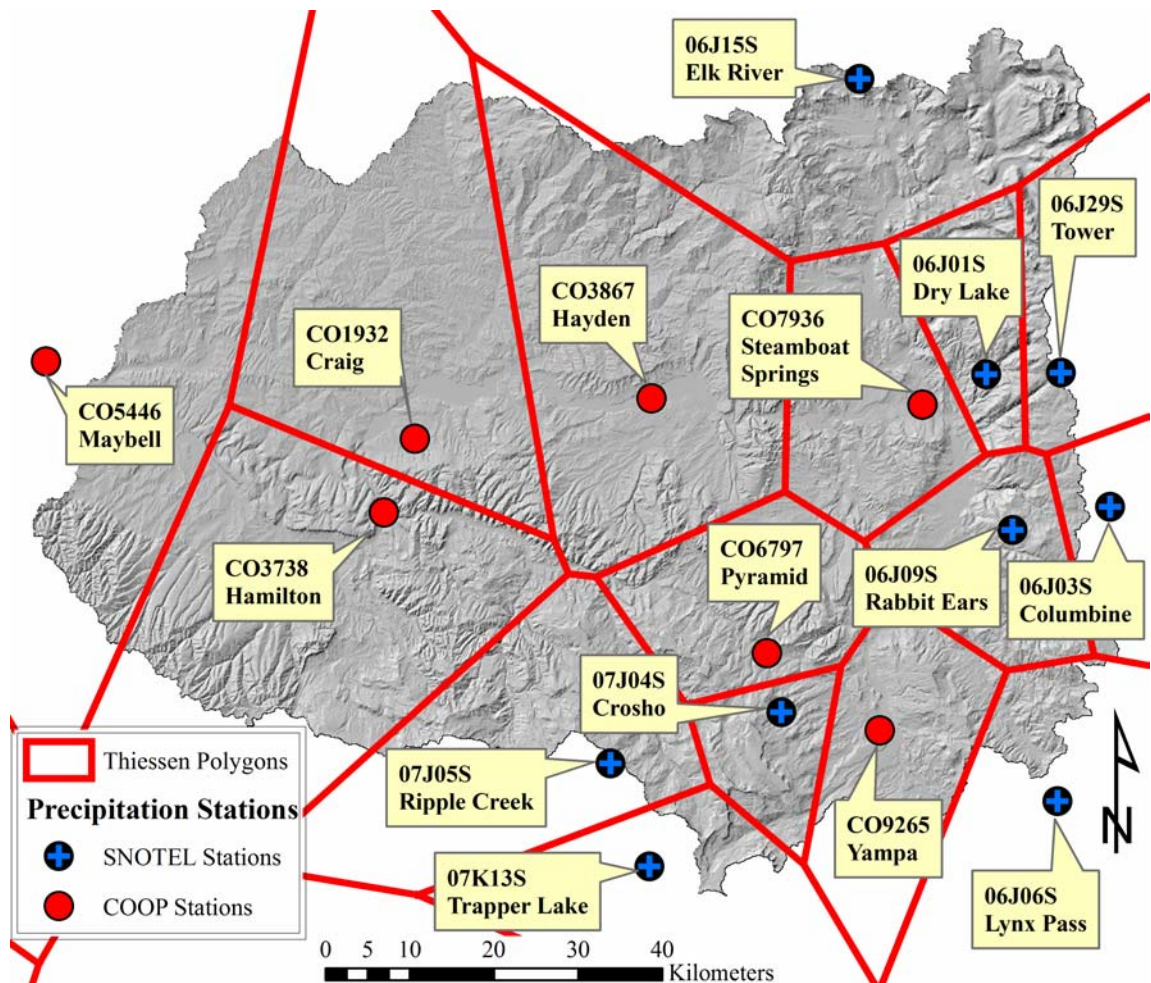


Figure 4.4. Thiessen polygons generated for the precipitation stations where the larger polygons encompass a relatively homogenous area while the smaller polygons encompass a relatively heterogenous area with respect to land cover.

Although Thiessen polygons were used in this study, presently the standard distribution method for the climate variables is the XYZ method (Hay et al., 2000; Leavesley et al., 2002; Hay et al, 2002). This method spatially distributes the climate variables using multiple linear regressions (MLRs) where the independent variables are latitude (x), longitude (y), and elevation (z), and the dependent variable is the climate variable (precipitation, maximum and minimum temperature) (Hay et al., 2002).

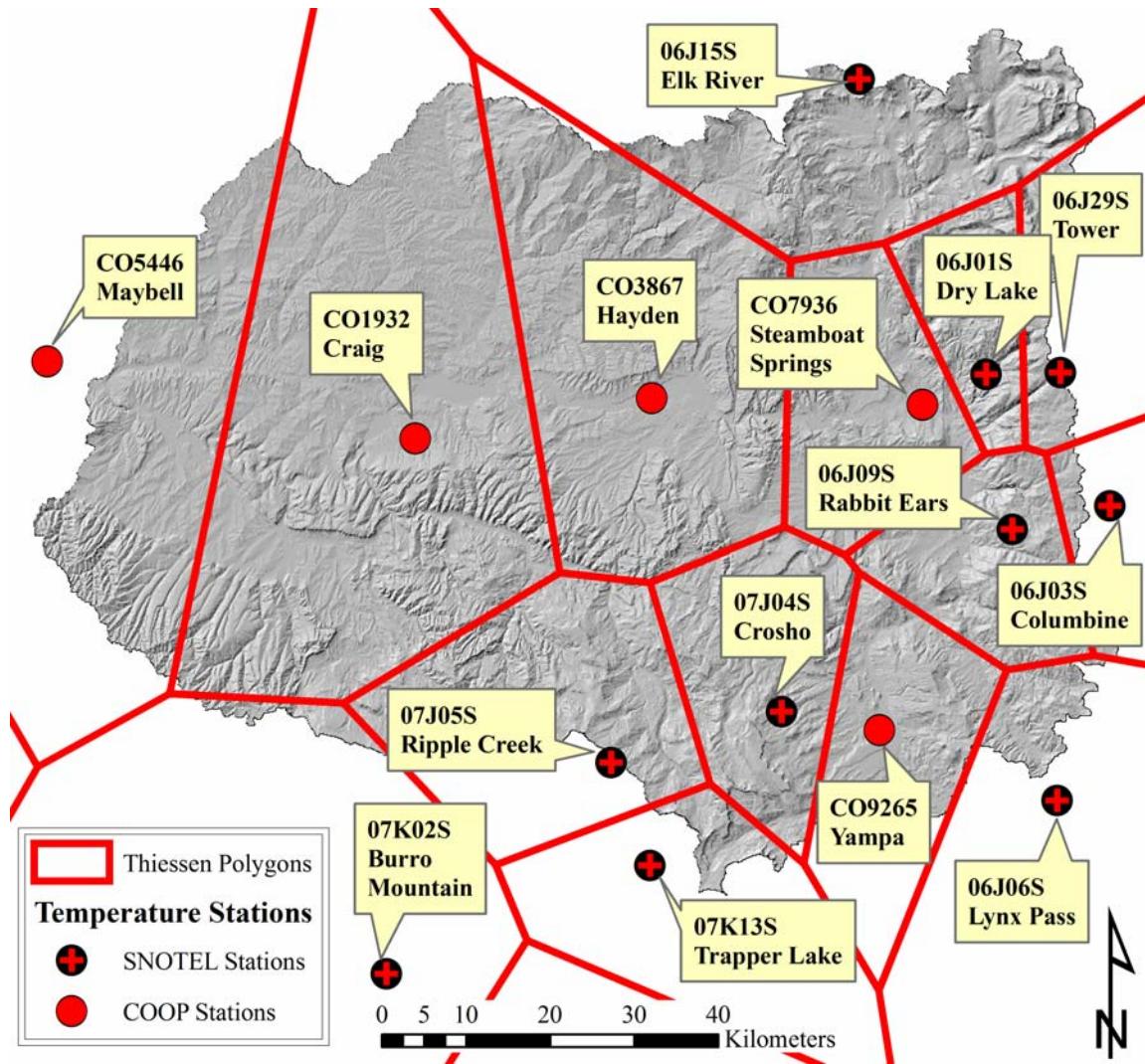


Figure 4.5. Thiessen polygons generated for the temperature stations where the same trend as for the precipitation stations is observed with respect to a large polygon size and homogeneous land cover.

Typically three stations are used to determine the occurrence of precipitation and three stations (can be the same, others, or a combination thereof) are used to determine precipitation amounts. The first criterion is useful for small watershed where the occurrence of precipitation is across the entire basin. However for the Yampa River, since the large basin exhibits a sharp contrast in climate with twice the precipitation in the mountainous regions and precipitation occurring 40% more often than in the lower

lying regions, the Thiessen polygon method was deemed to be more appropriate than the XYZ method.

After each HRU was assigned a climate station using the Thiessen polygon method, several steps were necessary to prepare the data for use in PRMS since the model did not directly handle missing data values.

IV.iv.i.iii.i. Preparing the Precipitation Data

The precipitation data contained daily precipitation amounts recorded at nine SNOTEL stations and eight COOP stations. The first step was to identify the missing data values which were represented as -99.9 in the uncorrected data file. The second step was to fill in values where it was probable that no precipitation had occurred. If all other stations did not observe precipitation on the day in question, then it was probable that the station with missing data also did not observe precipitation on that day. If all other stations did not observe precipitation except only one SNOTEL station, then it was also probable that the COOP stations with missing data also had no precipitation. These two assumptions were made since the average precipitation for the SNOTEL sites was approximately twice as much more than for the COOP sites. The final step was to examine the stations that had remaining missing values, and to fill in the missing data values with a linear regression. The three nearby stations with the highest correlation were used as the independent variables in the regression.

IV.iv.i.iii.ii. Preparing the Temperature Data

The temperature data contain daily maximum and minimum temperature values recorded at 10 SNOTEL stations and five COOP stations. The first step was to identify missing or erroneous data values. Missing data values were represented as -99.9 and were marked for correction. Data values were flagged as erroneous if they were below -40 °F or greater than 100 °F. Data values were also flagged as erroneous if T_{\max} was less than T_{\min} for any given day.

The next step was to replace the missing or erroneous values using a monthly average for the station (Leavesly, personal communication, 2005). If T_{\max} was less than T_{\min} , both values were corrected for that date using a monthly average. In cases where a month had less than three viable values for interpolation, a different method was used. When a month had nearly all erroneous or missing values, a linear regression was used to fill in the data values. All other stations were used as independent variables for the regression as long as they were not missing the same months of data as the dependent variable.

CHAPTER V: RESULTS

V.i. MODELED VEGETATION MAP

V.i.i. BINARY REGRESSION RESULTS FOR THE LANDSAT-DERIVED LAND COVER MAP

For the binary regression procedure, it was found that the overall classification accuracy could be increased by running hierarchical regressions rather than simply a single regression. Table 5.1 shows the classification accuracy results when running a single regression versus running hierarchical regressions where the independent variables were Landsat bands 1 through 6 and 8, MODIS bands 1-7, aspect, slope, elevation, and forest density.

Table 5.1. The classification accuracy results when running a single regression versus running multiple regressions.

Land Class	Multiple Regressions (%)	Single Regression (%)	Difference (%)
Coniferous Forest	95.1	87.8	7.3
Deciduous Forest	95.2	100.0	-4.8
Shrubland	86.7	81.7	5
Grassland / Herbaceous	89.7	88.2	1.5
Agricultural Land	86.2	83.1	3.1
Barren or Sparsely Vegetated	93.4	80.3	13.1
Overall Accuracy	91.0	86.8	4.2

In all cases with the exception of the deciduous class, the classification accuracy was increased by running hierarchical regressions rather than a single regression.

two coniferous forest points should have been classified as deciduous forest points, and three deciduous forest points should have been classified as coniferous forest points.

Figure 5.2 shows the regression tree used to develop the decision rules for the coniferous forest and the deciduous forest land classes.

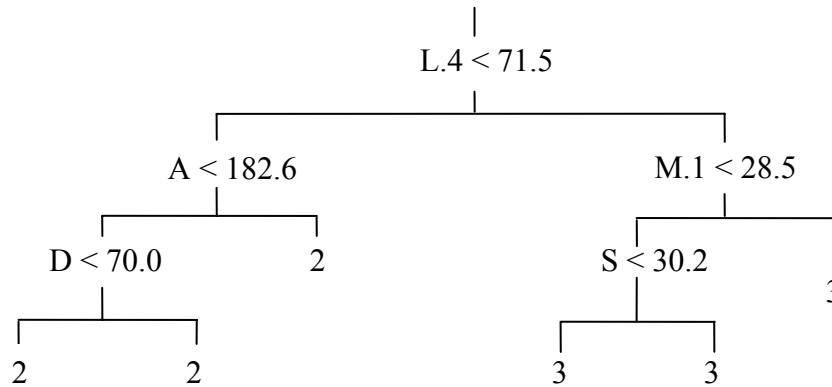


Figure 5.2. Regression tree used to develop the decision rules for the coniferous forest and the deciduous forest land classes. The number 2 represents the coniferous forest land class, and the number 3 represents the deciduous forest land class. Although only Landsat Band 4 is required to classify coniferous and deciduous classes, the additional discriminant variables show the other important factors for determining these land classes in this particular case. L.x represents Landsat band x, M.x represents MODIS band x, S represents slope, A represents aspect, and D represents canopy density.

The decision rules were then applied to only the forested pixels of the binary map created in the initial regression using ARGINFO 9.0 (ESRI, 2004). The important discriminating variables for classifying the forest classes were Landsat band 4, MODIS band 1, slope, aspect, and elevation.

The final regression was run using only the sample points representing non-forested areas, which included 254 points. Figure 5.3 shows the regression tree used to develop the decision rules for the shrubland (5), grassland or herbaceous (6), agricultural (7), and barren or sparsely vegetated (8) land classes. The discriminating variables for classifying the non-forest categories were elevation, slope, aspect, canopy density,

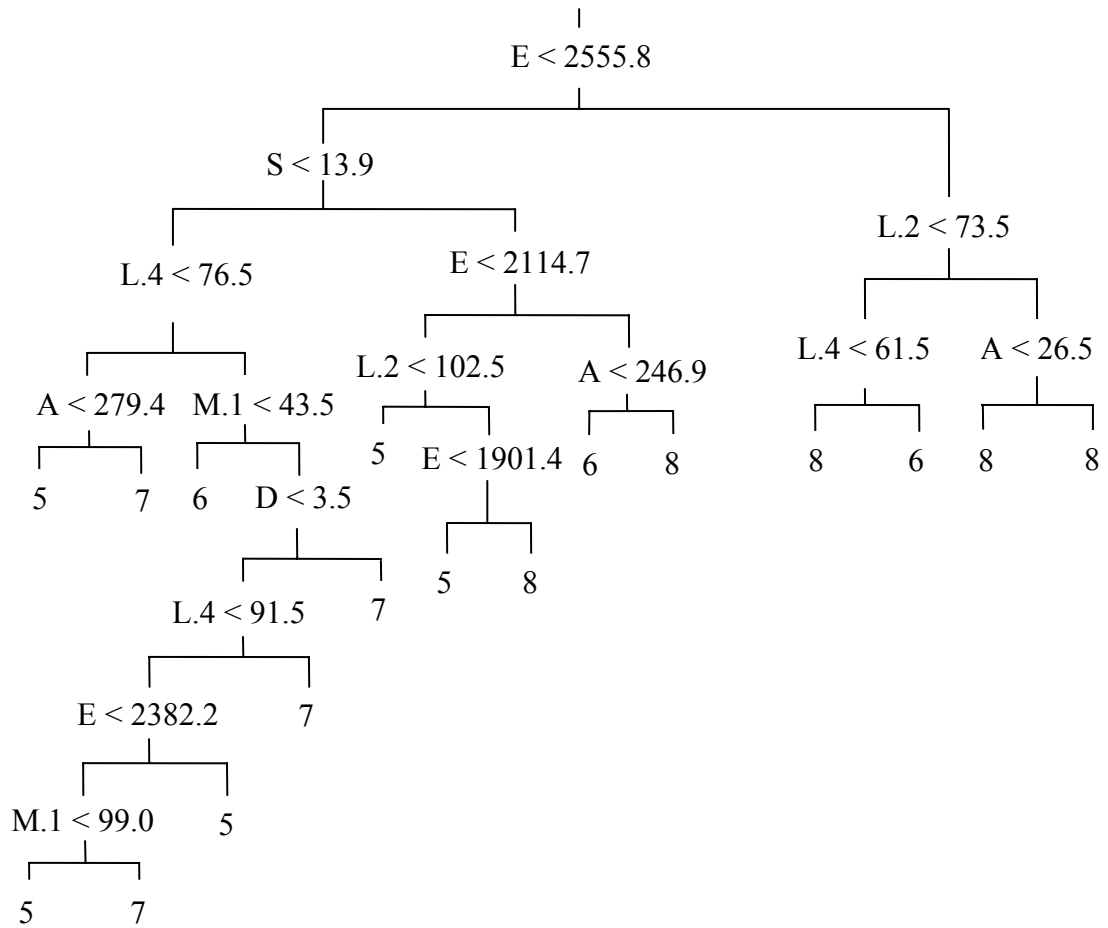


Figure 5.3. Regression tree used to develop the decision rules for the shrubland (5), grassland or herbaceous (6), agricultural (7), and barren or sparsely vegetated (8) land classes. L.x represents Landsat band x, M.x represents MODIS band x, E represents elevation, D represents canopy density, A represents aspect, and S represents slope.

MODIS band 1, and Landsat bands 2 and 4. The decision rules were then applied to only the non-forested pixels of the binary map created in the initial regression using ArcINFO[®] 9.0 (ESRI[®], 2004). The overall classification accuracy was 89.4%, and Table 5.2 shows the classification error matrix where the sample points are the reference data. The error matrix showed no significant classification outliers, so all classes had a similar performance with respect to classification accuracy.

Table 5.2. Classification error matrix where the sample points are the reference data. The columns represent the reference data, and the rows represent the classified data. The highlighted major diagonal shows the points that were correctly classified. In this case, both Landsat imagery and MODIS imagery were available as discriminating variables.

Classified Data	Reference Data			
	Shrub-land	Grassland/Herbaceous	Agricultural Land	Barren/Sparsely Vegetated
Shrubland	52	3	2	3
Grassland/Herbaceous	2	61	3	2
Agricultural Land	5	1	56	3
Barren/Sparsely Vegetated	2	0	2	57

V.i.ii. BINARY REGRESSION RESULTS FOR THE MODIS-DERIVED LAND COVER MAP

Since the Landsat imagery was the primary discriminating variable for the regressions, a small area of the map was unclassified due to a stretch of cloud cover on the imagery that obscured the spectral signatures of the land surface. Although the unclassified area was only 0.42% (37 km²) of the total area of the basin, the area was very distinct within the map. In order to remove this unclassified area, the three regressions described previously were rerun without the Landsat imagery. The intent was for the MODIS bands to replace the Landsat bands as the primary discriminating variables, hence the area of cloud cover was absent in the new regression. The new map was then applied to the unclassified portion of the MVM to have a land cover map that was 100% classified. Figure 5.4 shows a map highlighting the original unclassified area while showing the effect of under-laying the MODIS-derived land cover map. Appendix A shows the classification regression trees used to develop the decision rules for the MODIS-derived land cover map.

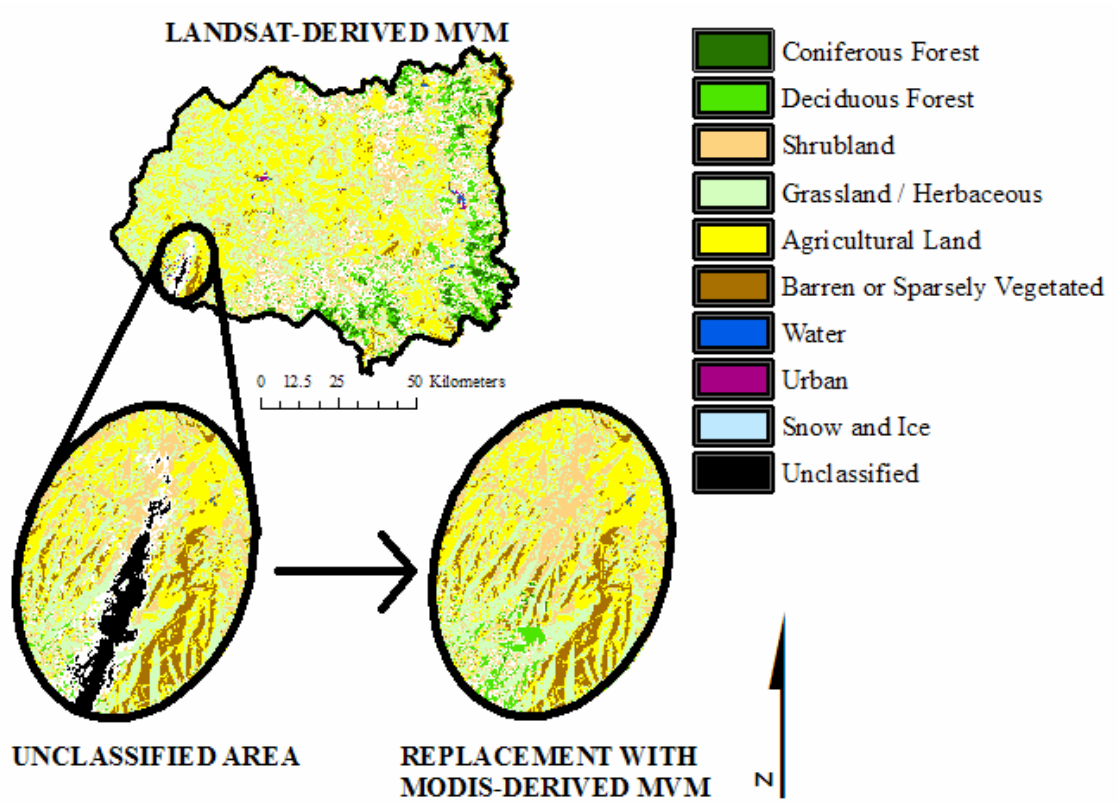


Figure 5.4. Map highlighting the original unclassified area while showing the effect of under-laying the MODIS-derived land cover map.

When the Landsat data were removed for the regressions, it was expected that the classification accuracy would be reduced. This expectation was based on the finer resolution of the Landsat data (30-m) compared to the MODIS data (1-km resampled to 30-m), as well as the observation that the Landsat data were the primary discriminating variables in the original regressions. Figure 5.5 shows the classification accuracy for each class using only the MODIS data compared to the classification accuracy for each class using both Landsat and MODIS data. In each case, canopy density, elevation, slope, and aspect were also used as discriminating variables. As expected, using both data sources resulted in overall higher classification accuracy than using the MODIS data

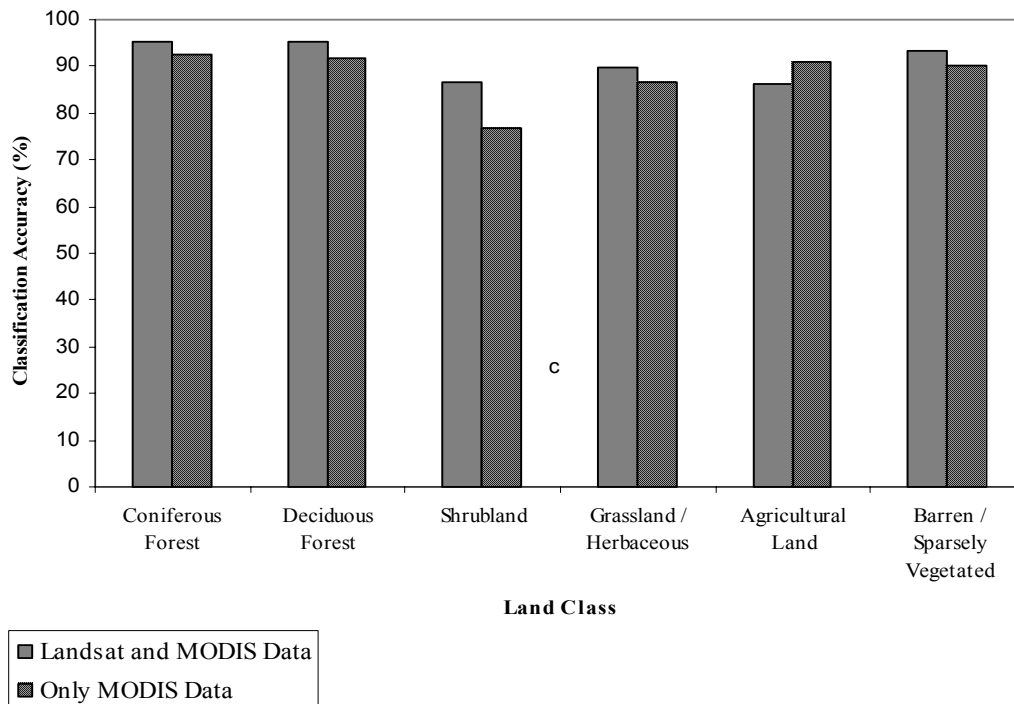


Figure 5.5. Classification accuracy for each class using only the MODIS data compared to the classification accuracy for each class using both Landsat and MODIS data. In each case, canopy density, elevation, slope, and aspect were also used as discriminating variables.

alone. Each land class had higher classification accuracy when using both imagery sources with the exception of the agricultural land class.

The overall accuracy for the binary forest/non-forest classification was 92.6% using 635 points where 27 points were misclassified as non-forest, and 20 points were misclassified as forest. The overall accuracy for the forest classification was 92.2%, which was only slightly lower than the binary forest/non-forest map. Out of a possible 103 points, three deciduous forest points were misclassified as coniferous forest, and five coniferous forest points were misclassified as deciduous forest. The overall accuracy for the non-forest classification was 86.2%, which was significantly lower than the forest/non-forest classification and the forest classification. Table 5.3 shows the error

matrix for the MODIS-derived classification where the sample points are the reference data and the total sample size is 254.

Table 5.3. Error matrix for the MODIS-derived classification where the sample points are the reference data and the total sample size is 254. The columns represent the reference data, and the rows represent the classified data. The highlighted major diagonal shows the points that were correctly classified.

Classified Data	Reference Data			
	Shrub-land	Grassland/Herbaceous	Agricultural Land	Barren/Sparsely Vegetated
Shrubland	46	3	8	3
Grassland/Herbaceous	3	59	1	5
Agricultural Land	4	1	59	1
Barren/Sparsely Vegetated	2	2	2	55

Again the error matrix showed no significant classification outliers, so all classes had a similar performance with respect to classification accuracy.

V.ii. COMPARISON RESULTS FOR THE DIGITAL LAND COVER MAPS

V.ii.i. DATA CROSS-WALK

Data “cross-walking” refers to reclassifying map categories to coincide with another map’s categories so they both share a common classification scheme. In practice, the aggregation of the original land cover categories to the lowest common classification scheme was a process that was somewhat subjective. The large number of classification schemes that needed to be condensed into one common scheme resulted in a high degree of aggregation for some maps, and a low degree of aggregation in others. Appendix B shows the results of cross-walking the land cover data sets to a common classification scheme.

In order to make the aggregation process as objective as possible, convention was followed from aggregations done by others in the past. For example, the woody savanna land class was consistently placed in the mixed forest land category as it had been done by Pietroniro and Soulis (2001), and the juniper woodland class was placed in the shrubland class as per Theobald et al. (2004).

When available, class definitions were also used to determine where to place the land classes in the aggregated classification scheme. Since the Anderson et al. (1976) Land Use Land Cover classification system outlined the definitions of the land classes in the greatest detail, this was the primary reference for determining which land class to place the sample points that could be placed into more than one class. The LULC classification system was also used to classify field points used in the MVM that could have been placed into more than one category. For example, there were many field points that could have been classified as either shrubland or barren or sparsely vegetated. However, the LULC classification system defines barren land in which less than one-third of the area has vegetation cover. This definition was used as the discriminating factor for classifying the sample point as either shrubland or barren or sparsely vegetated. The field photographs proved to be an invaluable tool for referencing these sample points.

The data cross-walk to the lowest common classification scheme and the USFS/USGS composite classification scheme affected the species resolution of the land cover maps to varying degrees. Figure 5.6 illustrates the effect of cross-walking the land cover classes with respect to the species resolution of the different land cover maps. The average reduction in species resolution was seven land classes after cross-walk to the

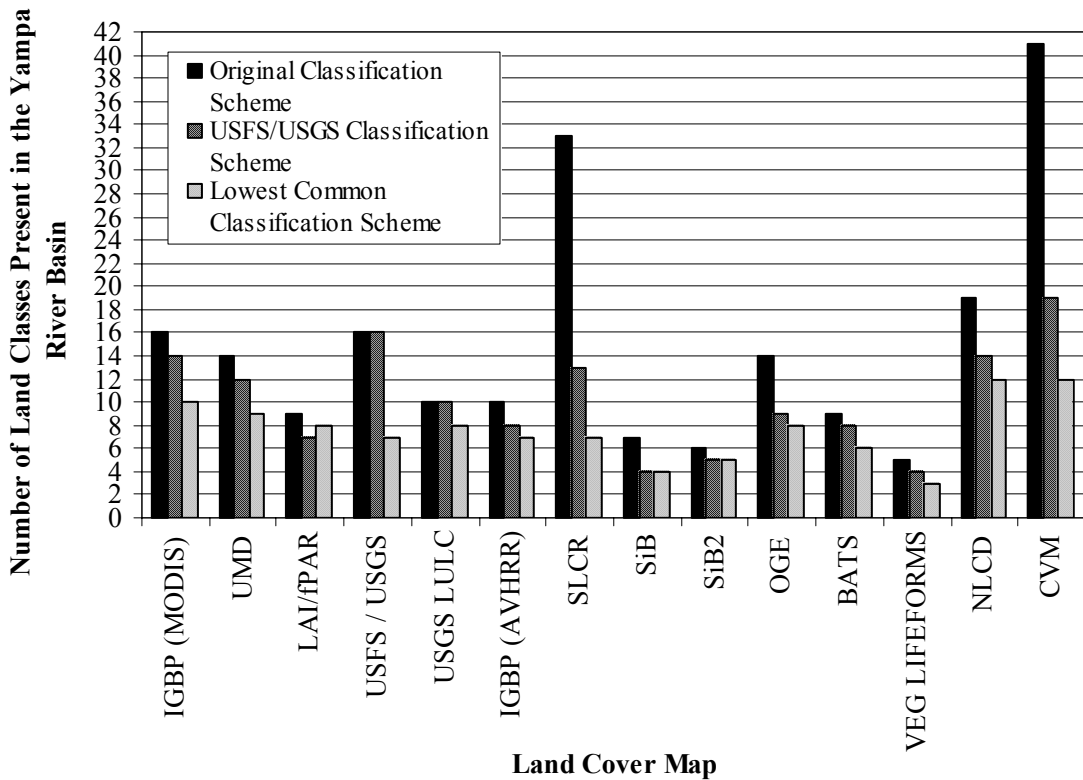


Figure 5.6. The effect of cross-walking the land cover classes with respect to the species resolution of the different land cover maps.

lowest classification scheme, and was five classes after cross-walk to the USFS/USGS composite classification scheme. The maximum reduction in resolution was observed in the CVM where 29 classes were lost after cross-walk to the lowest common classification scheme, and 22 classes were lost after cross-walk to the USFS/USGS composite classification scheme. The SLCR also had a dramatic loss in resolution where 26 classes were lost after cross-walk to the lowest common classification scheme, and 20 classes were lost after cross-walk to the USFS/USGS composite classification scheme. The other maps all lost less than 10 classes for the two cross-walk schemes, so there was not such a steep reduction in species resolution as in the CVM and the SLCR. The minimum number of classes lost from both the cross-walk to the lowest common classification

scheme and the USFS/USGS composite classification scheme was one. The SiB2 map had the lowest overall reduction in species resolution where one class was lost after cross-walk to the lowest common classification scheme, and one class was lost after cross-walk to the USFS/USGS composite classification scheme.

V.ii.ii. AGGREGATED LAND CLASS PERCENTAGES

The first comparison was a qualitative examination of the effect of aggregating the land classes through the data cross-walk procedure. Table 5.4 shows the percentage of pixels assigned to each land cover category for the different land cover data sets after cross-walk to the lowest common classification scheme. Overall the land cover maps had a larger percentage of forested pixels than the MVM. The CVM and NLCD maps showed nearly identical results, which is expected since the CVM was developed by dividing existing NLCD land classes into several more land categories. The SiB and SiB2 maps also yield nearly identical results, which is expected since the SiB and SiB2 classification schemes have only minor differences from one another - SiB2 has a grassland/herbaceous land class, and SiB has a more diverse shrubland class. The UMD and IGBP MODIS maps also yield similar aggregation results. Both are based on the same MODIS imagery, and the UMD is simply a modified IGBP classification scheme where the permanent wetlands, cropland/natural vegetation mosaic, and snow and ice land classes were removed (Hodges, 2002).

Table 5.5 shows the percentage of pixels assigned to each land cover category for the different land cover data sets after being cross-walked to the USFS/USGS composite classification scheme which is used to determine the parameters for the PRMS model.

Table 5.4. The percentage of pixels assigned to each land cover category for the different land cover datasets after cross-walk to the lowest common classification scheme.

Land Category	CVM	NLCD	LAI/ fPAR	UMD	IGBP - MODIS	IGBP - AVHRR	OGE	SiB	SiB2	SLCR	USGS LULC	USFS/ USGS	BATS	RUN	MVM	
1 Mixed forest	2.2	2.6	30.5	12.7	12.7	2.3	1.8			16.8	0.2	< 0.1				
2 Coniferous forest	29.7	29.6		17.2	17.2	21.9	22.1	22.	1	22.1	22.3	22.0	14.5	22.1	30.1	12.6
3 Deciduous forest	23.7	24.4		10.4	10.4	34.0	34.1	34.	7	34.7	19.3	34.9	37.8	34.7	48.4	18.3
4 Transitional forest	0.2	0.2														
5 Shrubs	21.4	19.8	14.2	14.2	14.2	19.4	19.8	41.	1	40.0	19.8	19.8	27.5	12.6		19.7
6 Grassland	14.2	14.9	10.3	42.3	42.3	20.2	20.6			1.1	20.1	21.5	19.2			20.5
7 Cropland and Pasture	7.7	7.5	44.6	2.8	2.8	2.1	1.4	2.1	2.1	1.8	1.5	0.9	21.5	21.5	19.2	
8 Barren or sparsely vegetated	0.4	0.5	< 0.1	< 0.1	< 0.1									6.9		9.0
9 Water	0.3	0.3	0.3	0.3	0.3											0.4
10 Wetlands	< 0.1	< 0.1			0.1											
11 Urban	0.1	0.2	0.1	0.1	0.1	0.1	0.1				0.1	0.1				0.3
12 Ice and snow	< 0.1	< 0.1														< 0.1
13 Forest / Field Mosaic							0.7				0.7		2.2			
255 Unclassified			< 0.1													

Table 5.5. The percentage of pixels assigned to each land cover category for the different land cover datasets after cross-walk to the USFS/USGS composite classification scheme used to determine the parameters for the PRMS model.

Land Category	CVM	NLCD	LAI / fPAR	UMD	IGBP - MODIS	IGBP - AVHRR	OGE	SiB	SiB2	SLC R	USFS / USGS	BATS	RUN	MVM
1 White-red-jack pine														
2 Spruce-fir	7.8									0.2				
3 Longleaf-slash pine														
4 Loblolly-shortleaf pine														
5 Oak-pine										12.3				
6 Oak-hickory														
7 Oak-gum-cypress														
8 Elm-ash-cottonwood														
9 Maple-beech-birch														
10 Aspen-birch	0.1													
11 Douglas-fir														
12 Hemlock-sitka spruce														
13 Ponderosa pine	1.0									7.0				
14 Western white pine											3.4			
15 Lodgepole pine	11.1													
16 Larch											8.0			
17 Fir-spruce											4.1			
18 Redwood														
19 Chaparral														
20 Pinyon-juniper	2.0									0.2	12.5			
21 Western hardwoods											3.5			
22 Aspen-birch	23.3									19.2	6.0			
101 Urban or built-up land	0.1	0.2	0.1	0.1	0.1	0.1	0.1				< 0.1			0.3
102 Dryland cropland and pasture	4.0	4.0									< 0.1			
103 Irrigated cropland and pasture	< 0.1	< 0.1					1.4			1.4	0.9	1.4		

104	Mixed dryland / irrigated cropland and pasture	3.6	3.5		2.8	2.7	1.4	< 0.1				< 0.1	21.8	19.2
105	Cropland / grassland mosaic			44.6					2.1	2.1	0.4			
106	Cropland/woodland mosaic					0.1	0.7	0.7			0.7	0.4	2.1	
107	Grassland	14.2			41.8	41.8	20.2				15.6	12.6	20.4	20.5
108	Shrubland	21.4	19.8	14.2	14.2	14.2	19.4	19.6	41.1	40.0		12.3	12.6	19.7
109	Mixed shrubland/grassland		14.9					20.2		1.1	11.5			
110	Chaparral													
111	Savanna			10.3	0.5	0.5						0.7		
112	Broadleaf deciduous forest	0.4	24.4		10.1	10.1	34.0	34.0	34.7	34.7		21.6	34.7	48.2
113	Evergreen coniferous forest	7.7	29.6		17.1	17.1	21.9	22.1	22.1	22.1	14.7	13.7	21.7	22.9
114	Subalpine forest										0.2			
115	Mixed forest	2.2	2.6	30.5	12.7	12.7	2.3	1.8			16.6	0.1		
116	Deciduous coniferous forest				0.2	0.2								
117	Evergreen broadleaf forest				<0.1	<0.1							7.1	
118	Water bodies	0.3	0.3	0.3	0.3	0.3								0.4
119	Herbaceous wetland	< 0.1	< 0.1			0.1								
120	Forested wetland	< 0.1	< 0.1											
121	Barren or sparsely vegetated	0.7	0.7	<0.1	<0.1	<0.1						7.1		9.0
122	Wooded tundra													
123	Herbaceous tundra													
124	Bare ground tundra													
125	Wet tundra													
126	Mixed tundra													
127	Perennial snowfields or glaciers	< 0.1	< 0.1											< 0.1

V.ii.iii. SCENE ACCURACY

Scene accuracy is presented as the percent of the land cover map that is correctly classified, irrespective of location, and is computed using only those classes present in the reference map, or the MVM. Table 5.6 summarizes the scene accuracy computed for each land cover map using the MVM as the reference map.

Table 5.6. Scene accuracy computed for each land cover map using the MVM as the reference map.

Land Cover Map	Scene Accuracy (%)
NLCD	73.9
CVM	73.3
IGBP (AVHRR)	72.7
OGE	72.5
USGS LULC	72.5
SLCR	72.2
USFS / USGS	70.7
BATS	69.6
UMD	60.9
IGBP (MODIS)	60.9
SIB2	53.8
SIB	52.7
VEGETATION LIFEFORMS	50.1
LAI/FPAR	44.1

The NLCD map had the highest scene accuracy compared to the MVM. However, the CVM map differed from the NLCD map by only 0.6%. Overall, the AVHRR-derived land cover maps had a higher scene accuracy than the MODIS-derived land cover maps. For example, the IGBP map derived from AVHRR imagery yielded a scene accuracy of 72.7%, while the IGBP map derived from MODIS imagery yielded a scene accuracy of 60.9%. Also, the USFS/USGS composite map had a slightly lower scene accuracy than the USGS LULC map alone.

Figure 5.7 shows histograms comparing the percentage of each land class present in the Yampa River Basin for each land cover map to the percentage present when using the MVM.

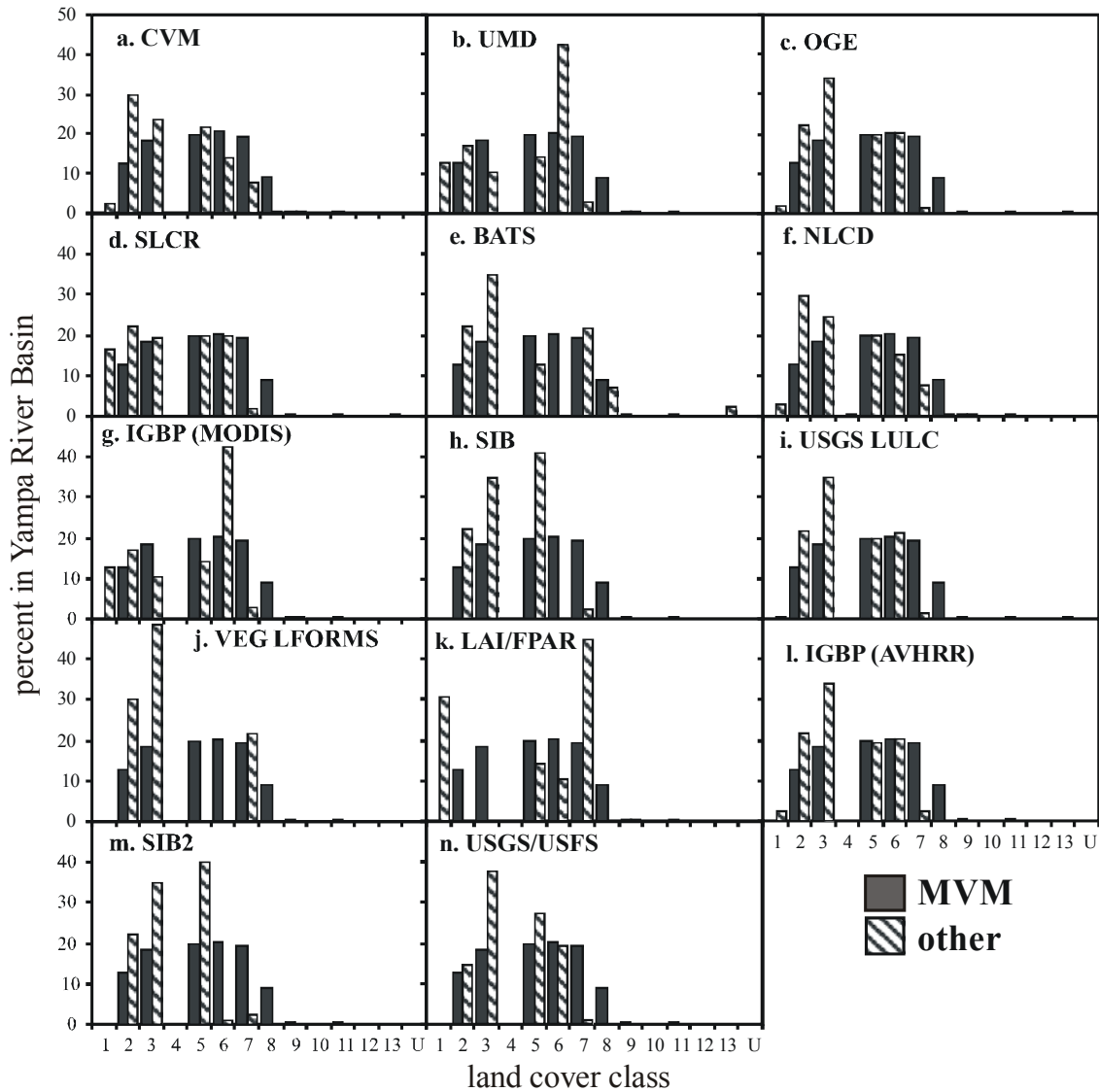


Figure 5.7. Histograms comparing the percentage of each land class present in the Yampa River Basin for each land cover map to the percentage present when using the MVM. The land cover classes are as follows: 1 = Mixed forest, 2 = Coniferous forest, 3 = Deciduous forest, 4 = Transitional forest, 5 = Shrubs, 6 = Grassland, 7 = Cropland and Pasture, 8 = Barren or sparsely vegetated, 9 = Water, 10 = Wetlands, 11 = Urban, 12 = Ice and snow, 13 = Forest / Field Mosaic, U = Unclassified.

The histograms help to explain the scene accuracy results because they show where too many pixels were allocated to a particular class, or conversely where not enough pixels were allocated to a particular class. For example, the LAI/fPAR map received the lowest rank with respect to scene accuracy, and this can be partially explained by the observation that too many pixels were assigned to the agricultural land class. In addition, all the forested pixels were assigned to the mixed forest class rather than to either the coniferous or deciduous class, and the mixed forest class is not represented in the MVM. Although the overall scene accuracy was often higher for the AVHRR-derived land cover maps, the histograms show that the MODIS-derived land cover maps had a closer forest to non-forest ratio to that observed in the MVM.

V.ii.iv. PIXEL ACCURACY

Pixel accuracy was assessed through the construction of error matrices, and like scene accuracy was only assessed for those classes present in the MVM. Appendix D provides the raw error matrices for each land cover map using the MVM for the reference points. The raw error matrices can be examined to identify the errors of inclusion and the errors of exclusion. Table 5.7 provides a summary of the producer's accuracy, user's accuracy, and overall accuracy for each of the land cover maps. For the coniferous category, the producer's accuracy was equal to or higher than the user's accuracy for all maps with a coniferous forest category. In other words, a larger proportion of the classification errors could be attributed to pixels being assigned to the incorrect category (errors of inclusion) rather than pixels being omitted from the correct category (errors of exclusion) according to the reference data. For the urban, water, barren/sparsely

Table 5.7. Summary of the producer's accuracy, user's accuracy, and overall accuracy for each of the land cover maps.

		Coniferous forest	Deciduous forest	Shrubland	Grassland / herbaceous	Cropland and Pasture	Barren / sparsely vegetated	Water	Urban	Snow and Ice	Overall Accuracy
VEG LFORMS	Producer's Accuracy	54.2	74.1	-	-	41	-	-	-	-	56.4
	User's Accuracy	45.9	50.6	-	-	93.2	-	-	-	-	
SIB	Producer's Accuracy	50.2	48.2	70.8	-	2.7	-	-	-	-	42.4
	User's Accuracy	48.3	40	41.9	-	35.1	-	-	-	-	
CVM	Producer's Accuracy	83.1	72.7	45.9	17.5	23.3	3	51.8	38	5.1	41.1
	User's Accuracy	34.1	52.3	42	24.8	58	58.7	69.5	79.4	52.4	
NLCD	Producer's Accuracy	81.6	74.9	44.1	18	22.7	3	51.4	43	5.7	40.8
	User's Accuracy	33.3	51.6	43.7	24.3	57.7	56.9	68.7	57.4	52.4	
SIB2	Producer's Accuracy	50.2	48.2	70.8	1.2	2.7	-	-	-	-	33
	User's Accuracy	33	28.1	37.7	28.1	27.3	-	-	-	-	
LAI/fPAR	Producer's Accuracy	-	-	8.5	21	78.5	< 0.1	10.6	18.4	-	32.1
	User's Accuracy	-	-	17.7	40.1	34.1	5.2	14.9	29.1	-	
BATS	Producer's Accuracy	55.3	47.7	1.3	-	41.1	6.2	-	-	-	30.8
	User's Accuracy	40.2	34.4	2.7	-	40.1	7.7	-	-	-	
SLCR	Producer's Accuracy	56.2	42.1	28.9	8.1	3.9	-	-	-	-	26.2
	User's Accuracy	32.9	38.6	25.5	7.2	35.6	-	-	-	-	
OGE	Producer's Accuracy	54.6	48.1	23.9	7.5	2.7	-	-	7.9	-	24.5
	User's Accuracy	32.9	28	25.5	7.9	40.3	-	-	26	-	
USGS LULC	Producer's Accuracy	51.5	48.3	23.8	8.3	2.7	-	-	3.6	-	24.4
	User's Accuracy	33	27.9	25.5	8.6	39.9	-	-	11.8	-	
IGBP (AVHRR)	Producer's Accuracy	53.1	47.9	23.3	7.1	2.7	-	-	3.6	-	24.1
	User's Accuracy	33	27.9	25.1	7.6	27.3	-	-	11.8	-	
IGBP (MODIS)	Producer's Accuracy	66.8	25.2	8.5	32.5	3.4	< 0.1	8.6	13.3	-	21.7
	User's Accuracy	42.7	36.5	11.2	13.2	20.9	5.2	11.3	29.1	-	
UMD	Producer's Accuracy	66.8	25.2	8.5	32.5	3.4	< 0.1	8.6	13.3	-	21.7
	User's Accuracy	42.7	36.5	11.2	13.2	20.8	5.2	11.3	29.1	-	
USFS / USGS	Producer's Accuracy	35.6	45.4	26.6	5.9	2	-	-	3.4	-	21.6
	User's Accuracy	35.6	24.1	21	6.8	46.6	-	-	11.5	52.4	

vegetated, and snow and ice classes, the user's accuracy was higher than the producer's accuracy for all maps. In this case, a larger proportion of the classification errors could be attributed to pixels being omitted from the correct category rather than pixels being assigned to the incorrect category according to the reference data.

For this study, the results for the producer's and user's accuracy correlated well with the histograms calculated for the scene accuracy (Figure 5.7). When the histograms showed that too many pixels were assigned to a category, the producer's accuracy was higher than the user's accuracy. When the histograms showed that not enough pixels were assigned to a category, then the user's accuracy was higher than the producer's accuracy. The histograms are insensitive to pixel location, while the producer's and user's accuracy are sensitive to pixel location. As a result of this difference, the histograms could only indicate a lower probability of an omission error when too many pixels were assigned to a category, and a higher probability of an omission error when not enough pixels were assigned to a category.

The error matrices were also summarized using the KHAT statistic, and Table 5.8 provides the calculated Kappa estimate, variance, Z statistic, and rank of agreement with respect to the MVM for each land cover map. The Vegetation Lifeforms map had the highest Kappa value of 0.35, and the USFS/USGS map had the lowest Kappa value of 0.02. All maps were significantly greater than 0 according to the Z statistic, so the maps were better than a random classification. According to Landis and Koch (1977), a Kappa value below 0.40 indicates poor agreement, so none of the maps showed strong agreement with the MVM even though all maps were significantly better than a random classification. Appendix E provides the normalized error matrices for each land cover

Table 5.8. The calculated Kappa value, variance, Z statistic, and rank of agreement with respect to the MVM for each land cover map.

Land Cover Map	Kappa value	Variance	Z statistic	Rank
VEG LFORMS	0.35	2.75×10^{-7}	658.04	1
NLCD	0.29	7.23×10^{-8}	1068.57	2
CVM	0.29	7.26×10^{-8}	1074.78	2
SIB	0.23	6.97×10^{-8}	852.18	4
SIB2	0.17	6.02×10^{-8}	681.71	5
BATS	0.12	5.90×10^{-8}	497.00	6
SLCR	0.08	5.25×10^{-8}	344.83	7
OGE	0.06	4.34×10^{-8}	291.61	8
IGBP (AVHRR)	0.06	4.23×10^{-8}	271.55	8
USGS LULC	0.06	4.25×10^{-8}	287.55	8
IGBP (MODIS)	0.04	5.14×10^{-8}	191.40	11
UMD	0.04	5.13×10^{-8}	191.51	11
LAI/fPAR	0.03	1.67×10^{-7}	64.88	13
USFS/USGS	0.02	3.96×10^{-8}	90.91	14

map using the MVM for the reference points. Appendix F compares the individual accuracies of each land class by specifying the original pixel total, producer's accuracy, user's accuracy, and normalized value for the main diagonal cell of each land class for each map. Table 5.9 summarizes the results of the error matrix analysis for each map by outlining the Kappa value, raw overall accuracy, and normalized overall accuracy; as well as the rank in terms of agreement with the MVM with respect to each of these analysis methods. The Vegetation Lifeforms map had the highest rank according to all three accuracy measures. The four highest ranking maps were the same for all three accuracy measures, but ranks for the maps were not consistent across the three accuracy measures.

Table 5.9. Results of the error matrix analysis for each map by outlining the Kappa value, raw overall accuracy, and normalized overall accuracy; as well as the rank in terms of agreement with the MVM with respect to each of these analysis methods.

Land Cover Map	Kappa Statistic		Raw Overall Accuracy		Normalized Overall Accuracy	
	Value	Rank	Value	Rank	Value	Rank
IGBP (MODIS)	0.04	11	21.7	12	35.7	9
UMD	0.04	11	21.7	12	35.7	9
LAI/fPAR	0.03	13	32.1	6	40.8	5
USFS/USGS	0.02	14	21.6	14	36.7	7
USGS LULC	0.06	8	24.4	10	36.3	8
VEG LFORMS	0.35	1	56.4	1	66.8	1
NLCD	0.29	2	40.8	4	59.3	3
OGE	0.06	8	24.5	9	38.0	6
BATS	0.12	6	30.8	7	28.2	14
SIB	0.23	4	42.4	2	41.7	4
SIB2	0.17	5	33	5	32.1	12
IGBP (AVHRR)	0.06	8	24.1	11	32.8	11
SLCR	0.08	7	26.2	8	29.5	12
CVM	0.29	2	41.1	3	60	2

V.ii.v. SIMULATED STREAMFLOW RESULTS USING THE PRMS MODEL

V.ii.v.i. Data Preparation

There were 5844 data values for each station for the 16-year period being modeled, and any missing values had to be interpolated. Table 5.10 shows the percentage of the total missing precipitation values for each station and the percent corrected by each method.

There were no missing data values for the SNOTEL stations for the period being modeled. The average percent of missing data for the COOP stations was 2.6%, of which 48.4% were deemed days when actual precipitation events probably occurred and regression analysis was used to fill in the data values. Table 5.11 shows the percent of missing or erroneous temperature values for each station and the percent corrected by each method. On average, 3.4% of the maximum temperature values for each station

Table 5.10. Percentage of the total missing precipitation values for each station and the percent corrected by each method. The symbol *n* represents the total number of precipitation stations.

	% of missing values	% Filled in as “0” because all other stations observed no precipitation	% Filled in as “0” because <i>n</i>-1 stations observed no precipitation	Filled in by regression using nearest 3 stations
Dry Lake (06J01S)	0	0	0	0
Columbine (06J03S)	0	0	0	0
Lynx Pass (06J06S)	0	0	0	0
Rabbit Ears (06J09S)	0	0	0	0
Elk River (06J15S)	0	0	0	0
Tower (06J29S)	0	0	0	0
Crosho (07J04S)	0	0	0	0
Ripple Creek (07J05S)	0	0	0	0
Trapper Lake (07K13S)	0	0	0	0
Craig (CO1932)	19.6	4.3	5.8	89.9
Hamilton (CO3738)	7.2	43.4	27.6	28.9
Hayden (CO3867)	1.1	50.0	50.0	0.0
Maybell (CO5446)	13.0	38.0	22.6	39.4
Pyramid (CO6797)	11.7	18.7	15.4	65.9
Steamboat Springs (CO7936)	26.5	23.7	19.4	57.0
Yampa (CO9265)	20.9	23.6	18.6	57.7

were marked as missing or erroneous, and 4.4% of the minimum temperature values for each station were marked as missing or erroneous. The station at Craig (CO1932) had the highest amount of missing or erroneous values where 27.9% of the total missing or erroneous maximum temperature data and 23.2% of the missing or erroneous minimum temperature data were from this station. Appendix G shows the regression results for the precipitation and temperature stations.

Table 5.11. Percent of missing or erroneous temperature values for each station and the percent corrected by each method.

Station	% of Missing or Erroneous Values		% Corrected using Monthly Average		% Corrected using Linear Regression	
	T_{max}	T_{min}	T_{max}	T_{min}	T_{max}	T_{min}
Dry Lake (06J01S)	2.5	2.0	60.0	60.0	40.0	40.0
Columbine (06J03S)	2.3	4.1	100.0	81.0	0.0	19.0
Lynx Pass (06J06S)	0.6	0.5	100.0	100.0	0.0	0.0
Rabbit Ears (06J09S)	5.7	10.5	82.6	62.1	17.4	37.9
Elk River (06J15S)	4.5	3.7	77.2	78.2	22.8	21.8
Tower (06J29S)	6.3	9.2	83.8	91.2	16.2	8.8
Crosho (07J04S)	2.5	4.6	100.0	64.9	0.0	35.1
Ripple Creek (07J05S)	4.4	3.6	76.9	77.2	23.1	22.8
Burro Mountain (07K02S)	14.0	11.2	64.3	64.6	35.7	35.4
Trapper Lake (07K13S)	3.5	6.8	71.4	53.3	28.6	46.7
Craig (CO1932)	27.9	23.2	92.8	93.1	7.2	6.9
Hayden (CO3867)	1.0	0.9	0.0	14.3	100.0	85.7
Maybell (CO5446)	6.5	5.3	54.3	55.7	45.7	44.3
Steamboat Springs (CO7936)	9.8	7.7	8.8	7.2	91.2	92.8
Yampa (CO9265)	8.3	6.7	96.0	5.5	4.0	94.5

V.ii.v.ii. PRMS Runs

V.ii.v.ii.i. Cumulative Streamflow Results

In order to test the general sensitivity of the model predictions toward the land cover parameters, several runs were performed using either homogeneous or binary land cover maps to derive the parameters. More specifically, either the land cover maps had only one category, or they were binary maps of forested versus non-forested areas.

Figure 5.8 shows the predicted cumulative streamflow for each of the test runs and the observed cumulative streamflow. Table 5.12 shows the summary of the mean absolute error (MAE) for simulated cumulative streamflow compared to observed cumulative streamflow over the 15-year modeling period using the test datasets. The range of MAE for the water years 1987 through 2001 was between 14.3 and 18.7 percent.

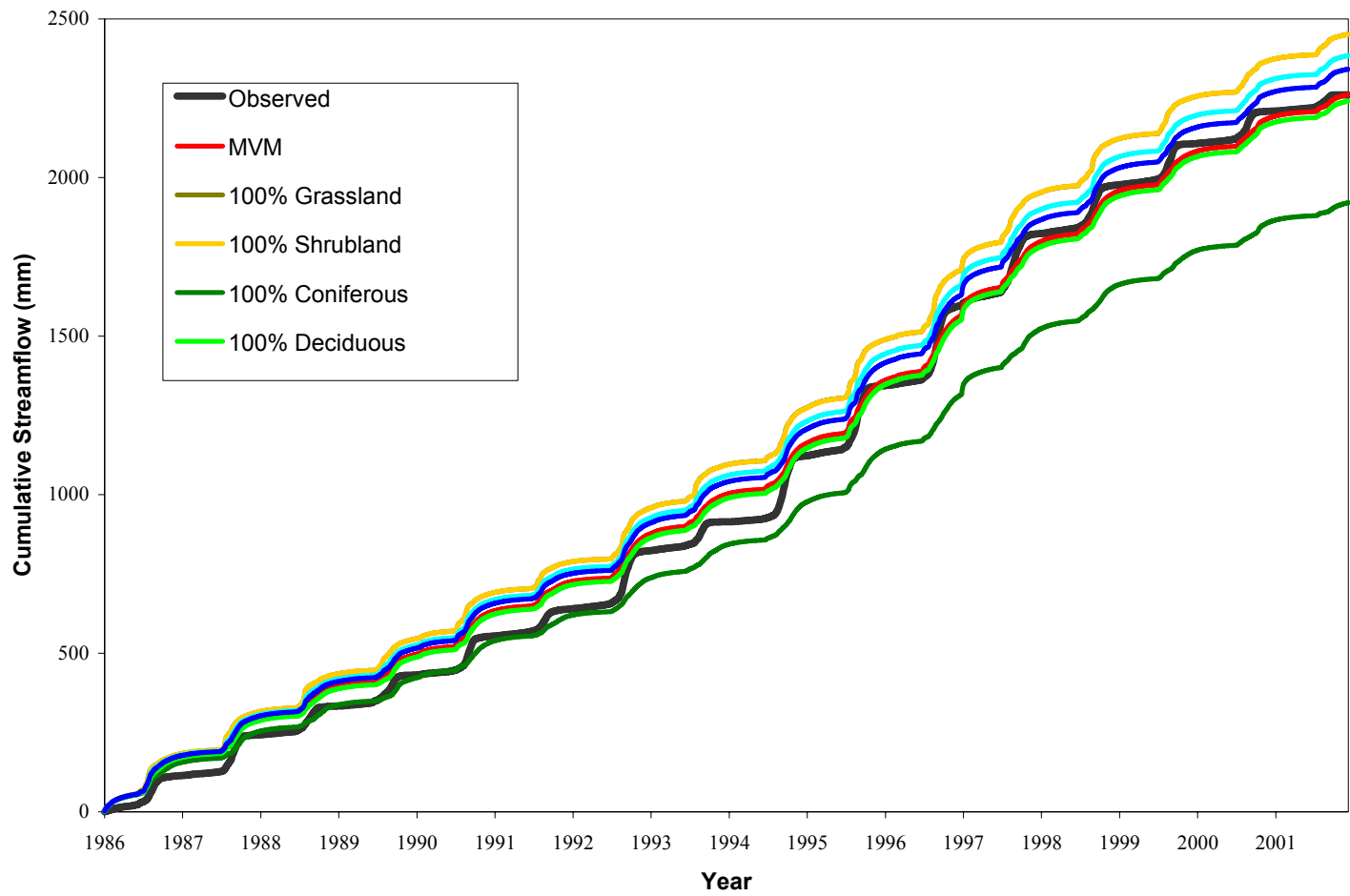


Figure 5.8. Predicted cumulative streamflow for each of the test runs and the observed cumulative streamflow.

Table 5.12. Summary of the mean absolute error (MAE) for simulated cumulative streamflow compared to observed cumulative streamflow over the 15-year modeling period using the test datasets.

Test Land Cover Dataset	Mean Absolute Error (MAE)
Grassland	16.7
Shrubland	16.7
Coniferous	18.7
Deciduous	14.3
Forest/Non-forest	14.8
Forest/Non-forest Reversal	15.3

Running the model using a land cover map of 100 percent deciduous forest land cover to derive the parameters had the closest predicted streamflow values with respect to the observed streamflow values.

There was a total of 13 model runs performed for the period 1 October 1986 to 31 August 2002. Appendix H provides the modeled annual water balance summary for each of the PRMS runs. Figure 5.9 shows the predicted cumulative streamflow for each of the model runs minus the observed cumulative streamflow. The range of MAE for the water years 1987 through 2001 was between 13.9 and 20.5 percent. The SLCR land cover map showed the most extreme deviation from observed cumulative streamflow. Table 5.13 is a summary of the total cumulative predicted streamflow minus observed streamflow ($P - O$), and the mean absolute error (MAE) for simulated cumulative streamflow compared to observed cumulative streamflow over the 15-year modeling period using each of the land cover maps to derive the land cover parameters.

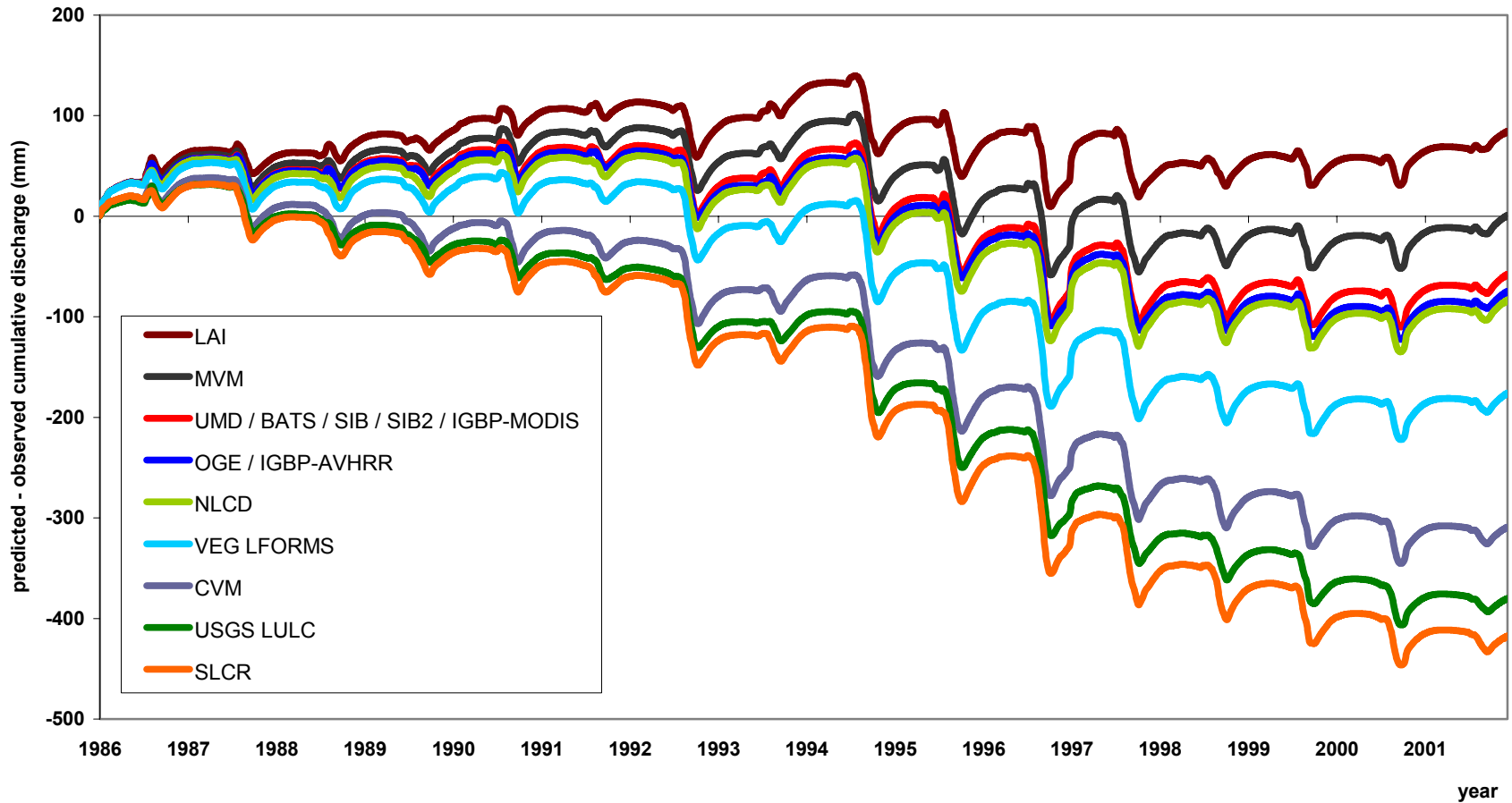


Figure 5.9 The predicted cumulative streamflow for each of the model runs minus the observed cumulative streamflow.

Table 5.13. Summary of the total cumulative predicted streamflow minus observed streamflow (P – O), and the mean absolute error (MAE) for simulated cumulative streamflow compared to observed cumulative streamflow over the 15-year modeling period using each of the land cover maps to derive the land cover parameters.

Land Cover Map	P – O (in)	MAE (%)	P – O Rank	MAE Rank	Sum	Overall Rank
SIB	-2.4 (2.7%)	13.9	3	1	4	1
SIB2	-2.4 (2.7%)	13.9	3	1	4	1
IGBP (MODIS)	-2.3 (2.6%)	14.0	1	3	4	1
UMD	-2.3 (2.6%)	14.0	1	3	4	1
BATS	-2.4 (2.7%)	14.1	3	6	9	5
NLCD	-3.3 (3.7%)	14.0	8	3	11	6
OGE	-3.0 (3.4%)	14.1	7	6	13	7
IGBP (AVHRR)	-2.9 (3.3%)	14.2	6	8	14	8
LAI/FPAR	3.3 (3.7%)	14.4	8	9	17	9
VEGETATION	14.4 (16.2%)	14.4	11	9	20	10
LIFEFORMS						
CVM	-12.2 (13.7%)	17.4	10	11	21	11
USFS/USGS	-15.0 (16.9%)	19.4	12	12	24	12
SLCR	-16.5 (18.6%)	20.5	13	13	26	13

V.ii.v.ii.i. Effect of Using Landsat-Derived Land Cover Parameters in the PRMS Runs

The NLCD map underestimated cumulative streamflow over the 15-year period by -3.3 inches. The maximum amount of overestimation in a single year was 2.1 inches, and the maximum underestimation of cumulative streamflow was 2.1 inches. Overall the NLCD received a rank of eight, but its CVM counterpart received a rank of eleven. The CVM under-estimated cumulative streamflow by 12.2 inches over the 15-year period. All years except 1987 and 1994 had a predicted net water balance that was below the observed net water balance. Both the NLCD and CVM yielded nearly identical results for the scene and pixel accuracy, so the difference in streamflow predictions is attributed to the cross-walk to the USFS/USGS composite classification scheme. The CVM had classes in both

the USFS and USGS classification sections while the NLCD had classes in only the USGS section.

V.ii.v.ii.i.ii. Effect of Using MODIS-Derived Land Cover Parameters in the PRMS Runs

The effect of using MODIS-derived IGBP and UMD land cover parameters to predict cumulative streamflow yielded identical results with respect to the annual water balance. The net annual water balance was overestimated by a maximum of 2.2 inches, and was underestimated by a maximum of 2.1 inches. These two maps performed the best in terms of matching predicted to observed cumulative streamflow using the MVM to calibrate the model. The LAI/fPAR model run overestimated streamflow by 3.3 over the 15-year period. Every year cumulative streamflow was overestimated, and in 1997 a maximum difference of 10.3 inches was observed between predicted and observed cumulative streamflow

V.ii.v.ii.i.iii. Effect of Using AVHRR-Derived Land Cover Parameters in the PRMS Runs

The SiB, SiB2, and BATS model runs had the highest rank out of the AVHRR-derived maps. All were ranked third, and all underestimated cumulative streamflow by 2.4 inches over the 15-year period. SiB and SiB2 yielded identical results with respect to annual predicted streamflow where the maximum overestimation of 2.2 inches occurred in 1987, and the maximum underestimation of 2.0 inches occurred in 1995. In 1990, predicted streamflow matched observed streamflow. The BATS results were identical to the SiB

and SiB2 results except for the years 1998 and 2001 where the difference was 0.1 inches in both cases.

Using the AVHRR-derived IGBP map to derive the land cover parameters resulted in the slightly larger difference of 2.9 inches in the underestimation of cumulative streamflow over the 15-year period. The maximum overestimation was 2.2 inches in 1987, and the maximum underestimation was 1.6 inches in 1993. The only difference between the OGE run and the AVHRR-derived IGBP run was that the OGE run overestimated streamflow by 0.1 inches more than IGBP in 1994, so the OGE underestimated cumulative streamflow by 3.0 inches over the 15-year period.

The Vegetation Lifeforms map underestimated cumulative streamflow by 7 inches over the 15-year period. The maximum overestimation of streamflow of 2.0 inches was observed in 1987, and the maximum underestimation of streamflow was 2.5 inches in 1995. In 1992, there was no annual difference between simulated and observed streamflow.

The USFS/USGS map, which was the default map for parameterization, underestimated cumulative streamflow by 15 inches over the 15-year period. Every year except 1987 and 1994 underestimated streamflow where the maximum difference was 2.9 inches. Consistent with the other maps, 1987 showed the largest difference (1.2 inches) with respect to overestimation of streamflow.

Finally, the SLCR map had the largest difference of all the maps between simulated cumulative streamflow and observed cumulative streamflow over the 15-year period. Using the SLCR map to derive the land cover parameters resulted in an underestimation of 16.5 inches over the modeling period. Every year except 1994

underestimated annual streamflow where the maximum difference was 3.1 inches in 1995.

V.ii.v.ii.ii. Daily Discharge Results

In addition to cumulative streamflow, the magnitude and timing of peak discharge was also examined for the PRMS runs. Each run was separated into two time series for ease of examination. Appendix I shows the predicted discharge versus observed discharge for the Yampa River Basin at Maybell from October 1986 to September 1994, as well as from October 1994 to August 2002. Overall the predicted timing of peak discharge was relatively close to the observed timing of the peak discharge for each of the PRMS runs. In addition, the predicted discharge consistently returned to base flow conditions at a slower rate and hence at a later date than observed discharge. An extremely sharp spike was observed for each of the PRMS runs in late September 1997. Examination of the precipitation data shows that a large amount of rain fell over a large area within a short amount of time that month. Three to eight inches fell at each station within the basin over a 17-day period between 11 September and 27 September. Many of these stations were located in the arid region of the basin and there was little precipitation surrounding the event, so overall this was a significant amount of precipitation. In all model runs, the receding limb of each yearly hydrograph for the predicted discharge was more gradual than the observed discharge, so the return to base flow conditions occurred at a later date for the predicted discharge.

V.ii.vi. OVERALL ACCURACY RESULTS FOR THE LAND COVER DATA SETS

Table 5.14 lists the ranks for each land cover dataset determined from the scene and pixel accuracy assessment methods as compared to the MVM. The CVM and NLCD had the

Table 5.14. Ranks for each land cover dataset determined from the quantitative assessment methods as compared to the MVM.

Land Cover Map	Scene Accuracy	Normalized Pixel Accuracy	Sum	Overall Rank
NLCD	1	3	4	1
CVM	2	2	4	1
OGE	4	6	10	3
IGBP (AVHRR)	3	10	13	4
VEG LFORMS	12	1	13	4
USFS/USGS	6	7	13	4
SIB	11	4	15	7
UMD	8	8	16	8
IGBP (MODIS)	8	8	16	8
SLCR	5	11	16	8
LAI/FPAR	13	5	18	11
BATS	7	13	20	12
SIB2	10	11	21	13

highest overall rank which means they have the highest agreement with the reference data. This is expected since the CVM and NLCD both have a significantly higher spatial resolution than the other land cover maps. The SiB2 map received the lowest overall rank, which was significantly different from the rank of its SiB counterpart. The major difference between the two maps was quantified by the pixel accuracy assessment, but for the pixel accuracy assessment the SiB2 map had an additional class being compared. The Vegetation Lifeforms map had the lowest rank for the scene accuracy comparison but had the highest rank for the pixel accuracy comparison. The low species resolution of the dataset may account for the low scene accuracy and the high pixel accuracy. A low

species resolution will have a negative effect on scene accuracy, but in some cases may have a positive effect on pixel accuracy. Since the pixel accuracy is based only on classes present in both the land cover map and the reference map, a lower number of similar land cover classes will increase the probability of chance agreement.

Once the overall rank based on scene and pixel accuracy was determined for each of the maps, it was compared to the rank assigned based on model performance. Figure 5.10 is a comparison chart where the overall rank based on scene and pixel accuracy is shown on the x-axis, and the rank based on model performance is shown on the y-axis.

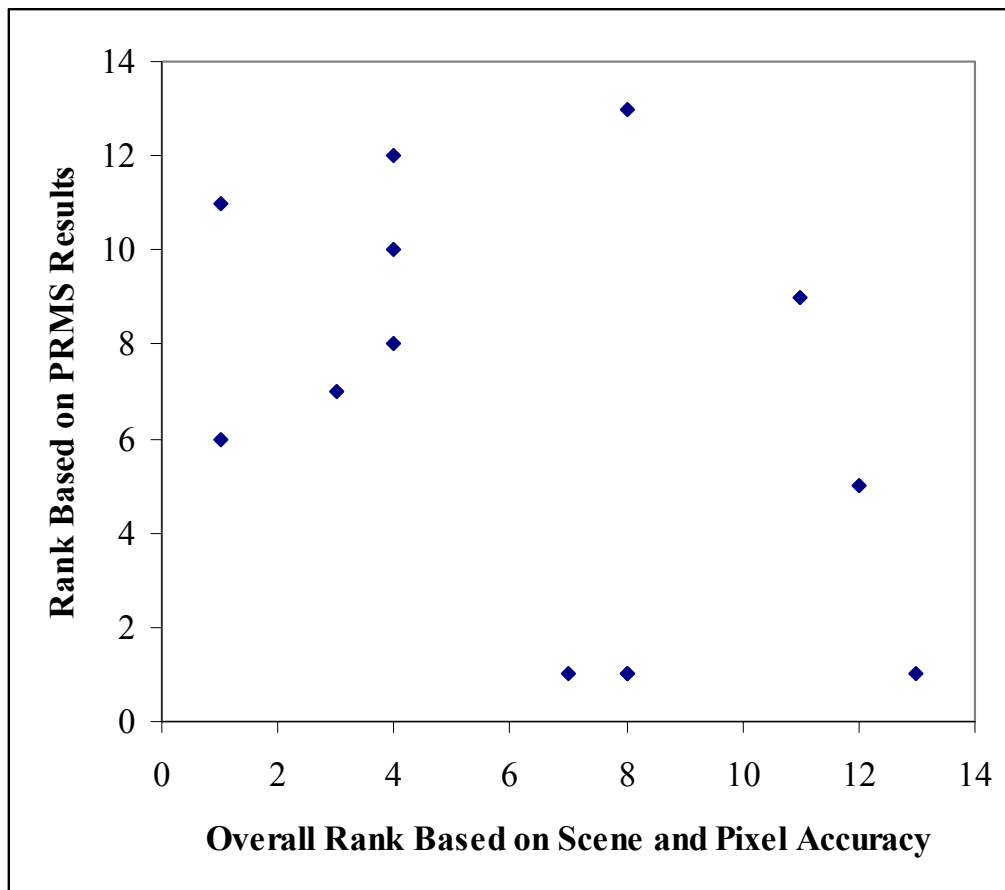


Figure 5.10. Comparison chart where the overall rank based on scene and pixel accuracy is shown on the x-axis, and the rank based on model performance is shown on the y-axis.

The chart shows no apparent correlation between model performance and scene and pixel accuracy. Logical reasoning would have one presume that the most accurate land cover map would have the best model performance, but this presumption is not supported by the results.

CHAPTER VI: DISCUSSION

VI.i. MODELED VEGETATION MAP

Several issues arose while trying to model the vegetation of a basin of this size. The primary goal was to obtain a representative sample of vegetation cover over an area of approximately 8758 km². When access restrictions through private property and limited road networks were considered, a large number of the sample points became inaccessible.

The binary regressions indicated that the 30-m Landsat imagery was a better indicator for land cover than the 1-km MODIS imagery that had been resampled to 30-m. Although the MODIS imagery had been resampled to 30-m, the spatial resolution was still 1-km. As a result, the higher correlation between the Landsat imagery and land cover characteristics of the Yampa River Basin as compared to the MODIS imagery is attributed to the finer spatial resolution of the data set.

VI.ii. METHODS FOR ASSESSMENT OF THE DIGITAL LAND COVER MAPS

VI.ii.i. DATA CROSS-WALK

Since one of the goals of this study was to compare public domain data sets, it was necessary to include all classification schemes of the AVHRR-derived data sets and the MODIS-derived data sets to maintain objectivity. This resulted in a very low resolution common classification scheme.

Since the data have been modified from their original form for the purposes of this study, it is important to note that some maps were altered to a greater degree than others. The effect of cross-walking the land cover maps with respect to the species resolution of the datasets was most pronounced with the SLCR and CVM land cover maps. This is attributed to the high number of land classes present in the original data sets.

VI.ii.ii. AGGREGATED LAND CLASS PERCENTAGES

The aggregated land class percentages provided a qualitative examination of the effects of cross-walking the data sets, and it proved a useful tool for quickly assessing the similarities and differences among the land cover data sets. This initial comparison showed that land cover maps derived from the same imagery had a tendency to have similar land class percentages after cross-walking to a common classification scheme. The preliminary comparison also showed that on average the MVM had significantly less area classified as forest than the other land cover maps. This was useful when trying to determine why certain maps under- or over-predicted streamflow since the total area of forest cover affects evapotranspiration rates which in turn affect the overall water balance.

VI.ii.iii. SCENE ACCURACY

Although the scene accuracy was insensitive to pixel location, it was sensitive to classification resolution. If a land cover map did not have a particular land class, such as water, the scene accuracy was lowered. The degree to which the scene accuracy was

lowered was proportional to the area the missing land cover class occupied in the Yampa River Basin according to the MVM.

In practice, a deficiency was noted with this method involving classes not present in the MVM. For example, the mixed forest land category was not present in the MVM, and it could not be broken down into either the coniferous or deciduous land cover category. As a result, the mixed forest category reduced the number of forested pixels available for the coniferous and deciduous forest category. However since on average the MVM had fewer forested pixels than the other maps, the scene accuracy had the potential for underestimating the accuracy of only the UMD and IGBP (MODIS) deciduous forest categories and the LAI/fPAR coniferous and deciduous forest categories. The accuracy of the UMD and IGBP (MODIS) was underestimated because they had fewer deciduous pixels than the MVM, while the accuracy of the LAI/fPAR coniferous and deciduous forest categories were underestimated since they were individually absent in the map, specifically, all forested pixels were classified as mixed forest.

VI.ii.iv. PIXEL ACCURACY

Since the pixel accuracy was only assessed for classes present in both the MVM and each other map being compared, a lower number of land classes will increase the probability of chance agreement. The Vegetation Lifeforms land cover map had the highest pixel accuracy, but it also had the lowest species resolution after cross-walking to the lowest common classification resolution. Since the Vegetation Lifeforms map had the lowest scene accuracy and the highest pixel accuracy, this verifies that using only

scene accuracy or only pixel accuracy is not sufficient to assess the differences among the land cover maps.

When the ranks derived from the scene and pixel accuracy methods are summed together, the individual biases of the methods seemed to balance out. For example, the NLCD and CVM had the highest overall rank which was expected due to the finer spatial resolution even though neither of the maps had the highest pixel or scene accuracy.

VI.ii.v. PRMS RUNS

Since the only difference between PRMS inputs were spatial parameters derived from land cover characteristics, there is a limited number of variables that can account for the differences observed in the PRMS runs. The general categories were soil moisture properties, vegetation density, canopy transmissivity, and canopy interception.

There were some significant land cover changes that occurred in the Yampa River Basin during the modeling period that affected the relationship between the land cover designated on a particular map to the land cover that is actually present in the basin. In 1997, a significant wind-throw event occurred that altered the composition of the coniferous forests on the western slopes of the Park Range. In 1998, a spruce beetle outbreak occurred within the wind-throw area that also modified the composition of the coniferous forests, and salvage logging accompanied both events.

Although the modeling period ended at the 2001 water year, several large fires occurred in 2002 that had a significant impact on the forested area within the Yampa River Basin. The Big Fish fire affected 68.8 km² of the Yampa River Basin, the Green Creek fire affected 16.2 km², and the Mount Zirkel fire affected 125 km² (Romme, 2004).

The fires collectively represent a major land cover change event that warrant further inquiry if the modeling is to be taken further. However, in terms of the modeling period under review, the years 1997 and 1998 were the landmark years for significant land cover change. The overall trend observed for predicted cumulative streamflow was to underestimate cumulative streamflow. Even PRMS runs that initially overestimated cumulative streamflow eventually underestimated cumulative streamflow. The transition years for these runs were 1995 to 1998, which briefly preceded the time of significant land cover change so the reason is not completely clear. The maps that were based on imagery acquired after the land cover change events initially overestimated cumulative streamflow, and later underestimated cumulative streamflow. This supports a model sensitivity to the land cover change since these maps would have a lower coverage of forested area for the years preceding the land cover change that would result in overestimation of cumulative streamflow.

VI.iii. OVERALL ASSESSMENT OF DIGITAL LAND COVER MAPS

One of the primary goals of this study was to determine the most suitable map for hydrological modeling of the Yampa River Basin. It was found that the basic accuracy assessment methods (scene and pixel accuracies) did not correlate with the PRMS results. This questions the logical assumption that the most accurate land cover map for a given area will be the most suitable map for a particular application.

To remain in the context of application within PRMS, it did not seem that detailed land cover representation resulted in improved model results. For example, deriving land cover parameters using a map of 100 percent deciduous forest land cover had only a 0.4%

difference in the MAE for cumulative streamflow than the highest ranking public domain land cover map. The model was sensitive to land cover to a moderate degree. The test runs showed that the model tended to overestimate streamflow when the land cover map was 100 percent non-forested area, and tended to underestimate streamflow when the land cover map was 100 percent coniferous area. In terms of the spatial distribution of forested and non-forested areas, there was only a slight difference of the MAEs (0.5%) between the binary maps where one represented forested and non-forested areas based on the reference map (14.8%), and the other was the binary opposite (15.3%). The binary opposite means that forested areas in the reference map were coded as non-forested areas, and non-forested areas in the reference map were coded as forested areas. It is important to note that the study basin was very large, so the sensitivity to land cover conditions might be more pronounced in smaller watersheds.

However, after examining the different accuracy measures, some broad recommendations can be made. If a relatively recent, accurate map is available with a high spatial resolution that is tailored to the basin of interest, as was the case with the MVM, it will likely prove to be an invaluable asset. If this type of map is not available or time or resource limitations prohibit the creation of this type of map, various public-domain maps are available that will yield adequate results with a minimal amount of invested time or resources. The following overall assessment of each of the sets of land cover maps highlights the general sensitivities of the land cover maps based on the assessment methods used in this study. Care must be taken in the interpretation of the assessment because the comparison was only conducted for the Yampa River Basin. As a result the assessment does not attempt to determine “good” maps and “bad” maps,

rather it is meant to summarize performance compared to the reference map and to explain reasons for the differences observed among the land cover data sets.

VI.iii.i. LANDSAT-DERIVED LAND COVER MAPS

Overall the Landsat-derived land cover maps had the highest quantitative accuracy with respect to scene and pixel accuracy compared to the MVM, even though these maps are based on imagery eight to nine years older than the MVM. This is attributed to the relatively high spatial resolution of the data sets compared to the other land cover data sets. Although in the quantitative assessment there was no significant difference between these two data sets, it is important to note that the data were modified from their original form through the data cross-walk. The CVM has 47 land cover categories compared to 21 for the NLCD, so the CVM may be more suitable for ecological studies where a high vegetation species resolution may be critical.

VI.iii.i.i. National Land Cover Dataset (NLCD)

The NLCD had the highest scene accuracy for all the land cover maps measured at 73.9%, but it differed from the CVM by only 0.6%. The higher spatial resolution gives the NLCD an advantage that is more pronounced in heterogeneous terrain. For example, a small meadow of approximately 100 square meters surrounded by coniferous forest would not be detected by a 1-km land cover block. If there were many small meadows, the overall area of grassland would add up while remaining undetected by the 1-km land cover blocks. Based on the same reasoning, if the terrain is largely homogeneous the effect of a higher spatial resolution would be less pronounced. The pixel accuracy was

also relatively high for the NLCD at 59.3% (Rank #3), even though there were a relatively large number of classes being compared.

The preliminary evaluation of the NLCD through the aggregated land class percentages indicated that the NLCD had a significantly higher percentage of forest cover than the reference map. This helps to explain why the NLCD tended to underestimate streamflow. A higher degree of forest cover results in larger amounts of precipitation lost through sublimation, evapotranspiration, and vegetation uptake, which reduces the amount of water available for runoff (Lundberg et al., 2004; Waring and Running, 1998). The NLCD underestimated total cumulative streamflow by 3.3 inches, which was fairly close to observed total cumulative streamflow with respect to the other PRMS runs.

VI.iii.i.ii. Colorado Vegetation Model (CVM)

The CVM had a high scene accuracy of 73.3% (Rank #2). Although the scene accuracy was 0.6% lower than the NLCD, the pixel accuracy was 0.7% higher for the CVM. As with the NLCD, the CVM also had a significantly higher percentage of forest cover than the reference map. As a result the CVM tended to underestimate streamflow, which is explained by the same reasoning used for the streamflow underestimation observed in the NLCD. However, the CVM underestimated total cumulative streamflow by 12.2 inches compared to 3.3 inches for the NLCD. There was a difference between the two maps after cross-walk to the USFS/USGS composite scheme used in the PRMS model where the CVM had classes in the USFS section while the NCLD only had classes in the USGS LULC section.

VI.iii.ii. MODIS-DERIVED LAND COVER MAPS

Although the MODIS-derived land cover maps have a lower spatial resolution than the Landsat-derived land cover maps, the MODIS-derived land cover maps are based on imagery collected 8-9 years after the Landsat-derived land cover maps. The MODIS-derived land cover maps were also collected 8-9 years after the AVHRR-derived land cover maps. It was expected that the MODIS-derived land cover maps would match more closely with the MVM than the AVHRR-derived land cover maps since it is based on more recent imagery, but this was not necessarily the case.

VI.iii.ii.i. International Geosphere Biosphere Programme (IGBP)

The scene accuracy for the MODIS-derived IGBP land cover map was 60.9%, which was less than the AVHRR-derived IGBP counterpart (72.7%). As stated previously, the scene accuracy appears to be biased towards a higher species resolution with respect to the MVM, however the MODIS-derived IGBP has more classes present in the Yampa River Basin (eight) than the AVHRR-derived IGBP (six). This indicates that the AVHRR-derived IGBP map may have a classification algorithm more sensitive to the land cover conditions present in the Yampa River Basin, or the combination of band widths used for the remote sensing component were more sensitive to differences in vegetation. The MODIS-derived IGBP land cover map did have a higher pixel accuracy (35.7%)

compared to the AVHRR-derived MODIS land cover map (32.8%), but the margin of difference was less (2.9%).

For the PRMS runs, the MODIS-derived IGBP map was slightly closer to the observed cumulative streamflow total than the AVHRR-derived map, but the difference between the MAE's was 0.2%. In general, the MODIS-derived IGBP map underestimated the magnitude of peak discharge, but the underestimation was more pronounced during the period from 1995 to 2001 when there was typically a higher observed peak discharge. The underestimation of peak discharge and cumulative streamflow is attributed to the larger overall percent of forest cover present in the MODIS-derived IGBP map compared to the reference map.

VI.iii.ii.ii. University of Maryland Modified IGBP (UMD)

After the UMD was cross-walked to the lowest common classification scheme, the aggregated land class percentages were identical to the MODIS-derived IGBP with the exception of a wetlands class present in the MODIS-derived IGBP that constituted 0.1% of the total area of the map. Data cross-walk to the USFS/USGS composite classification scheme was also nearly identical with a discrepancy of only 0.2% between the two maps. The scene and pixel accuracy for the UMD map was identical to the scene and pixel accuracy for the MODIS-derived IGBP map. The overall cumulative streamflow results were identical for the two land cover maps, and no significant differences were observed in the discharge graphs. These results are expected since the UMD classification scheme is simply a slightly modified version of the IGBP classification scheme, and both maps were derived from the same imagery.

VI.iii.ii.iii. Leaf Area Index / fraction of Photosynthetically Active Radiation (LAI/fPAR)

Biome Scheme

The general purpose of the LAI/fPAR map was to characterize vegetation types that facilitate LAI and fPAR retrievals from MODIS and Multiangle Imaging Spectroradiometer (MISR) imagery (Lotsch et al., 2003). The significant characteristic of the LAI/fPAR land cover map was that it did not have a coniferous or deciduous land cover category. All forested pixels were placed in the mixed forest category because neither of the LAI/fPAR forest classes were exclusively coniferous nor deciduous - both the broadleaf forest category and the needleleaf forest categories can contain both coniferous and deciduous species. This helps explain the extremely low scene accuracy of the LAI/fPAR land cover map (44.1%) because the scene accuracy was highly sensitive to the absence of a coniferous or deciduous land class. Together the two classes constitute approximately 30% of the total land cover with respect to the MVM, which reduces the scene accuracy of the LAI/fPAR map by 30%. In this case, the scene accuracy was deemed a poor assessment method for the map because of the ambiguous land class definitions. The pixel accuracy yielded a more intermediate rating of the land cover map receiving a rank of five (40.8%).

In terms of estimating peak discharge, the LAI/fPAR map performed quite well. Although the map overestimated total cumulative streamflow, the difference was only 2.3 inches over a 15 year time period. The relative agreement between the LAI/fPAR PRMS runs and observed streamflow is attributed to the overall scene accuracy in terms of

forested and nonforested pixels. In the LAI/fPAR map, 30.5% of the total area is forested pixels, and in the MVM 30.9% of the total area is forested pixels equating to a difference of only 0.4%.

VI.iii.iii. AVHRR-DERIVED LAND COVER MAPS

The AVHRR-derived land cover maps were not expected to perform as well as the Landsat- or MODIS-derived land cover products with respect to the different comparison methods. This assumption was based on the poor spatial resolution compared to the Landsat-derived land cover products, and the datedness of the imagery compared to the MODIS-derived land cover products. In practice, it became apparent that this assumption was not completely valid because in some instances the AVHRR land cover products outperformed the other land cover products.

VI.iii.iii.i. Vegetation Lifeforms (RUN)

The scene accuracy for the RUN map was ranked second to last at 50.1%. This is attributed to an over-allocation of forested pixels within the land cover map. In contrast, the pixel accuracy for the RUN map was ranked the highest at 66.8%. There were only three land classes used for the pixel accuracy, so chance agreement may have accounted for this extreme change in rank. The aggregated land class percentages showed that the RUN map classified 78.5% of the map as forest compared to 30.9% for the MVM. The expected result was an underestimation of cumulative streamflow and peak discharge due to a high amount of evapotranspiration that would be calculated from the over-represented forested area. The results confirmed this expectation both in terms of peak

discharge and cumulative streamflow where the RUN PRMS total predicted cumulative streamflow was less than total observed cumulative streamflow by 7 inches.

VI.iii.iii.ii. USGS Land Use / Land Cover (LULC)

The USGS LULC land cover map had the apparent advantage of being merged with the USFS land cover map when used to parameterize the PRMS model. However for the scene accuracy the USGS LULC map was calculated as 72.5% accurate, but after being merged with the USFS map the accuracy was decreased to 70.7%. Both accuracies were intermediate relative to the other maps. Pixel accuracy was only slightly better with the USGS/USFS composite scheme (36.7% compared to 36.3%), so the maps were close to each other in regards to overall accuracy due to the balancing effect of the two methods. In terms of PRMS simulations, only the USGS/USFS composite was run since this was the default map for PRMS and there would be no reason to exclude the USFS scheme in a PRMS application outside this study. Underestimation of peak discharge was the overall trend when using the USGS/USFS map to parameterize the model. In addition, the total predicted cumulative streamflow was 15 inches less than the total observed cumulative streamflow, which was significant with respect to the other PRMS simulations. Again the underestimation of cumulative streamflow is attributed to an overestimation of forest cover, but the RUN map was closer to observed streamflow while having a larger overestimation of forest cover than the USGS/USFS map. The reason for this is unclear, but perhaps it relates to the higher pixel accuracy of the RUN map (66.8%) compared to the USGS/USFS map (36.7%).

VI.iii.iii.iii. Global Ecosystems (OGE)

The OGE had a high-to-intermediate scene accuracy (72.5%) and an intermediate pixel accuracy (38.0%) with respect to the other land cover maps. Although the OGE had a tendency to underestimate peak discharge, overall it matched closer to observed peak discharge than most of the other maps. The OGE underestimated total cumulative streamflow by 3.0 inches over the 15-year simulation. The OGE forested area was overestimated by 25.9% with respect to the MVM, which may account for the underestimation of cumulative streamflow.

VI.iii.iii.iv. Biosphere-Atmosphere Transfer Scheme (BATS)

The BATS map had an intermediate scene accuracy (69.6%) and had the lowest pixel accuracy (28.2%). Surprisingly, the BATS PRMS simulation for peak discharge had a relatively good fit with observed peak discharge. Total simulated cumulative streamflow was only 2.4 inches less than total observed cumulative streamflow over the 15-years. The underestimation of cumulative streamflow is attributed to the overestimation of forest cover (56.8%) compared to the MVM (30.9%).

VI.iii.iii.v. Simple Biosphere Model (SiB)

The scene accuracy of the SiB map was relatively low at 52.7%, but the pixel accuracy was relatively high at 41.7%. In terms of total simulated cumulative streamflow, the SiB map yielded 2.4 inches less than total observed cumulative streamflow. Along with the SiB2 map, the SiB map had the lowest MAE (13.9%) for predicting cumulative

streamflow. The peak discharge had a tendency to be underestimated by the SiB run, but overall the fit was acceptable compared to the other PRMS runs.

VI.iii.iii.vi. Simple Biosphere 2 Model (SiB2)

The SiB2 map was almost identical to the SiB map. In terms of aggregated land class percentages, there was only a 1.1% discrepancy that was between the grassland/herbaceous category and the shrubland category. The SiB2 map also had a relatively low scene accuracy at 53.8%, and was only 1.1% higher than the SiB map. This was attributed to the aggregated land class percentage discrepancy resulting from the data cross-walk. Although the scene accuracy was similar, the SiB2 map had a significantly lower pixel accuracy (32.1%) compared to the SiB map (41.7%). The normalized error matrices revealed that the SiB2 map had five classes used in the comparison compared to four in the SiB map, and the forest classes were less accurate for the SiB2 map. For total simulated streamflow, the SiB2 simulation yielded the same total cumulative streamflow as the SiB simulation and both yielded the same annual predicted runoff every year. The SiB run showed nearly identical discharge results compared to the SiB2, so the SiB run also had an acceptable fit with observed discharge.

VI.iii.iii.vii. International Geosphere Biosphere Programme (IGBP)

The AVHRR-derived IGBP map had a relatively high scene accuracy of 72.7%, but a relatively low pixel accuracy of 32.8%. The AVHRR-derived IGBP PRMS run underestimated total cumulative streamflow by 3.9 inches, while the MODIS-derived IGBP run underestimated total cumulative streamflow by 3.3 inches. The discharge

graphs revealed the map had a tendency to underestimate peak discharge which is consistent with the underestimation of total cumulative streamflow. The IGBP map classified 62.2% of the total area as forest, which was over twice the amount classified as forest in the MVM (30.9%). This large discrepancy supports the observation that the IGBP simulations underestimated both peak discharge and cumulative streamflow.

VI.iii.iii.viii. Seasonal Land Cover Regions (SLCR)

The SLCR had an intermediate-to-high scene accuracy of 72.2%, but had a relatively low pixel accuracy of 29.5% which was second to last with respect to the other maps. The SLCR PRMS run underestimated total cumulative streamflow by 16.5 inches, which was the largest degree of underestimation observed out of all the PRMS runs. The SLCR had a tendency to underestimate peak discharge, and the underestimation was highly pronounced between 1995 and 2001. The SLCR map classified 58.4% of the total area as forest, which was nearly double the amount classified as forest in the MVM (30.9%). This partially explains the underestimation of peak discharge and cumulative streamflow. The other contributing factor might be related to the low pixel accuracy measured for this map.

VI.iv. DISCUSSION

Ultimately, the purpose of this study was to evaluate the differences among the public domain land cover datasets, as well as to provide specific answers for the optimal spatial, spectral, and classification resolution for modeling basins of this size. In order to simplify the discussion, the maps will be grouped by their respective imagery source.

VI.iv.i. OVERALL DIFFERENCES AMONG THE PUBLIC DOMAIN LAND COVER DATASETS

For the MODIS-derived land cover maps, it was found that they had the closest ratio of forest to non-forest area to that observed in the MVM. Even without the MVM, a total forested area of approximately 30% is also supported by the distribution of land ownership. Approximately 30.2% of the area was designated as National Forest Land, 8.1% was designated as BLM land, and 61.7% was designated as private property. From field visits, it was found that private property was primarily cropland, pasture, shrubland, or urban. The only forested areas, primarily cottonwood groves, were found along riparian corridors, but the total of these areas was small in proportion to the size of the basin. The BLM land was mostly distributed in the arid lowlands, and were either shrubland or barren or sparsely vegetated. This leaves 30.2% of the total area available for forested land. Inside the National Forest land there were many meadows, blow-downs, and burned areas so not all of the National Forest land was forest. After consideration of both the National Forest land and the riparian corridors, an approximate proportion of 30% forested area is reasonable. The AVHRR-derived land cover maps had a higher proportion of forested area ranging from 56.8% to 78.5%, and the Landsat-derived land cover maps had a higher proportion as well ranging from 55.6% to 56.6%.

The high spatial resolution of the Landsat-derived land cover maps is attributed to their high performance in the scene accuracy and pixel accuracy assessments even though the imagery was approximately 12 years older than the imagery used to derive the reference map. There is another NLCD land cover product that will soon be available

based on 2001 Landsat imagery, so this will help resolve the datedness issue of the current NLCD land cover product.

For the AVHRR-derived land cover maps, similarities were observed in the aggregated land class percentages for some of the maps, but all had varying performance levels for each of the comparison levels. There was no distinct difference between the AVHRR-derived land cover maps and the MODIS-derived land cover maps except for what was observed in the PRMS results, which is discussed in the next section.

VI.iv.ii. IMPLICATIONS OF THE ASSESSMENT ON MODELING CONSIDERATIONS

In terms of hydrological modeling, the maps with the closest ratio of forest to non-forest area (UMD and MODIS IGBP) to that observed in the MVM had model simulations of total cumulative streamflow that were closest to observed total cumulative streamflow. However, the SiB and SiB2 had lower MAEs than the UMD and MODIS IGBP maps, but the difference was not significant (0.1%). The LAI/fPAR also had a forest to non-forest ratio that agreed with the ratio for the MVM, and the LAI/fPAR map performed well even though there was no deciduous or coniferous land category.

For the NLCD and CVM maps, the spatial resolution was not deemed to be as an important factor in the model results. The model results showed that the Landsat-derived maps exhibited a relatively moderate performance when deriving land cover parameters to model streamflow using the USGS PRMS in a basin of this size. The modeling blocks had a 2-km resolution, so a mosaic, or GRU, approach may yield more favorable results for the higher resolution land cover maps. A GRU is a grouping of areas with similar

attributes (i.e., land cover) so a modeling cell would have zones of distinct GRUs. The simulated runoff from the different zones of GRUs are then added together to contribute to the drainage system (Pietroniro and Soulis, 2003).

Since the Landsat- and AVHRR-derived land cover maps were based on imagery from 1992 and 1993, it was thought that these maps would perform poorly in the latter end of the model period because the area had been exposed to extreme winds resulting in blow-downs, as well as other land cover changes that occurred after the maps had been created. It was also thought that the MODIS-derived land cover maps would perform better in the latter end of the model year since these maps were based on imagery collected in 2000 and 2001. However after examination of the annual net water balance summaries, no discernible trend was observed throughout the model years to support this reasoning.

The overall recommendation based on the results of this study is that the accuracy of the proportion of forested area is more important than the spatial, classification, or temporal resolution for modeling a basin of this size using the USGS PRMS model and the conditions of this study. However, the test runs using erroneous land cover maps outperformed several legitimate land cover maps. The model did not appear to be particularly sensitive to pixel location, and none of the accuracy assessment measures correlated with model performance. It is important to note that the results of this study are specific to modeling a basin of this size, so when modeling basins of a different size or these recommendations may not be valid. In addition, the model results are specific to the USGS PRMS model when using the automated parameterization process in the USGS

GIS Weasel program. This is partly due to the data cross-walk to the USFS/USGS composite classification scheme which altered the original datasets in a specific way.

CHAPTER VII: CONCLUSIONS

The goal of this study was to assess the different public domain land cover data sets and to investigate their suitability for hydrological modeling in the Yampa River Basin using the USGS PRMS model. Individual ranks were given to each land cover map for each comparison method and were summed to yield an overall rank. However, the sets ranks are not meant to be absolute; they were meant to simplify interpretation of the streamflow results. In practice, it was found that the accuracy measures performed in this study did not correlate with the model results.

For the quantitative comparison methods, it was shown that one method alone does not provide an adequate summation of differences between data sets. There was no single method that could adequately summarize the data sets while accounting for differences in species resolution, spatial resolution, date-of-creation, and source imagery. Although in some cases the comparison methods provided an indication of how well the maps would perform in the PRMS model, it was not possible to accurately predict which maps would perform the best based on the comparison methods. For example, the significant difference between the NLCD simulated streamflow and the CVM simulated streamflow was not expected. All comparison methods had shown the NLCD and CVM land cover maps were not significantly different after cross-walk to a common classification scheme, but after cross-walk to the USFS/USGS composite scheme used in the PRMS model there was a difference between which categories the pixels were

allocated to. Whether or not this would account for the large difference observed in the streamflow results is unclear.

In an attempt to transfer the results of this study to other land cover data users, some general recommendations are provided. First of all, the most ideal scenario is to have a land cover map that was created based on the specific land cover characteristics of the study basin. If the basin is small, unregulated, and accessible, then a map can be generated on one's own with relative ease. If the time or resources are not available, there are numerous public domain land cover data sets that are available at little or no cost. Please note that all public domain land cover datasets used in this study with the exception of the CVM was designed to characterize land cover on a continental or global scale, so it is expected that these land cover maps may not be suitable if a high degree of accuracy is required within a small area. This does not imply a deficiency in the data sets, rather it was a calculated loss in order to gain large coverage capabilities.

In terms of spatial resolution, it was found that the 30-m maps outperformed the 1-km maps for this particular study. Although the Landsat imagery used in this study was based on 1992 imagery, an NLCD map based on 2001 Landsat imagery is now available in selected areas and will serve to complement the 1992 NLCD. As a word of caution, the 30-m maps are not "better" in the sense that optimal spatial resolution will depend on many factors including desired accuracy, scale of study, and cost. For example, a 30-m map may not be sufficient for a study basin that is only 100 m² in size.

In terms of the PRMS runs, the model did not prove to be very sensitive to accurate land cover. Only a broad generalization can be made where a map that contributed to a relatively good match between simulated and observed streamflow

generally had the proper ratio of forest to nonforest cover with respect to the MVM. When the forested to nonforest ratio was too high, the simulated PRMS runs had the tendency to underestimate peak discharge and cumulative streamflow. The only map that contributed to an overestimation of cumulative streamflow was the LAI/fPAR map, and the forested area was 0.4% less for the LAI/fPAR map than for the MVM. In this study, the PRMS simulated streamflow runs were not partial to the 30-m data even though they had the highest rank when the scene accuracy and pixel accuracy were combined. The overall conclusion is that the quantitative comparison methods together could not predict which map to use to derive simulated streamflow that compared best with observed streamflow. However the quantitative comparisons can be used to explain why simulated streamflow results differ from observed streamflow.

REFERENCES

- Anderson, J.R., Hardy, E.E., Roach, J.T., and R.E. Witmer. 1976. A land use and land cover classification system for use with remote sensor data. USGS Professional Paper 964.
- Belward, A.S., J.E. Estes, and K.D. Kline. 1999. The IGBP-DIS Global 1-km Land-Cover Data Set DISCover: A project overview. *Photogrammetric Engineering and Remote Sensing*. 65: 1013-1020.
- Bewket, W., and G. Sterk. 2004. Dynamics in land cover and its effect on stream flow in the Chemoga watershed, Blue Nile basin, Ethiopia. *Hydrological Processes*. IN PRESS – FIND DATE.
- Bossong, C.R., Caine, J.S., Stannard, D.I., Flynn, J.L., Stevens, M.R., and J.S. Heiny-Dash. 2003. Hydrologic conditions and assessment of water resources in the Turkey Creek watershed, Jefferson County, Colorado, 1998-2001. U.S. Geological Survey Water-Resources Investigations Report 03 (4034). 140 pp.
- Congalton, R.G., and K. Green. 1999. *Assessing the Accuracy of Remotely Sensed Data: Principles and Practices*. CRC Press, Inc, Boca Raton, Florida. 137 pp.
- Congalton, R., Mead, R., Oderwalk, R., and J. Heinen. 1981. Analysis of forest classification accuracy. *Remote Sensing Research Report*. 13-1134. 85 pp.
- Defries, R.S., and J.G.R. Townshend. 1994. NDVI derived land cover classifications at a global scale. *International Journal of Remote Sensing*. 5: 3567-3586.
- Defries, R., Hansen, M., Townshend, J.G.R., and R. Sohlberg. 1998. Global land cover classifications at 8 km resolution: the use of training data derived from Landsat imagery in decision tree classifiers. *International Journal of Remote Sensing*. 19: 3141-3168.
- Fassnacht, S.R., L.M. Christel, R.C. Bales, S. Yool, K. A. Dressler, and G.H. Leavesley. 2000. The impact of different vegetation representations on hydrologic modelling. *EOS Trans., AGU, Fall Meet. Suppl.*, 81(48): F484-F485.
- Fassnacht, S.R., and E.D. Soulis. 2002. Implications during transitional periods of improvements to the snow processes in the land surface scheme – hydrological model WATCLASS. *Atmosphere-Ocean*. 40 (4): 389-403.

- Friedl, M.A., McIver, D.K., Hodges, J.C.F., Zhang, X.Y., Muchoney, D., Strahler, A.H., Woodcock, C.E., Gopal, S., Schneider, A., Cooper, A., Baccini, A., Gao, F., and C. Schaaf. 2002. Global land cover mapping from MODIS: algorithms and early results. *Remote Sensing of Environment*. 83: 287-302.
- Gebelein, J., and J.E. Estes. 2000. Validation of current land cover maps utilizing astronaut acquired photography. CP504, Space Technology and Applications International Forum-2000.
- Global Land Cover Characteristics Data Base. Version 2.0, last updated 12.05.2003. USGS – NASA Distributed Active Archive Center. 1.23.2005.
http://LPDAAC.usgs.gov/glcc/globdoc2_0.asp.
- Hansen, M.C., Defries, R.S., Townshend, R.G. and R. Sohlberg. 2000. Global land cover classification at the 1km spatial resolution using a classification tree approach. *International Journal of Remote Sensing*. 21: 1331-1364.
- Hay, L.E., Clark, M.P, Wilby, R.L., Gutowski Jr, W.J., Leavesley, G.H., Pan, Z., Arritt, R.W., and E.S. Takle. 2002. Use of regional climate model output for hydrologic simulations. *Journal of Hydrometeorology*. 3: 571-590.
- Hay, L.E., Wilby, R.L., and G.H. Leavesley. 2000. A comparison of delta change and downscaled GCM scenarios for three mountainous basins in the United States. *Journal of American Water Resources*. 36 (2): 387-397.
- Hodges, J. 2002. MODIS MOD12 Land Cover and Land Cover Dynamics Products User Guide. <http://geography.bu.edu/landcover/userguide/lc.html>. 16 December.
- Justice, C.O., Townshend, J.R.G., Vermote, E.F., Masuoka, E., Wolfe, R.E., Saleous, N., Roy, D.P., and J.T. Morisette. 2002. An overview of MODIS Land data processing and product status. *Remote Sensing of Environment*. 83: 3-15.
- Landis, J., and G. Koch. 1977. The measurement of observer agreement for categorical data. *Biometrics*. 33: 159-174
- Leavesley, G.H., Lichty, R.W., Troutman, B.M., and Saindon, L.G. 1983. Precipitation runoff modeling system – user’s manual. U.S. Geological Survey Water-Resources Investigations Report 83 (4238). pp. 207.
- Leavesley, G.H., Markstrom, S.L., Restrepo, P.J. and R.J. Viger. 2002. A modular approach to addressing model design, scale, and parameter estimation issues in distributed hydrological modelling. *Hydrological Processes*. 16: 173-187.

- Lotsch, A., Tian, Y., Friedl, M.A., and R.B. Myneni. 2003. Land cover mapping in support of LAI and FPAR retrievals from EOS-MODIS and MISR: classification methods and sensitivities to errors. *International Journal of Remote Sensing*. 24 (10): 1997-2016.
- Loveland, T.R., Merchant, J.W., Ohlen, D.O. and J.F. Brown. 1991. Development of a land-cover characteristics database for the conterminous U.S. *Photogrammetric Engineering and Remote Sensing*. 57 (11): 1453-1463.
- Loveland, T.R., Reed, B.C., Brown, J.F., Ohlen, D.O., Zhu, J., Yang, L., and J.W. Merchant. 2000. Development of a global land cover characteristics database and IGBP DISCover from 1-km AVHRR Data. *International Journal of Remote Sensing*. 21 (6/7): 1303 – 1330.
- Lundberg, A., and S. Halldin. 2001. Snow interception evaporation – rates, processes and measurement techniques. In *Land-surface/Atmosphere Exchange in High-latitudes Landscapes*, Grassl, H., Halldin, S., Gryning, S.E., and C.R. Lloyd (eds). *Theoretical and Applied Climatology*. 70 (1-4): 117-133.
- Merriam-Webster's Desk Dictionary. 1995. Merriam-Webster, Inc. 765 pp.
- MODIS Web. Curator: MODARCH Webmaster. Authorized by: Barbara Conboy, MAST leader. <http://modis.gsfc.nasa.gov/data/dataproducts.html>.
- Myneni, R.B., Nemani, R.R., and S.W. Running. 1997. Estimation of global leaf area index and absorbed PAR using radiative transfer model. *IEEE Trans. Geosci. Remote Sens.* 35: 1380-1393.
- Pietroniro, A., and E.D. Soulis. 2003. A hydrology modelling framework for the Mackenzie GEWEX programme. *Hydrological Processes*. 17: 673-676.
- Pietroniro, A., and E.D. Soulis. 2001. Comparison of global land-cover databases in the Mackenzie basin, Canada. *Remote Sensing and Hydrology*. IAHS: no. 267.
- Pomeroy, J.W., Gray, D.M., Hedstrom, N.R., and J.R. Janowicz. 2002. Prediction of seasonal snow accumulation in cold climate forests. *Hydrological Processes*. 16: 3543-3558.
- Romme, W.H. 2004. Personal Communication. Department of Forest, Rangeland, and Watershed Stewardship. Colorado State University.
- Running, S.W., Loveland, T.R., and L.L. Pierce. 1994. A vegetation classification logic based on remote sensing for use in global scale biogeochemical models. *Ambio*. 23: 77-81.

- Sabins, F. 1997. Remote Sensing, Principles and Interpretation. New York, W.H. Freeman and Company. pp. 200-315.
- Scepan, J. 1999. Thematic validation of high-resolution global land-cover data sets. Photogrammetric Engineering and Remote Sensing. 65:1051-1060.
- Scurlock, J.M.O., Asner, G.P., and S.T. Gower. 2001. Global leaf area index data from field measurements, 1932-2000. Data set. Available on-line <http://www.daac.ornl.gov> from the Oak Ridge National Laboratory Distributed Active Archive Center, Oak Ridge, Tennessee, USA.
- Smith, D.H., Nichols, R.H. and F. M. Smith. 1998. Irrigation water use in the Yampa River Basin. Colorado Water Resources Research Institute. No. 8.
- Smits, P.C., Dellepiane, S.G., and R.A. Schowengerdt. 1999. Quality assessment of image classification algorithms for land-cover mapping: a review and a proposal for a cost-based approach. International Journal of Remote Sensing. 20: 1461-1486.
- Storck, P. 2000. Trees, snow and flooding: an investigation of forest canopy effects on snow accumulation and melt at the plot and watershed scales in the Pacific Northwest. Water Resources Series, Technical Report 161. University of Washington, 176 pp.
- Stocks, C.E., and S. Wise. 2000. The role of GIS in environmental modeling. Geographical and Environmental Modelling. 4 (2): 219-235.
- Theobald,, D.M., Peterson, N. and W. Romme. 2004. The Colorado vegetation model: using National Land Cover Data and ancillary spatial data to produce a high resolution, fine-classification map of Colorado (v8). 4 February. Unpublished report. Natural Resource Ecology Lab, Colorado State University.
- US Department of Agriculture. 1992. Forest land distribution data for the United States. http://www.epa.gov/docs/grd/forest_inventory/. Forest Service.
- US Department of Agriculture. 1994. State soil geographic (STATSGO) database – Data use information. Natural Resources Conservation Service. Miscellaneous Publication No. 1492. pp. 107.
- Waring, R.H., and S.W. Running. 1998. Forest Ecosystems: Analysis at Multiple Scales. 2nd edition. Academic Press: San Diego. Pp. 161-164.
- Williams, Darrel. 2004. <http://landsat.gsfc.nasa.gov/project/Comparison.html>. Web Curator: Laura Rocchio. Last modified 21 May 2004. Site visited on 2 Feb 2005.

- VanShaar, J.R., Haddeland, I., and D.P Lettenmaier. 2002. Effects of land-cover changes on the hydrological response of interior Columbia River basin forested catchments. *Hydrological Processes*. 16: 2499-2520.
- Vogelmann, J.E., Sohl, T.L., Campbell, P.V., and D.M. Shaw. 1998. Regional land cover characterization using Landsat Thematic Mapper data ancillary data sources. *Environmental Monitoring and Assessment*. 51: 415-428.
- Zhu, Z. and D.L. Evans. 1992. Mapping midsouth forest distributions. *Journal of Forestry*.

APPENDIX A: MODIS-DERIVED REGRESSION TREES

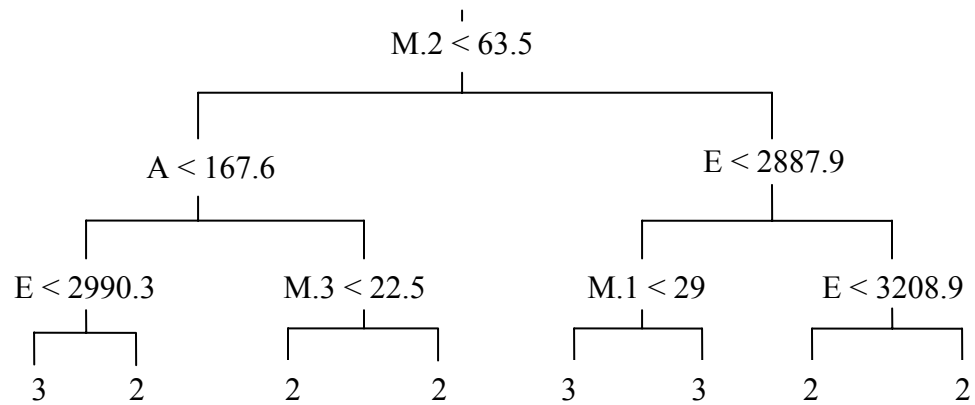


Figure A.1. Forest classification regression tree without the use of Landsat imagery as discriminating variables. Variables used for classification include MODIS bands 1-3 (M.x), elevation (E), and aspect (A). The two forest classes are coniferous forest (2) and deciduous forest (3).

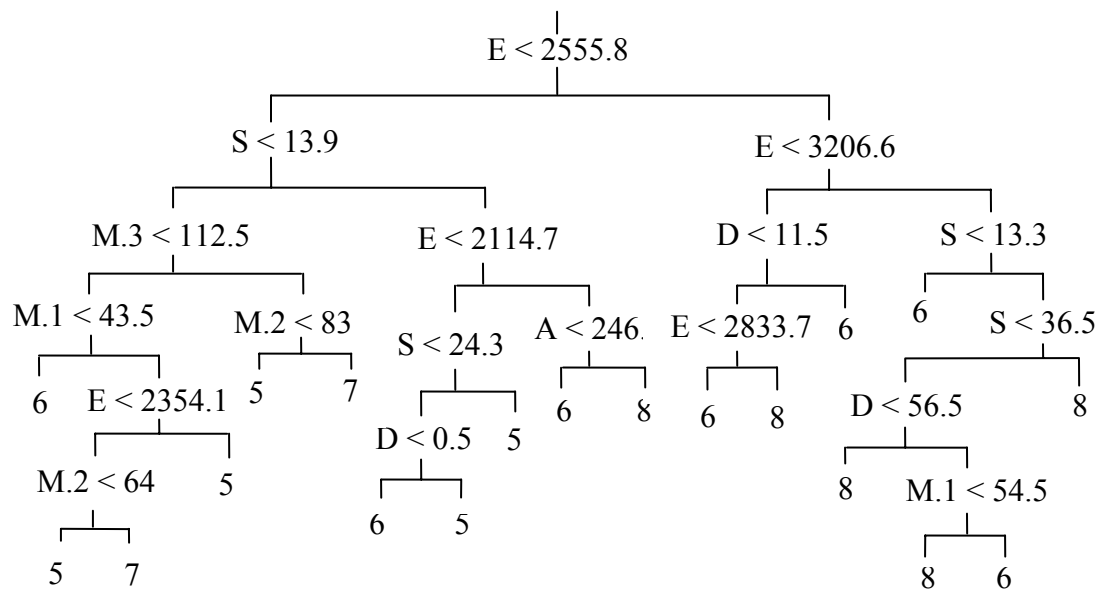


Figure A.2. Non-forest classification regression tree without the use of Landsat imagery as discriminating variables. Variables used for classification include MODIS bands 1-3 (M.x), elevation (E), canopy density (D), slope (S), and aspect (A). The non-forest classes are shrubland (5), grassland/herbaceous (6), agricultural land (7), and barren/sparsely vegetated (8).

APPENDIX B: DATA CROSSWALK TO LOWEST COMMON CLASSIFICATION SCHEME

Table B.1. Crosswalk of IGBP (MODIS) classes to a common framework with respect to classes present in the Yampa River Basin.

Aggregated Class	IGBP (MODIS)
1 Mixed forest	Mixed forests (5) Woody savanna (8)
2 Coniferous forest	Evergreen needleleaf forest (1) Evergreen broadleaf forest (2)
3 Deciduous forest	Deciduous needleleaf forest (3) Deciduous broadleaf forest (4)
4 Transitional forest	
5 Shrubland	Closed shrubland (6) Open shrublands (7)
6 Grassland/herbaceous	Savannas (9) Grasslands (10)
7 Agricultural land	Croplands (12) Cropland/natural vegetation mosaic (14)
8 Barren/sparsely vegetated	Barren or sparsely vegetated (16)
9 Water	Water (0)
10 Wetlands	Permanent wetlands (11)
11 Urban	Urban and built-up (13)
12 Snow and ice	
13 Forest/field mosaic	
255 Unclassified	

Table B.2. Crosswalk of UMD classes to a common framework with respect to classes present in the Yampa River Basin.

Aggregated Class	UMD
1 Mixed forest	Mixed forests (5) Woody savannas (8)
2 Coniferous forest	Evergreen needleleaf forest (1) Evergreen broadleaf forest (2)
3 Deciduous forest	Deciduous needleleaf forest (3) Deciduous broadleaf forest (4)
4 Transitional forest	
5 Shrubland	Closed shrubland (6) Open shrublands (7)
6 Grassland/herbaceous	Savannas (9) Grasslands (10)
7 Agricultural land	Croplands (12)
8 Barren/sparsely vegetated	Barren or sparsely vegetated (16)
9 Water	Water (0)
10 Wetlands	
11 Urban	Urban and built-up (13)
12 Snow and ice	
13 Forest/field mosaic	
255 Unclassified	

Table B.3. Crosswalk of LAI/fPAR classes to a common framework with respect to classes present in the Yampa River Basin.

Aggregated Class	LAI/fPAR (MODIS)
1 Mixed forest	Broadleaf forest (5) Needleleaf forest (6)
2 Coniferous forest	
3 Deciduous forest	
4 Transitional forest	
5 Shrubland	Shrubs (2)
6 Grassland/herbaceous	Savanna (4)
7 Agricultural land	Grasses/cereal crops (1)
8 Barren/sparsely vegetated	Unvegetated (7)
9 Water	Water (0)
10 Wetlands	
11 Urban	Urban (8)
12 Snow and ice	
13 Forest/field mosaic	
255 Unclassified	Unclassified 255

Table B.4. Crosswalk of composite USFS/USGS classes to a common framework with respect to classes present in the Yampa River Basin.

Aggregated Class	USFS/USGS
1 Mixed forest	Mixed Forest (115)
2 Coniferous forest	Western white pine (14) Redwood (18) Evergreen coniferous forest (113)
3 Deciduous forest	Larch (16) Broadleaf deciduous forest (112) Western hardwoods (21) Aspen-birch (22)
4 Transitional forest	
5 Shrubland	Pinyon-juniper (20) Shrubland (108)
6 Grassland/herbaceous	Grassland (107) Savanna (111)
7 Agricultural land	Dryland cropland and pasture (102) Irrigated cropland and pasture (103) Cropland/woodland mosaic (106)
8 Barren/sparsely vegetated	
9 Water	
10 Wetlands	
11 Urban	Urban or built-up land (101)
12 Snow and ice	
13 Forest/field mosaic	
255 Unclassified	

Table B.5. Crosswalk of USGS LULC classification scheme to a common framework with respect to classes present in the Yampa River Basin.

Aggregated Class	USGS LULC
1 Mixed forest	Mixed forest (15)
2 Coniferous forest	Evergreen needleleaf forest (14)
3 Deciduous forest	Deciduous broadleaf forest (11)
4 Transitional forest	
5 Shrubland	Shrubland (8)
6 Grassland/herbaceous	Grassland (7) Savanna (10)
7 Agricultural land	Dryland cropland and pasture (2) Irrigated cropland and pasture (3)
8 Barren/sparsely vegetated	
9 Water	
10 Wetlands	
11 Urban	Urban and built-up land (1)
12 Snow and ice	
13 Forest/field mosaic	Cropland/woodland mosaic (6)
255 Unclassified	

Table B.6. Crosswalk of IGBP (AVHRR) classification scheme to a common framework with respect to classes present in the Yampa River Basin.

Aggregated Class	IGBP (AVHRR)
1 Mixed forest	Mixed forests (5) Woody savanna (8)
2 Coniferous forest	Evergreen needleleaf forest (1)
3 Deciduous forest	Deciduous broadleaf forest (4)
4 Transitional forest	
5 Shrubland	Closed shrubland (6) Open shrublands (7)
6 Grassland/herbaceous	Grasslands (10)
7 Agricultural land	Croplands (12) Cropland/natural vegetation mosaic (14)
8 Barren/sparsely vegetated	
9 Water	
10 Wetlands	
11 Urban	Urban and built-up (13)
12 Snow and ice	
13 Forest/field mosaic	
255 Unclassified	

Table B.7. Crosswalk of SLCR classification scheme to a common framework with respect to classes present in the Yampa River Basin.

Aggregated Class	SLCR
1 Mixed forest	Mixed boreal forest (aspen, birch, spruce, pine) (16) Deciduous woodlands (aspen)/shrubland (mountain mahogany) (46) Open mixed forest (aspen, birch, white spruce, black spruce) (64) Mixed forest (aspen, birch, balsam poplar, black and white spruce) (65) Mixed forest (black and white spruce, aspen, birch) (67) Mixed forest (aspen, birch, spruce, balsam fir) (70) Open deciduous woodland (oak, populus) with evergreen needleleaf species (110)
2 Coniferous forest	Spruce forest (1) Ponderosa, lodgepole pine forest (4) Evergreen needleleaf forest (lodgepole pine and douglas fir) (6) Needleleaf forest (douglas fir, spruce, western red cedar) (7) Open evergreen needleleaf forest (ponderosa pine) (8) Evergreen needleleaf forest (lodgepole pine, englemann spruce, ponderosa pine) (10) Ponderosa/lodgepole pine woodland (12) Evergreen needleleaf forest (ponderosa pine, douglas fir, western red cedar) (14) Evergreen needleleaf forest (douglas fir, lodgepole pine, larch, western red cedar) (15) Open needleleaf forest (ponderosa pine and lodgepole pine) (17) Needleleaf forest (western red cedar, lodgepole pine, douglas fir, larch, ponderosa pine) (18) Needleleaf forest (ponderosa, lodgepole and white pine, douglas fir) (21) Needleleaf forest (douglas fir, lodgepole pine, western white pine) (24) Evergreen needleleaf forest (douglas fir, ponderosa, jeffrey pine) (26) Subalpine forest (englemann spruce, subalpine fir, douglas fir) (54)
3 Deciduous forest	Deciduous forest (aspen) (48)
4 Transitional forest	
5 Shrubland	Deciduous shrubland (oak) with pinyon juniper (84) Shrubland/grassland (needlegrass, big sage, rabbitbrush) (102) Juniper woodland (108)
6 Grassland/herbaceous	Grassland (short- mid grass prairie) (123) Grassland with shrubland (127)
7 Agricultural land	Grassland/shrubland with crops, fallow (131) Irrigated agriculture (144) Irrigated agriculture (150)
8 Barren/sparsely vegetated	
9 Water	
10 Wetlands	
11 Urban	
12 Snow and ice	
13 Forest/field mosaic	Cropland (corn, other row crops, forage crops) with woodland (151) Cropland/deciduous dry forest mosaic (187)
255 Unclassified	

Table B.8. Crosswalk of SiB classification scheme to a common framework with respect to classes present in the Yampa River Basin.

Aggregated Class	SiB Class
1 Mixed forest	
2 Coniferous forest	Evergreen needleleaf trees (4)
3 Deciduous forest	Broadleaf deciduous trees (2)
4 Transitional forest	
5 Shrubland	Ground cover with trees and shrubs (6) Broadleaf shrubs with perennial ground cover (8) Broadleaf shrubs with bare soil (9) Groundcover with dwarf trees and shrubs (10)
6 Grassland/herbaceous	
7 Agricultural land	Agriculture or C3 grassland (12)
8 Barren/sparsely vegetated	
9 Water	
10 Wetlands	
11 Urban	
12 Snow and ice	
13 Forest/field mosaic	
255 Unclassified	

Table B.9. Crosswalk of SiB2 classification scheme to a common framework with respect to classes present in the Yampa River Basin.

Aggregated Class	SiB2 Class
1 Mixed forest	
2 Coniferous forest	Needleleaf evergreen trees (4)
3 Deciduous forest	Broadleaf deciduous trees (2)
4 Transitional forest	
5 Shrubland	Shrubs with bare soil (7) Dwarf trees and shrubs (8)
6 Grassland/herbaceous	Short vegetation/C4 grassland (6)
7 Agricultural land	Agriculture or C3 grassland (9)
8 Barren/sparsely vegetated	
9 Water	
10 Wetlands	
11 Urban	
12 Snow and ice	
13 Forest/field mosaic	
255 Unclassified	

Table B.10. Crosswalk of OGE classification scheme to a common framework with respect to classes present in the Yampa River Basin.

Aggregated Class	OGE Class
1 Mixed forest	Small leaf mixed woods (60) Woody savanna (91)
2 Coniferous forest	Conifer boreal forest (21) Cool conifer forest (22) Narrow conifers (62)
3 Deciduous forest	Deciduous broadleaf forest (5)
4 Transitional forest	
5 Shrubland	Shrub deciduous (17) Dry woody scrub (47) Semi desert sage (52)
6 Grassland/herbaceous	Cool grasses and shrubs (40)
7 Agricultural land	Cool crops and towns (30) Cool irrigated cropland (38)
8 Barren/sparsely vegetated	
9 Water	
10 Wetlands	
11 Urban	Urban (1)
12 Snow and ice	
13 Forest/field mosaic	Forest and field (56)
255 Unclassified	

Table B.11. Crosswalk of BATS classification scheme to a common framework with respect to classes present in the Yampa River Basin.

Aggregated Class	BATS Class
1 Mixed forest	
2 Coniferous forest	Evergreen needleleaf trees (3)
3 Deciduous forest	Deciduous broadleaf trees (5)
4 Transitional forest	
5 Shrubland	Evergreen shrubs (16) Deciduous shrubs (17)
6 Grassland/herbaceous	
7 Agricultural land	Crops, mixed farming (1) Irrigated crops (10) Short grass (2)
8 Barren/sparsely vegetated	Semidesert (11)
9 Water	
10 Wetlands	
11 Urban	
12 Snow and ice	
13 Forest/field mosaic	Forest/field mosaic (19)
255 Unclassified	

Table B.12. Crosswalk of VEGETATION LIFEFORMS classification scheme to a common framework with respect to classes present in the Yampa River Basin.

Aggregated Class	Vegetation Lifeforms Class
1 Mixed forest	
2 Coniferous forest	Evergreen needleleaf vegetation (1) Evergreen broadleaf vegetation (2)
3 Deciduous forest	Deciduous broadleaf vegetation (4)
4 Transitional forest	
5 Shrubland	
6 Grassland/herbaceous	
7 Agricultural land	Annual broadleaf vegetation (5) Annual grass vegetation (6)
8 Barren/sparsely vegetated	
9 Water	
10 Wetlands	
11 Urban	
12 Snow and ice	
13 Forest/field mosaic	
255 Unclassified	

Table B.13. Crosswalk of NLCD classification scheme to a common framework with respect to classes present in the Yampa River Basin.

Aggregated Class	NLCD
1 Mixed forest	Mixed forest (43)
2 Coniferous forest	Evergreen forest (42)
3 Deciduous forest	Deciduous forest (41)
4 Transitional forest	Transitional (33)
5 Shrubland	Shrubland (51)
6 Grassland/herbaceous	Grasslands/herbaceous (71)
7 Agricultural land	Pasture/hay (81) Row crops (82) Small grains (83) Urban/recreational grasses (85)
8 Barren/sparsely vegetated	Bare rock/sand/clay (31) Quarries/strip mines/gravel pits (32)
9 Water	Open water (11)
10 Wetlands	Woody wetlands (91) Emergent herbaceous wetlands (92)
11 Urban	Residential (low intensity) (21) Residential (high density) (22) Commercial/industrial/transportation (23)
12 Snow and ice	Perennial ice/snow (12)
13 Forest/field mosaic	
255 Unclassified	

Table B.14. Crosswalk of CVM classification scheme to a common framework with respect to classes present in the Yampa River Basin.

Aggregated Class	CVM Class
1 Mixed forest	Mixed forest (43)
2 Coniferous forest	Ponderosa pine foothill (421) Ponderosa pine montane (422) Ponderosa pine with douglas fir (423) Douglas fir (424) Lodgepole pine with douglas fir (428) Lodgepole pine (429) Engelmann spruce/subalpine fir (432) Limber pine (435) Mixed woodland (440) Pinyon-juniper (441) Krummholtz (450)
3 Deciduous forest	Deciduous riparian (411) Aspen (412)
4 Transitional forest	Transitional (33)
5 Shrubland	Shrub - alpine (510) Shrub - subalpine (511) Subalpine riparian shrub (512) Shrub - riparian (513) Deciduous western intermountain (514) Deciduous central/front range (515) Salt desert shrub (516) Sagebrush intermountain (517) Gambel oak (520)
6 Grassland/herbaceous	Alpine meadow (711) Subalpine meadow (712) Riparian grass (713) Foothills/intermountain (716)
7 Agricultural land	Agriculture - pasture/hay (81) Agriculture - row crops (82) Agriculture - small grains (83) Urban-recreational grass (85)
8 Barren/sparsely vegetated	Bare rock/sand/clay (31) Quarries/mines/gravels (32)
9 Water	Water (11)
10 Wetlands	Wetland - woody (91) Wetland - herbaceous (92)
11 Urban	Residential (low density) (21) Residential (high density) (22) Commercial/ind./trans. (23)
12 Snow and ice	Ice/snow (12)
13 Forest/field mosaic	
255 Unclassified	

APPENDIX C: DATA CROSSWALK TO LOWEST USFS/USGS COMPOSITE CLASSIFICATION SCHEME

Table C.1. Crosswalk of IGBP (MODIS) classes to USFS/USGS composite classification scheme with respect to classes present in the Yampa River Basin.

USFS/USGS Class	IGBP (MODIS) Class
1 White-red-jack pine	
2 Spruce-fir	
3 Longleaf-slash pine	
4 Loblolly-shortleaf pine	
5 Oak-pine	
6 Oak-hickory	
7 Oak-gum-cypress	
8 Elm-ash-cottonwood	
9 Maple-beech-birch	
10 Douglas-fir	
12 Hemlock-sitka spruce	
13 Ponderosa pine	
14 Western white pine	
15 Lodgepole pine	
16 Larch	
17 Fir-spruce	
18 Redwood	
19 Chaparral	
20 Pinyon-juniper	
21 Western hardwoods	
22 Aspen-birch	
23 Nonforest	
101 Urban or built-up land	Urban and built-up (13)
102 Dryland cropland and pasture	
103 Irrigated cropland and pasture	
104 Mixed dryland/irrigated cropland and pasture	Croplands (12)
105 Cropland/grassland mosaic	
106 Cropland/woodland mosaic	Cropland/natural vegetation mosaic (14)
107 Grassland	Grasslands (10)

108 Shrubland	Closed shrubland (6) Open shrublands (7)
109 Mixed shrubland/grassland	
110 Chaparral	
111 Savanna	Savannas (9)
112 Broadleaf deciduous forest	Deciduous broadleaf forest (4)
113 Evergreen coniferous forest	Evergreen needleleaf forest (1)
114 Subalpine forest	
115 Mixed forest	Mixed forests (5) Woody savanna (8)
116 Deciduous coniferous forest	Deciduous needleleaf forest (3)
117 Evergreen broadleaf forest	Evergreen broadleaf forest (2)
118 Water bodies	Water (0)
119 Herbaceous wetland	Permanent wetlands (11)
120 Forested wetland	
121 Barren or sparsely vegetated	Barren or sparsely vegetated (16)
122 Wooded tundra	
123 Herbaceous tundra	
124 Bare ground tundra	
125 Wet tundra	
126 Mixed tundra	
127 Perennial snowfields or glaciers	

Table C.2. Crosswalk of UMD classes to USFS/USGS composite classification scheme with respect to classes present in the Yampa River Basin.

USFS/USGS Class	UMD Class
1 White-red-jack pine	
2 Spruce-fir	
3 Longleaf-slash pine	
4 Loblolly-shortleaf pine	
5 Oak-pine	
6 Oak-hickory	
7 Oak-gum-cypress	
8 Elm-ash-cottonwood	
9 Maple-beech-birch	
10 Douglas-fir	
12 Hemlock-sitka spruce	
13 Ponderosa pine	
14 Western white pine	
15 Lodgepole pine	
16 Larch	
17 Fir-spruce	
18 Redwood	
19 Chaparral	
20 Pinyon-juniper	
21 Western hardwoods	
22 Aspen-birch	

23 Nonforest	
101 Urban or built-up land	Urban and built-up (13)
102 Dryland cropland and pasture	
103 Irrigated cropland and pasture	
104 Mixed dryland/irrigated cropland and pasture	Croplands (12)
105 Cropland/grassland mosaic	
106 Cropland/woodland mosaic	
107 Grassland	Grasslands (10)
108 Shrubland	Closed shrubland (6) Open shrublands (7)
109 Mixed shrubland/grassland	
110 Chaparral	
111 Savanna	Savannas (9)
112 Broadleaf deciduous forest	Deciduous broadleaf forest (4)
113 Evergreen coniferous forest	Evergreen needleleaf forest (1)
114 Subalpine forest	
115 Mixed forest	Mixed forests (5) Woody savannas (8)
116 Deciduous coniferous forest	Deciduous needleleaf forest (3)
117 Evergreen broadleaf forest	Evergreen broadleaf forest (2)
118 Water bodies	Water (0)
119 Herbaceous wetland	
120 Forested wetland	
121 Barren or sparsely vegetated	Barren or sparsely vegetated (16)
122 Wooded tundra	
123 Herbaceous tundra	
124 Bare ground tundra	
125 Wet tundra	
126 Mixed tundra	
127 Perennial snowfields or glaciers	

Table C.3. Crosswalk of LAI/fPAR classes to USFS/USGS composite classification scheme with respect to classes present in the Yampa River Basin.

USFS/USGS Class	LAI/fPAR Class
1 White-red-jack pine	
2 Spruce-fir	
3 Longleaf-slash pine	
4 Loblolly-shortleaf pine	
5 Oak-pine	
6 Oak-hickory	
7 Oak-gum-cypress	
8 Elm-ash-cottonwood	
9 Maple-beech-birch	
10 Douglas-fir	
12 Hemlock-sitka spruce	
13 Ponderosa pine	
14 Western white pine	

15 Lodgepole pine	
16 Larch	
17 Fir-spruce	
18 Redwood	
19 Chaparral	
20 Pinyon-juniper	
21 Western hardwoods	
22 Aspen-birch	
23 Nonforest	
101 Urban or built-up land	Urban (8)
102 Dryland cropland and pasture	
103 Irrigated cropland and pasture	
104 Mixed dryland/irrigated cropland and pasture	
105 Cropland/grassland mosaic	Grasses/cereal crops (1)
106 Cropland/woodland mosaic	
107 Grassland	
108 Shrubland	Shrubs (2)
109 Mixed shrubland/grassland	
110 Chaparral	
111 Savanna	Savanna (4)
112 Broadleaf deciduous forest	
113 Evergreen coniferous forest	
114 Subalpine forest	
115 Mixed forest	Broadleaf forest (5) Needleleaf forest (6)
116 Deciduous coniferous forest	
117 Evergreen broadleaf forest	
118 Water bodies	Water (0)
119 Herbaceous wetland	
120 Forested wetland	
121 Barren or sparsely vegetated	Unvegetated (7)
122 Wooded tundra	
123 Herbaceous tundra	
124 Bare ground tundra	
125 Wet tundra	
126 Mixed tundra	
127 Perennial snowfields or glaciers	

Table C.4. Crosswalk of USGS LULC classes to USFS/USGS composite classification scheme with respect to classes present in the Yampa River Basin.

USFS/USGS Class	USGS LULC Class
1 White-red-jack pine	
2 Spruce-fir	
3 Longleaf-slash pine	
4 Loblolly-shortleaf pine	
5 Oak-pine	
6 Oak-hickory	
7 Oak-gum-cypress	
8 Elm-ash-cottonwood	
9 Maple-beech-birch	
10 Douglas-fir	
12 Hemlock-sitka spruce	
13 Ponderosa pine	
14 Western white pine	
15 Lodgepole pine	
16 Larch	
17 Fir-spruce	
18 Redwood	
19 Chaparral	
20 Pinyon-juniper	
21 Western hardwoods	
22 Aspen-birch	
23 Nonforest	
101 Urban or built-up land	Urban and built-up land (1)
102 Dryland cropland and pasture	Dryland cropland and pasture (2)
103 Irrigated cropland and pasture	Irrigated cropland and pasture (3)
104 Mixed dryland/irrigated cropland and pasture	
105 Cropland/grassland mosaic	
106 Cropland/woodland mosaic	Cropland/woodland mosaic (6)
107 Grassland	Grassland (7)
108 Shrubland	Shrubland (8)
109 Mixed shrubland/grassland	
110 Chaparral	
111 Savanna	Savanna (10)
112 Broadleaf deciduous forest	Deciduous broadleaf forest (11)
113 Evergreen coniferous forest	Evergreen needleleaf forest (14)
114 Subalpine forest	
115 Mixed forest	Mixed forest (15)
116 Deciduous coniferous forest	
117 Evergreen broadleaf forest	
118 Water bodies	
119 Herbaceous wetland	
120 Forested wetland	
121 Barren or sparsely vegetated	
122 Wooded tundra	
123 Herbaceous tundra	

124 Bare ground tundra	
125 Wet tundra	
126 Mixed tundra	
127 Perennial snowfields or glaciers	

Table C.5. Crosswalk of IGBP (AVHRR) classes to USFS/USGS composite classification scheme with respect to classes present in the Yampa River Basin.

USFS/USGS Class	IGBP (AVHRR) Class
1 White-red-jack pine	
2 Spruce-fir	
3 Longleaf-slash pine	
4 Loblolly-shortleaf pine	
5 Oak-pine	
6 Oak-hickory	
7 Oak-gum-cypress	
8 Elm-ash-cottonwood	
9 Maple-beech-birch	
10 Douglas-fir	
12 Hemlock-sitka spruce	
13 Ponderosa pine	
14 Western white pine	
15 Lodgepole pine	
16 Larch	
17 Fir-spruce	
18 Redwood	
19 Chaparral	
20 Pinyon-juniper	
21 Western hardwoods	
22 Aspen-birch	
23 Nonforest	
101 Urban or built-up land	Urban and built-up (13)
102 Dryland cropland and pasture	
103 Irrigated cropland and pasture	
104 Mixed dryland/irrigated cropland and pasture	Croplands (12)
105 Cropland/grassland mosaic	
106 Cropland/woodland mosaic	Cropland/natural vegetation mosaic (14)
107 Grassland	Grasslands (10)
108 Shrubland	Closed shrubland (6) Open shrublands (7)
109 Mixed shrubland/grassland	
110 Chaparral	
111 Savanna	
112 Broadleaf deciduous forest	Deciduous broadleaf forest (4)
113 Evergreen coniferous forest	Evergreen needleleaf forest (1)
114 Subalpine forest	
115 Mixed forest	Mixed forests (5) Woody savanna (8)

116	Deciduous coniferous forest	
117	Evergreen broadleaf forest	
118	Water bodies	
119	Herbaceous wetland	
120	Forested wetland	
121	Barren or sparsely vegetated	
122	Wooded tundra	
123	Herbaceous tundra	
124	Bare ground tundra	
125	Wet tundra	
126	Mixed tundra	
127	Perennial snowfields or glaciers	

Table C.6. Crosswalk of SLCR classes to USFS/USGS composite classification scheme with respect to classes present in the Yampa River Basin.

USFS/USGS Class	SLCR Class	
1	White-red-jack pine	
2	Spruce-fir	Spruce forest (1)
3	Longleaf-slash pine	
4	Loblolly-shortleaf pine	
5	Oak-pine	Deciduous shrubland (oak) with pinyon juniper (84)
6	Oak-hickory	
7	Oak-gum-cypress	
8	Elm-ash-cottonwood	
9	Maple-beech-birch	
10	Douglas-fir	
12	Hemlock-sitka spruce	
13	Ponderosa pine	Open evergreen needleleaf forest (ponderosa pine) (8)
14	Western white pine	
15	Lodgepole pine	
16	Larch	
17	Fir-spruce	
18	Redwood	
19	Chaparral	
20	Pinyon-juniper	Juniper woodland (108)
21	Western hardwoods	
22	Aspen-birch	Deciduous forest (aspen) (48)
23	Nonforest	
101	Urban or built-up land	
102	Dryland cropland and pasture	
103	Irrigated cropland and pasture	Irrigated agriculture (144) Irrigated agriculture (150)
104	Mixed dryland/irrigated cropland and pasture	
105	Cropland/grassland mosaic	Grassland/shrubland with crops, fallow (131)

106 Cropland/woodland mosaic	Cropland (corn, other row crops, forage crops) with woodland (151) Cropland/deciduous dry forest mosaic (187)
107 Grassland	Grassland (short- mid grass prairie) (123)
108 Shrubland	
109 Mixed shrubland/grassland	Shrubland/grassland (needlegrass, big sage, rabbitbrush) (102) Grassland with shrubland (127)
110 Chaparral	
111 Savanna	
112 Broadleaf deciduous forest	
113 Evergreen coniferous forest	Ponderosa, lodgepole pine forest (4) Evergreen needleleaf forest (lodgepole pine and douglas fir) (6) Needleleaf forest (douglas fir, spruce, western red cedar) (7) Evergreen needleleaf forest (lodgepole pine, englemann spruce, ponderosa pine) (10) Ponderosa/lodgepole pine woodland (12) Evergreen needleleaf forest (ponderosa pine, douglas fir, western red cedar) (14) Evergreen needleleaf forest (douglas fir, lodgepole pine, larch, western red cedar) (15) Open needleleaf forest (ponderosa pine and lodgepole pine) (17) Needleleaf forest (western red cedar, lodgepole pine, douglas fir, larch, ponderosa pine) (18) Needleleaf forest (ponderosa, lodgepole and white pine, douglas fir) (21) Needleleaf forest (douglas fir, lodgepole pine, western white pine) (24) Evergreen needleleaf forest (douglas fir, ponderosa, jeffrey pine) (26)
114 Subalpine forest	Subalpine forest (englemann spruce, subalpine fir, douglas fir) (54)
115 Mixed forest	Mixed boreal forest (aspen, birch, spruce, pine) (16) Deciduous woodlands (aspen)/shrubland (mountain mahogany) (46) Open mixed forest (aspen, birch, white spruce, black spruce) (64) Mixed forest (aspen, birch, balsam poplar, black and white spruce) (65) Mixed forest (black and white spruce, aspen, birch) (67) Mixed forest (aspen, birch, spruce, balsam fir) (70) Open deciduous woodland (oak, populus) with evergreen needleleaf species (110)

116	Deciduous coniferous forest	
117	Evergreen broadleaf forest	
118	Water bodies	
119	Herbaceous wetland	
120	Forested wetland	
121	Barren or sparsely vegetated	
122	Wooded tundra	
123	Herbaceous tundra	
124	Bare ground tundra	
125	Wet tundra	
126	Mixed tundra	
127	Perennial snowfields or glaciers	

Table C.7. Crosswalk of SiB classes to USFS/USGS composite classification scheme with respect to classes present in the Yampa River Basin.

USFS/USGS Class	SiB Class	
1	White-red-jack pine	
2	Spruce-fir	
3	Longleaf-slash pine	
4	Loblolly-shortleaf pine	
5	Oak-pine	
6	Oak-hickory	
7	Oak-gum-cypress	
8	Elm-ash-cottonwood	
9	Maple-beech-birch	
10	Douglas-fir	
12	Hemlock-sitka spruce	
13	Ponderosa pine	
14	Western white pine	
15	Lodgepole pine	
16	Larch	
17	Fir-spruce	
18	Redwood	
19	Chaparral	
20	Pinyon-juniper	
21	Western hardwoods	
22	Aspen-birch	
23	Nonforest	
101	Urban or built-up land	
102	Dryland cropland and pasture	
103	Irrigated cropland and pasture	
104	Mixed dryland/irrigated cropland and pasture	
105	Cropland/grassland mosaic	Agriculture or C3 grassland (12)
106	Cropland/woodland mosaic	
107	Grassland	

108 Shrubland	Ground cover with trees and shrubs (6) Broadleaf shrubs with perennial ground cover (8) Broadleaf shrubs with bare soil (9) Groundcover with dwarf trees and shrubs (10)
109 Mixed shrubland/grassland	
110 Chaparral	
111 Savanna	
112 Broadleaf deciduous forest	Broadleaf deciduous trees (2)
113 Evergreen coniferous forest	Evergreen needleleaf trees (4)
114 Subalpine forest	
115 Mixed forest	
116 Deciduous coniferous forest	
117 Evergreen broadleaf forest	
118 Water bodies	
119 Herbaceous wetland	
120 Forested wetland	
121 Barren or sparsely vegetated	
122 Wooded tundra	
123 Herbaceous tundra	
124 Bare ground tundra	
125 Wet tundra	
126 Mixed tundra	
127 Perennial snowfields or glaciers	

Table C.8. Crosswalk of SiB2 classes to USFS/USGS composite classification scheme with respect to classes present in the Yampa River Basin.

USFS/USGS Class	SiB2 Class
1 White-red-jack pine	
2 Spruce-fir	
3 Longleaf-slash pine	
4 Loblolly-shortleaf pine	
5 Oak-pine	
6 Oak-hickory	
7 Oak-gum-cypress	
8 Elm-ash-cottonwood	
9 Maple-beech-birch	
10 Douglas-fir	
12 Hemlock-sitka spruce	
13 Ponderosa pine	
14 Western white pine	
15 Lodgepole pine	
16 Larch	
17 Fir-spruce	
18 Redwood	
19 Chaparral	
20 Pinyon-juniper	

21 Western hardwoods	
22 Aspen-birch	
23 Nonforest	
101 Urban or built-up land	
102 Dryland cropland and pasture	
103 Irrigated cropland and pasture	
104 Mixed dryland/irrigated cropland and pasture	
105 Cropland/grassland mosaic	Agriculture or C3 grassland (9)
106 Cropland/woodland mosaic	
107 Grassland	
108 Shrubland	Shrubs with bare soil (7) Dwarf trees and shrubs (8)
109 Mixed shrubland/grassland	Short vegetation/C4 grassland (6)
110 Chaparral	
111 Savanna	
112 Broadleaf deciduous forest	Broadleaf deciduous trees (2)
113 Evergreen coniferous forest	Needleleaf evergreen trees (4)
114 Subalpine forest	
115 Mixed forest	
116 Deciduous coniferous forest	
117 Evergreen broadleaf forest	
118 Water bodies	
119 Herbaceous wetland	
120 Forested wetland	
121 Barren or sparsely vegetated	
122 Wooded tundra	
123 Herbaceous tundra	
124 Bare ground tundra	
125 Wet tundra	
126 Mixed tundra	
127 Perennial snowfields or glaciers	

Table C.9. Crosswalk of OGE classes to USFS/USGS composite classification scheme with respect to classes present in the Yampa River Basin.

USFS/USGS Class	OGE Class
1 Whit-red-jack pine	
2 Spruce-fir	
3 Longleaf-slash pine	
4 Loblolly-shortleaf pine	
5 Oak-pine	
6 Oak-hickory	
7 Oak-gum-cypress	
8 Elm-ash-cottonwood	
9 Maple-beech-birch	
10 Douglas-fir	
12 Hemlock-sitka spruce	
13 Ponderosa pine	

14	Western white pine	
15	Lodgepole pine	
16	Larch	
17	Fir-spruce	
18	Redwood	
19	Chaparral	
20	Pinyon-juniper	
21	Western hardwoods	
22	Aspen-birch	
23	Nonforest	
101	Urban or built-up land	Urban (1)
102	Dryland cropland and pasture	
103	Irrigated cropland and pasture	Cool irrigated cropland (38)
104	Mixed dryland/irrigated cropland and pasture	Cool crops and towns (30)
105	Cropland/grassland mosaic	
106	Cropland/woodland mosaic	Forest and field (56)
107	Grassland	
108	Shrubland	Shrub deciduous (17) Dry woody scrub (47) Semi desert sage (52)
109	Mixed shrubland/grassland	Cool grasses and shrubs (40)
110	Chaparral	
111	Savanna	
112	Broadleaf deciduous forest	Deciduous broadleaf forest (5)
113	Evergreen coniferous forest	Conifer boreal forest (21) Cool conifer forest (22) Narrow conifers (62)
114	Subalpine forest	
115	Mixed forest	Woody savanna (91) Small leaf mixed woods (60)
116	Deciduous coniferous forest	
117	Evergreen broadleaf forest	
118	Water bodies	
119	Herbaceous wetland	
120	Forested wetland	
121	Barren or sparsely vegetated	
122	Wooded tundra	
123	Herbaceous tundra	
124	Bare ground tundra	
125	Wet tundra	
126	Mixed tundra	
127	Perennial snowfields or glaciers	

Table C.10. Crosswalk of BATS classes to USFS/USGS composite classification scheme with respect to classes present in the Yampa River Basin.

USFS/USGS Class	BATS Class
1 White-red-jack pine	
2 Spruce-fir	
3 Longleaf-slash pine	
4 Loblolly-shortleaf pine	
5 Oak-pine	
6 Oak-hickory	
7 Oak-gum-cypress	
8 Elm-ash-cottonwood	
9 Maple-beech-birch	
10 Douglas-fir	
12 Hemlock-sitka spruce	
13 Ponderosa pine	
14 Western white pine	
15 Lodgepole pine	
16 Larch	
17 Fir-spruce	
18 Redwood	
19 Chaparral	
20 Pinyon-juniper	
21 Western hardwoods	
22 Aspen-birch	
23 Nonforest	
101 Urban or built-up land	
102 Dryland cropland and pasture	
103 Irrigated cropland and pasture	Irrigated Crops (10)
104 Mixed dryland/irrigated cropland and pasture	Crops, Mixed Farming (1)
105 Cropland/grassland mosaic	
106 Cropland/woodland mosaic	Forest/Field Mosaic (19)
107 Grassland	Short Grass (2)
108 Shrubland	Evergreen Shrubs (16) Deciduous Shrubs (17)
109 Mixed shrubland/grassland	
110 Chaparral	
111 Savanna	
112 Broadleaf deciduous forest	Deciduous Broadleaf Trees (5)
113 Evergreen coniferous forest	Evergreen Needleleaf Trees (3)
114 Subalpine forest	
115 Mixed forest	
116 Deciduous coniferous forest	
117 Evergreen broadleaf forest	
118 Water bodies	
119 Herbaceous wetland	
120 Forested wetland	
121 Barren or sparsely vegetated	Semidesert (11)
122 Wooded tundra	

123 Herbaceous tundra	
124 Bare ground tundra	
125 Wet tundra	
126 Mixed tundra	
127 Perennial snowfields or glaciers	

Table C.11. Crosswalk of VEGETATION LIFEFORMS classes to USFS/USGS composite classification scheme with respect to classes present in the Yampa River Basin.

USFS/USGS Class	Vegetation Lifeforms Class
1 White-red-jack pine	
2 Spruce-fir	
3 Longleaf-slash pine	
4 Loblolly-shortleaf pine	
5 Oak-pine	
6 Oak-hickory	
7 Oak-gum-cypress	
8 Elm-ash-cottonwood	
9 Maple-beech-birch	
10 Douglas-fir	
12 Hemlock-sitka spruce	
13 Ponderosa pine	
14 Western white pine	
15 Lodgepole pine	
16 Larch	
17 Fir-spruce	
18 Redwood	
19 Chaparral	
20 Pinyon-juniper	
21 Western hardwoods	
22 Aspen-birch	
23 Nonforest	
101 Urban or built-up land	
102 Dryland cropland and pasture	
103 Irrigated cropland and pasture	
104 Mixed dryland/irrigated cropland and pasture	Annual Broadleaf Vegetation (5) Annual Grass Vegetation (6)
105 Cropland/grassland mosaic	
106 Cropland/woodland mosaic	
107 Grassland	
108 Shrubland	
109 Mixed shrubland/grassland	
110 Chaparral	
111 Savanna	
112 Broadleaf deciduous forest	Deciduous Broadleaf Vegetation (4)
113 Evergreen coniferous forest	Evergreen Needleleaf Vegetation (1)
114 Subalpine forest	

115 Mixed forest	
116 Deciduous coniferous forest	
117 Evergreen broadleaf forest	Evergreen Broadleaf Vegetation (2)
118 Water bodies	
119 Herbaceous wetland	
120 Forested wetland	
121 Barren or sparsely vegetated	
122 Wooded tundra	
123 Herbaceous tundra	
124 Bare ground tundra	
125 Wet tundra	
126 Mixed tundra	
127 Perennial snowfields or glaciers	

Table C.12. Crosswalk of NLCD classes to USFS/USGS composite classification scheme with respect to classes present in the Yampa River Basin.

USFS/USGS Class	
1 White-red-jack pine	
2 Spruce-fir	
3 Longleaf-slash pine	
4 Loblolly-shortleaf pine	
5 Oak-pine	
6 Oak-hickory	
7 Oak-gum-cypress	
8 Elm-ash-cottonwood	
9 Maple-beech-birch	
10 Douglas-fir	
12 Hemlock-sitka spruce	
13 Ponderosa pine	
14 Western white pine	
15 Lodgepole pine	
16 Larch	
17 Fir-spruce	
18 Redwood	
19 Chaparral	
20 Pinyon-juniper	
21 Western hardwoods	
22 Aspen-birch	
23 Nonforest	
101 Urban or built-up land	Residential (low intensity) (21) Residential (high density) (22) Commercial/industrial/transportation (23)
102 Dryland cropland and pasture	Pasture/hay (81)
103 Irrigated cropland and pasture	Urban/recreational grasses (85)
104 Mixed dryland/irrigated cropland and pasture	Row crops (82) Small grains (83)
105 Cropland/grassland mosaic	

106 Cropland/woodland mosaic	
107 Grassland	
108 Shrubland	Shrubland (51)
109 Mixed shrubland/grassland	Grasslands/herbaceous (71)
110 Chaparral	
111 Savanna	
112 Broadleaf deciduous forest	Deciduous forest (41)
113 Evergreen coniferous forest	Evergreen forest (42)
114 Subalpine forest	
115 Mixed forest	Mixed forest (43)
116 Deciduous coniferous forest	
117 Evergreen broadleaf forest	
118 Water bodies	Open water (11)
119 Herbaceous wetland	Emergent herbaceous wetlands (92)
120 Forested wetland	Woody wetlands (91)
121 Barren or sparsely vegetated	Bare rock/sand/clay (31) Quarries/strip mines/gravel pits (32) Transitional (33)
122 Wooded tundra	
123 Herbaceous tundra	
124 Bare ground tundra	
125 Wet tundra	
126 Mixed tundra	
127 Perennial snowfields or glaciers	Perennial ice/snow (12)

Table C.13. Crosswalk of CVM classes to USFS/USGS composite classification scheme with respect to classes present in the Yampa River Basin.

USFS/USGS Class	CVM Class
1 White-red-jack pine	
2 Spruce-fir	Engelmann spruce/subalpine fir (432)
3 Longleaf-slash pine	
4 Loblolly-shortleaf pine	
5 Oak-pine	
6 Oak-hickory	
7 Oak-gum-cypress	
8 Elm-ash-cottonwood	
9 Maple-beech-birch	
10 Douglas-fir	Douglas fir (424)
12 Hemlock-sitka spruce	
13 Ponderosa pine	Ponderosa pine foothill (421) Ponderosa pine montane (422)
14 Western white pine	
15 Lodgepole pine	Lodgepole pine (429)
16 Larch	
17 Fir-spruce	
18 Redwood	
19 Chaparral	

20 Pinyon-juniper	Pinyon-juniper (441)
21 Western hardwoods	
22 Aspen-birch	Aspen (412)
23 Nonforest	
101 Urban or built-up land	Residential (low density) (21) Residential (high density) (22) Commercial/ind./trans. (23)
102 Dryland cropland and pasture	Agriculture - pasture/hay (81)
103 Irrigated cropland and pasture	
104 Mixed dryland/irrigated cropland and pasture	Agriculture - row crops (82) Agriculture - small grains (83)
105 Cropland/grassland mosaic	
106 Cropland/woodland mosaic	
107 Grassland	Alpine meadow (711) Subalpine meadow (712) Riparian grass (713) Foothills/intermountain (716)
108 Shrubland	Shrub - alpine (510) Shrub - subalpine (511) Subalpine riparian shrub (512) Shrub - riparian (513) Deciduous western intermountain (514) Deciduous central/front range (515) Salt desert shrub (516) Sagebrush intermountain (517) Gambel oak (520)
109 Mixed shrubland/grassland	
110 Chaparral	
111 Savanna	
112 Broadleaf deciduous forest	Deciduous riparian (411)
113 Evergreen coniferous forest	Ponderosa pine with douglas fir (423) Lodgepole pine with douglas fir (428) Limber pine (435) Krummholtz (450) Mixed woodland (440)
114 Subalpine forest	
115 Mixed forest	Mixed forest (43)
116 Deciduous coniferous forest	
117 Evergreen broadleaf forest	
118 Water bodies	Water (11)
119 Herbaceous wetland	Wetland - herbaceous (92)
120 Forested wetland	Wetland - woody (91)
121 Barren or sparsely vegetated	Bare rock/sand/clay (31) Quarries/mines/gravels (32) Transitional (33)
122 Wooded tundra	
123 Herbaceous tundra	
124 Bare ground tundra	
125 Wet tundra	

126 Mixed tundra	
127 Perennial snowfields or glaciers	Ice/snow (12)

APPENDIX D: RAW ERROR MATRICES

Table D.1. Raw error matrix for the IGBP (MODIS) land cover map using the MVM for the reference points.

	2	3	5	6	7	8	9	11	Row Total
2	712396	366365	29134	374660	43293	131026	8629	3021	1668524
3	63002	367529	55642	299590	129740	83168	2889	5966	1007526
5	212321	296264	154147	366133	156770	185627	5960	2007	1379229
6	68674	371986	1517014	540702	1264914	322917	16424	8985	4111616
7	6905	52698	42126	79490	57279	34240	664	1129	274531
8	1	11	610	271	1234	117	0	0	2244
9	2594	4247	3989	3099	10749	841	3259	0	28778
11	0	0	3454	0	3592	843	0	3233	11122
Column Total	1065893	1459100	1806116	1663945	1667571	758779	37825	24341	8483570

Table D.2. Raw error matrix for the UMD land cover map using the MVM for the reference points.

	2	3	5	6	7	8	9	11	Row Total
2	712396	366365	29134	374660	43293	131026	8629	3021	1668524
3	63057	368236	55642	299969	129740	83183	2889	5966	1008682
5	212321	296264	154147	366133	156770	185627	5960	2007	1379229
6	68674	371986	1517014	540702	1264914	322917	16424	8985	4111616
7	6908	53924	42267	80070	57486	34395	664	1129	276843
8	1	11	610	271	1234	117	0	0	2244
9	2594	4247	3989	3099	10749	841	3259	0	28778
11	0	0	3454	0	3592	843	0	3233	11122
Column Total	1065951	1461033	1806257	1664904	1667778	758949	37825	24341	8487038

Table D.3. Raw error matrix for the LAI/fPAR land cover map using the MVM for the reference points.

	5	6	7	8	9	11	Row Total
5	154147	366133	156770	185627	5960	2007	870644
6	100715	259079	187939	91566	4435	2255	645989
7	1558234	604786	1317417	354149	17051	10114	3861751
8	610	271	1234	117	0	0	2232
9	3989	3099	10749	841	3259	0	21937
11	3454	0	3592	843	0	3233	11122
Column Total	1821149	1233368	1677701	633143	30705	17609	5413675

Table D.4. Raw error matrix for the USFS/USGS land cover map using the MVM for the reference points.

	2	3	5	6	7	11	Row Total
2	436762	246521	67285	359256	114440	2422	1226686
3	709710	806423	433842	821249	563346	11151	3345721
5	70085	701438	508969	689393	453992	3528	2427405
6	7954	21617	866796	116703	699891	8703	1721664
7	736	1417	33945	6413	37268	133	79912
11	0	0	4079	0	3022	924	8025
Column Total	1225247	1777416	1914916	1993014	1871959	26861	8809413

Table D.5. Raw error matrix for the USGS LULC land cover map using the MVM for the reference points.

	2	3	5	6	7	11	Row Total
2	609172	414925	83043	582164	158534	560	1848398
3	157458	856053	435636	909890	690893	14229	3064159
5	351962	444687	455043	288638	245148	2479	1787957
6	62587	45880	896143	162870	723068	8638	1899186
7	2354	10194	40700	23405	50905	0	127558
11	0	0	4113	0	3017	955	8085
Column Total	1183533	1771739	1914678	1966967	1871565	26861	8735343

Table D.6. Raw error matrix for the IGBP (AVHRR) land cover map using the MVM for the reference points.

	2	3	5	6	7	11	Row Total
2	609172	414925	83043	582164	158534	560	1848398
3	136675	835923	434913	887963	688461	14229	2998164
5	351962	444622	442527	288638	235034	2479	1765262
6	10354	35209	896099	138028	722385	8638	1810713
7	38423	15399	40744	41683	51109	0	187358
11	0	0	4113	0	3017	955	8085
Column Total	1146586	1746078	1901439	1938476	1858540	26861	8617980

Table D.7. Raw error matrix for the SLCR land cover map using the MVM for the reference points.

	2	3	5	6	7	Row Total
2	612997	415260	83045	590785	158543	1860630
3	112472	657622	94145	551540	287804	1703583
5	351962	444687	455043	288638	245148	1785478
6	8659	22216	897865	128264	719583	1776587
7	3847	22844	43047	32732	56724	159194
Column Total	1089937	1562629	1573145	1591959	1467802	7285472

Table D.8. Raw error matrix for the SiB land cover map using the MVM for the reference points.

	2	3	5	7	Row Total
2	614734	415368	83045	158543	1271690
3	157458	856053	435636	690893	2140040
5	414549	490567	1355299	971233	3231648
7	38423	15399	40744	51109	145675
Column Total	1225164	1777387	1914724	1871778	6789053

Table D.9. Raw error matrix for the SiB2 land cover map using the MVM for the reference points.

	2	3	5	6	7	Row Total
2	614734	415368	83045	590897	158543	1862587
3	157458	856053	435636	909890	690893	3049930
5	362316	479896	1355255	426666	970550	3594683
6	52233	10671	44	24842	683	88473
7	38423	15399	40744	41683	51109	187358
Column Total	1225164	1777387	1914724	1993978	1871778	8783031

Table D.10. Raw error matrix for the OGE land cover map using the MVM for the reference points.

	2	3	5	6	7	11	Row Total
2	610188	423124	79361	591151	151469	638	1855931
3	145198	838610	428615	876759	687939	14070	2991191
5	348882	433997	457480	294917	252561	2990	1790827
6	11554	37115	905635	145031	722937	7040	1829312
7	2450	11167	39573	22333	50907	0	126430
11	0	0	3187	0	2860	2123	8170
Column Total	1118272	1744013	1913851	1930191	1868673	26861	8601861

Table D.11. Raw error matrix for the BATS land cover map using the MVM for the reference points.

	2	3	5	7	8	Row Total
2	623961	410498	87734	160927	267145	1550265
3	150541	838928	452537	698486	300157	2440649
5	339608	464359	25475	48519	57587	935548
7	13575	42785	930701	768122	159464	1914647
8	623	533	417356	194589	51496	664597
Column Total	1128308	1757103	1913803	1870643	835849	7505706

Table D.12. Raw error matrix for the VEGETATION LIFEFORMS land cover map using the MVM for the reference points.

	2	3	7	Row Total
2	664343	418149	365252	1447744
3	546828	1316423	738497	2601748
7	13575	42785	768122	824482
Column Total	1224746	1777357	1871871	4873974

Table D.13. Raw error matrix for the NLCD land cover map using the MVM for the reference points.

	2	3	5	6	7	8	9	11	12	Row Total
2	958987	311612	394000	553182	343533	306086	5688	3081	12	2876181
3	135794	1226331	40989	696514	147539	124282	4402	851	4	2376706
5	2182	10291	840659	294887	606082	164031	1380	3831	42	1923385
6	68899	25068	464834	351280	328185	200937	3347	2533	1512	1446595
7	3765	62054	157806	44218	422070	31869	4500	4876	1	731159
8	3269	511	1369	8071	3796	25522	708	33	1614	44893
9	2306	789	2697	1180	2079	694	21520	40	3	31308
11	500	614	2777	1132	2654	539	292	11480	0	19988
12	2	2	0	39	0	133	0	0	194	370
Column Total	1175704	1637272	1905131	1950503	1855938	854093	41837	26725	3382	9450585

Table D.14. Raw error matrix for the CVM land cover map using the MVM for the reference points.

	2	3	5	6	7	8	9	11	12	Row Total
2	985672	294766	386140	557540	344522	315683	5840	3283	5	2893451
3	125019	1204949	33193	691411	128986	115926	4026	97	4	2303611
5	4226	73772	874884	315956	638396	170776	1838	5194	18	2085060
6	61495	21102	445340	342417	305703	195497	2984	2718	1569	1378825
7	3673	62372	162152	42936	433154	31900	4812	5195	0	746194
8	3169	464	1216	7187	3535	25370	677	22	1608	43248
9	2320	736	2707	1054	2033	644	21781	68	3	31346
11	49	194	567	380	1219	145	90	10166	0	12810
12	1	1	0	33	0	123	0	0	174	332
Column Total	1185624	1658356	1906199	1958914	1857548	856064	42048	26743	3381	9494877

APPENDIX E: NORMALIZED ERROR MATRICES USING MARGFIT

Table E.1. Normalized error matrix for the IGBP (MODIS) land cover map using the MVM for the reference points.

	2	3	5	6	7	8	9	11	Row Total
2	53.1	15.1	1.0	12.2	1.0	9.9	6.2	1.4	100.0
3	10.2	33.1	4.2	21.4	6.8	13.8	4.5	5.9	100.0
5	23.1	17.8	7.8	17.5	5.5	20.6	6.3	1.3	100.0
6	3.2	9.5	32.6	10.9	18.9	15.1	7.3	2.5	100.0
7	4.4	18.5	12.5	22.2	11.8	22.2	4.1	4.4	100.0
8	0.1	0.7	30.6	12.8	43.0	12.8	0.0	0.0	100.0
9	5.9	5.3	4.2	3.1	7.9	1.9	71.6	0.0	100.0
11	0.0	0.0	6.9	0.0	5.0	3.7	0.0	84.5	100.0
Column Total	100.0	100.0	100.0	100.0	100.0	100.0	100.0	100.0	

Table E.2. Normalized error matrix for the UMD land cover map using the MVM for the reference points.

	2	3	5	6	7	8	9	11	Row Total
2	53.1	15.1	1.0	12.2	1.0	10.0	6.2	1.4	100.0
3	10.3	33.0	4.2	21.4	6.8	13.8	4.5	5.9	100.0
5	23.1	17.8	7.9	17.5	5.5	20.6	6.3	1.3	100.0
6	3.2	9.4	32.6	10.9	18.9	15.1	7.3	2.5	100.0
7	4.4	18.8	12.5	22.1	11.8	22.1	4.1	4.4	100.0
8	0.1	0.7	30.7	12.8	43.0	12.8	0.0	0.0	100.0
9	5.9	5.3	4.2	3.1	7.9	1.9	71.6	0.0	100.0
11	0.0	0.0	6.9	0.0	5.0	3.7	0.0	84.5	100.0

Column

Total 100.0 100.0 100.0 100.0 100.0 100.0 100.0 100.0

Table E.3. Normalized error matrix for the LAI/fPAR land cover map using the MVM for the reference points.

	5	6	7	8	9	11	Row Total
5	12.4	32.3	8.7	35.6	8.1	2.9	100.0
6	11.9	33.5	15.2	25.8	8.8	4.8	100.0
7	35.0	14.9	20.4	19.0	6.5	4.1	100.0
8	30.0	14.6	41.7	13.7	0.0	0.0	100.0
9	5.6	4.7	10.3	2.8	76.6	0.0	100.0
11	5.2	0.0	3.7	3.0	0.0	88.1	100.0

Column

Total 100.0 100.0 100.0 100.0 100.0 100.0

Table E.4. Normalized error matrix for the USFS/USGS land cover map using the MVM for the reference points.

	2	3	5	6	7	11	Row Total
2	52.1	20.3	1.7	21.2	3.0	1.7	100.0
3	36.4	28.5	4.6	20.8	6.3	3.4	100.0
5	6.3	43.2	9.4	30.4	8.9	1.9	100.0
6	1.7	3.2	38.6	12.4	33.1	11.0	100.0
7	3.5	4.7	33.6	15.2	39.2	3.8	100.0
11	0.0	0.0	12.1	0.0	9.5	78.3	100.0
Column Total	100.0	100.0	100.0	100.0	100.0	100.0	

Table E.5. Normalized error matrix for the USGS LULC land cover map using the MVM for the reference points.

	2	3	5	6	7	11	Row Total
2	46.9	22.0	2.2	24.2	4.4	0.4	100.0
3	8.9	33.1	8.5	27.7	13.9	7.9	100.0
5	32.5	28.2	14.5	14.4	8.1	2.3	100.0
6	7.5	3.8	37.0	10.5	31.0	10.2	100.0
7	4.3	12.9	25.9	23.3	33.6	0.0	100.0
11	0.0	0.0	11.9	0.0	9.0	79.1	100.0
Column Total	100.0	100.0	100.0	100.0	100.0	100.0	

Table E.6. Normalized error matrix for the IGBP (AVHRR) land cover map using the MVM for the reference points.

	2	3	5	6	7	11	Row Total
2	39.2	24.6	2.9	27.0	5.9	0.5	100.0
3	5.7	32.3	9.8	26.9	16.7	8.6	100.0
5	25.5	29.7	17.2	15.1	9.8	2.6	100.0
6	0.9	2.8	41.3	8.6	35.8	10.7	100.0
7	28.7	10.6	16.3	22.4	22.0	0.0	100.0
11	0.0	0.0	12.5	0.0	9.8	77.7	100.0

Column							
Total	100.0	100.0	100.0	100.0	100.0	100.0	100.0

Table E.7. Normalized error matrix for the SLCR land cover map using the MVM for the reference points.

	2	3	5	6	7	Row Total
2	48.6	18.6	2.9	24.5	5.5	100.0
3	12.0	39.5	4.4	30.7	13.3	100.0
5	33.3	23.7	18.8	14.2	10.0	100.0
6	1.1	1.6	49.5	8.4	39.3	100.0
7	5.0	16.7	24.4	22.1	31.8	100.0

Column					
Total	100.0	100.0	100.0	100.0	100.0

Table E.8. Normalized error matrix for the SiB land cover map using the MVM for the reference points.

	2	3	5	7	Row Total
2	50.1	32.4	6.5	11.0	100.0
3	7.9	41.3	21.2	29.6	100.0
5	13.7	15.5	43.3	27.4	100.0
7	28.3	10.8	28.9	32.0	100.0
Column Total	100.0	100.0	100.0	100.0	

Table E.9. Normalized error matrix for the SiB2 land cover map using the MVM for the reference points.

	2	3	5	6	7	Row Total
2	25.1	29.0	7.0	27.0	11.8	100.0
3	3.3	30.5	18.8	21.2	26.3	100.0
5	5.8	13.2	45.0	7.7	28.4	100.0
6	52.5	18.3	0.1	27.9	1.3	100.0
7	13.3	9.1	29.2	16.2	32.3	100.0
Column Total	100.0	100.0	100.0	100.0	100.0	

Table E.10. Normalized error matrix for the OGE land cover map using the MVM for the reference points.

	2	3	5	6	7	11	Row Total
2	49.1	21.2	2.0	23.6	3.9	0.3	100.0
3	9.5	34.1	8.7	28.3	14.2	5.3	100.0
5	34.7	26.9	14.2	14.5	7.9	1.7	100.0
6	1.8	3.5	42.9	10.9	34.7	6.2	100.0
7	5.0	14.2	25.2	22.6	32.9	0.0	100.0
11	0.0	0.0	7.0	0.0	6.4	86.6	100.0
Column Total	100.0	100.0	100.0	100.0	100.0	100.0	

Table E.11. Normalized error matrix for the BATS land cover map using the MVM for the reference points.

	2	3	5	7	8	Row Total
2	45.4	20.6	2.5	6.0	25.5	100.0
3	9.1	34.8	10.7	21.7	23.7	100.0
5	44.1	41.6	1.3	3.2	9.8	100.0
7	1.3	2.9	36.1	39.0	20.6	100.0
8	0.2	0.1	49.3	30.1	20.3	100.0
Column Total	100.0	100.0	100.0	100.0	100.0	

Table E.12. Normalized error matrix for the VEGETATION LIFEFORMS land cover map using the MVM for the reference points.

	2	3	7	Row Total
2	62.3	29.2	8.5	100.0
3	32.0	57.3	10.7	100.0
7	5.7	13.5	80.8	100.0
Column Total	100.0	100.0	100.0	

Table E.13. Normalized error matrix for the NLCD land cover map using the MVM for the reference points.

	2	3	5	6	7	8	9	11	12	Row Total
2	54.8	12.4	6.9	12.3	5.2	7.3	0.6	0.5	0.0	100.0
3	9.9	62.3	0.9	19.6	2.8	3.8	0.6	0.2	0.0	100.0
5	0.3	1.2	41.4	18.3	25.7	10.9	0.4	1.8	0.0	100.0
6	12.5	3.2	25.9	24.6	15.7	15.1	1.0	1.3	0.6	100.0
7	1.4	16.7	18.7	6.6	43.0	5.1	3.0	5.4	0.0	100.0
8	13.9	1.5	1.8	13.3	4.3	45.1	5.2	0.4	14.6	100.0
9	5.5	1.3	2.0	1.1	1.3	0.7	87.9	0.3	0.0	100.0
11	1.4	1.2	2.3	1.2	1.9	0.6	1.4	90.1	0.0	100.0
12	0.4	0.3	0.0	3.1	0.0	11.4	0.0	0.0	84.8	100.0
Column Total	100.0	100.0	100.0	100.0	100.0	100.0	100.0	100.0	100.0	

Table E.14. Normalized error matrix for the CVM land cover map using the MVM for the reference points.

	2	3	5	6	7	8	9	11	12	Row Total
2	56.3	10.8	7.1	12.4	5.3	7.3	0.6	0.3	0.0	100.0
3	9.9	61.1	0.8	21.2	2.7	3.7	0.5	0.0	0.0	100.0
5	0.6	6.7	39.8	17.3	24.1	9.8	0.4	1.2	0.0	100.0
6	11.7	2.6	27.3	25.3	15.6	15.1	1.0	0.8	0.6	100.0
7	1.4	15.5	20.2	6.5	44.9	5.0	3.2	3.2	0.0	100.0
8	14.1	1.3	1.7	12.5	4.2	46.1	5.2	0.2	14.7	100.0
9	5.5	1.1	2.1	1.0	1.3	0.6	88.2	0.3	0.0	100.0
11	0.3	0.7	1.0	0.8	1.9	0.3	0.9	94.0	0.0	100.0
12	0.2	0.2	0.0	3.0	0.0	11.9	0.0	0.0	84.7	100.0
Column Total	100.0	100.0	100.0	100.0	100.0	100.0	100.0	100.0	100.0	

APPENDIX F: CLASS ACCURACIES DERIVED FROM ERROR MATRIX DATA

Table F.1. The original pixel total, producer's accuracy, user's accuracy, and normalized accuracy for the *coniferous forest* category with respect to each land cover map.

Land Cover Map	Original Pixel Total	Producer's Accuracy	User's Accuracy	Normalized Accuracy
IGBP (MODIS)	712396	66.8	42.7	53.1
UMD	712396	66.8	42.7	53.1
LAI/fPAR	-	-	-	-
USFS/USGS	436762	35.6	35.6	52.1
USGS LULC	609172	51.5	33	46.9
VEG LFORMS	664343	54.2	45.9	62.3
NLCD	958987	81.6	33.3	54.8
OGE	610188	54.6	32.9	49.1
BATS	623961	55.3	40.2	45.4
SIB	614734	50.2	48.3	50.1
SIB2	614734	50.2	33	25.1
IGBP (AVHRR)	609172	53.1	33	39.2
SLCR	612997	56.2	32.9	48.6
CVM	985672	83.1	34.1	56.3

Table F.2. The original pixel total, producer’s accuracy, user’s accuracy, and normalized accuracy for the *deciduous forest* category with respect to each land cover map.

Land Cover Map	Original Pixel Total	Producer's Accuracy	User's Accuracy	Normalized Accuracy
IGBP (MODIS)	367529	25.2	36.5	33.1
UMD	368236	25.2	36.5	33
LAI/fPAR	-	-	-	-
USFS/USGS	806423	45.4	24.1	28.5
USGS LULC	856053	48.3	27.9	33.1
VEG LFORMS	1316423	74.1	50.6	57.3
NLCD	1226331	74.9	51.6	62.3
OGE	838610	48.1	28	34.1
BATS	838928	47.7	34.4	34.8
SIB	856053	48.2	40	41.3
SIB2	856053	48.2	28.1	30.5
IGBP (AVHRR)	835923	47.9	27.9	32.3
SLCR	657622	42.1	38.6	39.5
CVM	1204949	72.7	52.3	61.1

Table F.3. The original pixel total, producer’s accuracy, user’s accuracy, and normalized accuracy for the *shrubland* category with respect to each land cover map.

Land Cover Map	Original Pixel Total	Producer's Accuracy	User's Accuracy	Normalized Accuracy
IGBP (MODIS)	154147	8.5	11.2	7.8
UMD	154147	8.5	11.2	7.9
LAI/fPAR	154147	8.5	17.7	12.4
USFS/USGS	508969	26.6	21	9.4
USGS LULC	455043	23.8	25.5	14.5
VEG LFORMS	-	-	-	-
NLCD	840659	44.1	43.7	41.4
OGE	457480	23.9	25.5	14.2
BATS	25475	1.3	2.7	1.3
SIB	1355299	70.8	41.9	43.3
SIB2	1355255	70.8	37.7	45
IGBP (AVHRR)	442527	23.3	25.1	17.2
SLCR	455043	28.9	25.5	18.8
CVM	874884	45.9	42	39.8

Table F.4. The original pixel total, producer’s accuracy, user’s accuracy, and normalized accuracy for the *grassland/herbaceous* category with respect to each land cover map.

Land Cover Map	Original Pixel Total	Producer's Accuracy	User's Accuracy	Normalized Accuracy
IGBP (MODIS)	540702	32.5	13.2	10.9
UMD	540702	32.5	13.2	10.9
LAI/fPAR	259079	21	40.1	33.5
USFS/USGS	162870	5.9	6.8	12.4
USGS LULC	116703	8.3	8.6	10.5
VEG LFORMS	-	-	-	-
NLCD	351280	18	24.3	24.6
OGE	145031	7.5	7.9	10.9
BATS	-	-	-	-
SIB	-	-	-	-
SIB2	24842	1.2	28.1	27.9
IGBP (AVHRR)	138028	7.1	7.6	8.6
SLCR	128264	8.1	7.2	8.4
CVM	342417	17.5	24.8	25.3

Table F.5. The original pixel total, producer’s accuracy, user’s accuracy, and normalized accuracy for the *cropland and pasture* category with respect to each land cover map.

Land Cover Map	Original Pixel Total	Producer's Accuracy	User's Accuracy	Normalized Accuracy
IGBP (MODIS)	57279	3.4	20.9	11.8
UMD	57486	3.4	20.8	11.8
LAI/fPAR	1317417	78.5	34.1	20.4
USFS/USGS	37268	2	46.6	39.2
USGS LULC	50905	2.7	39.9	33.6
VEG LFORMS	768122	41	93.2	80.8
NLCD	422070	22.7	57.7	43
OGE	50907	2.7	40.3	32.9
BATS	768122	41.1	40.1	39
SIB	51109	2.7	35.1	32
SIB2	51109	2.7	27.3	32.3
IGBP (AVHRR)	51109	2.7	27.3	22
SLCR	56724	3.9	35.6	31.8
CVM	433154	23.3	58	44.9

Table F.6. The original pixel total, producer’s accuracy, user’s accuracy, and normalized accuracy for the *barren/sparsely vegetated* category with respect to each land cover map.

Land Cover Map	Original Pixel Total	Producer's Accuracy	User's Accuracy	Normalized Accuracy
IGBP (MODIS)	117	< 0.1	5.2	12.8
UMD	117	< 0.1	5.2	12.8
LAI/fPAR	117	< 0.1	5.2	13.7
USFS/USGS	-	-	-	-
USGS LULC	-	-	-	-
VEG LFORMS	-	-	-	-
NLCD	25522	3	56.9	45.1
OGE	-	-	-	-
BATS	51496	6.2	7.7	20.3
SIB	-	-	-	-
SIB2	-	-	-	-
IGBP (AVHRR)	-	-	-	-
SLCR	-	-	-	-
CVM	25370	3	58.7	46.1

Table F.7. The original pixel total, producer’s accuracy, user’s accuracy, and normalized accuracy for the *water* category with respect to each land cover map.

Land Cover Map	Original Pixel Total	Producer's Accuracy	User's Accuracy	Normalized Accuracy
IGBP (MODIS)	3259	8.6	11.3	71.6
UMD	3259	8.6	11.3	71.6
LAI/fPAR	3259	10.6	14.9	76.6
USFS/USGS	-	-	-	-
USGS LULC	-	-	-	-
VEG LFORMS	-	-	-	-
NLCD	21520	51.4	68.7	87.9
OGE	-	-	-	-
BATS	-	-	-	-
SIB	-	-	-	-
SIB2	-	-	-	-
IGBP (AVHRR)	-	-	-	-
SLCR	-	-	-	-
CVM	21781	51.8	69.5	88.2

Table F.8. The original pixel total, producer’s accuracy, user’s accuracy, and normalized accuracy for the *urban* category with respect to each land cover map.

Land Cover Map	Original Pixel Total	Producer's Accuracy	User's Accuracy	Normalized Accuracy
IGBP (MODIS)	3233	13.3	29.1	84.5
UMD	3233	13.3	29.1	84.5
LAI/fPAR	3233	18.4	29.1	88.1
USFS/USGS	924	3.4	11.5	78.3
USGS LULC	955	3.6	11.8	79.1
VEG LFORMS	-	-	-	-
NLCD	11480	43	57.4	90.1
OGE	2123	7.9	26	86.6
BATS	-	-	-	-
SIB	-	-	-	-
SIB2	-	-	-	-
IGBP (AVHRR)	955	3.6	11.8	77.7
SLCR	-	-	-	-
CVM	10166	38	79.4	94

Table F.9. The original pixel total, producer’s accuracy, user’s accuracy, and normalized accuracy for the *snow and ice* category with respect to each land cover map.

Land Cover Map	Original Pixel Total	Producer's Accuracy	User's Accuracy	Normalized Accuracy
IGBP (MODIS)	-	-	-	-
UMD	-	-	-	-
LAI/fPAR	-	-	-	-
USFS/USGS	-	-	-	-
USGS LULC	-	-	-	-
VEG LFORMS	-	-	-	-
NLCD	194	5.7	52.4	84.8
OGE	-	-	-	-
BATS	-	-	-	-
SIB	-	-	-	-
SIB2	-	-	-	-
IGBP (AVHRR)	-	-	-	-
SLCR	-	-	-	-
CVM	174	5.1	52.4	84.7

APPENDIX G: REGRESSION RESULTS FOR THE PRECIPITATION AND TEMPERATURE STATIONS

Table G.1. Regression results for the precipitation stations.

Dependent Variable	Independent Variables				r-value
Maybell	Craig	Hamilton	Hayden		0.494
Craig	Hamilton	Hayden	Maybell		0.611
Hamilton	Craig	Maybell	Hayden		0.534
Pyramid	Hayden	Crosho	Yampa		0.579
Steamboat Springs	Dry Lake	Hayden	Yampa		0.600
Yampa	Crosho	Pyramid	Hayden		0.448

Table G.2. Regression results for the Dry Lake (06j01s) temperature station.

Independent Variable	T_{MAX}				T_{MIN}			
	Value	Std. Error	t value	Pr(> t)	Value	Std. Error	t value	Pr(> t)
(Intercept)	4.43	0.23	19.33	0.00	3.35	0.09	38.35	0.00
Columbine	0.01	0.01	1.13	0.26	0.04	0.01	7.21	0.00
Lynx Pass	0.12	0.01	10.09	0.00	0.28	0.01	33.71	0.00
Rabbit Ears	0.16	0.01	14.26	0.00	0.10	0.01	9.72	0.00
Elk River	0.14	0.01	13.84	0.00	0.22	0.01	17.35	0.00
Tower	0.17	0.01	14.69	0.00	0.21	0.01	20.47	0.00
Crosho	-0.01	0.01	-0.53	0.60	0.03	0.01	2.47	0.01
Ripple Creek	0.14	0.01	10.91	0.00	0.04	0.01	2.71	0.01
Burro Mountain	0.12	0.02	7.43	0.00	0.00	0.01	-0.04	0.97
Trapper Lake	0.17	0.02	9.38	0.00	0.04	0.01	4.02	0.00
R²	0.95				0.98			

Table G.3. Regression results for the Columbine (06j03s) temperature station.

Independent Variable	T _{MAX}				T _{MIN}			
	Value	Std. Error	t value	Pr(> t)	Value	Std. Error	t value	Pr(> t)
Intercept	3.03	0.61	4.98	0.00	2.11	0.23	9.09	0.00
Dry Lake	0.04	0.04	1.13	0.26	0.26	0.03	7.66	0.00
Lynx Pass	0.23	0.03	7.34	0.00	0.10	0.02	4.63	0.00
Rabbit Ears	0.04	0.03	1.23	0.22	-	-	-	-
Elk River	-0.17	0.03	-6.32	0.00	0.11	0.03	3.61	0.00
Tower	0.23	0.03	7.46	0.00	0.14	0.02	5.68	0.00
Crosho	0.15	0.03	4.44	0.00	0.02	0.03	0.64	0.52
Ripple Creek	-0.39	0.03	-12.00	0.00	-0.05	0.03	-1.34	0.18
Burro Mountain	0.21	0.04	4.93	0.00	-0.06	0.02	-3.48	0.00
Trapper Lake	0.51	0.05	10.84	0.00	0.42	0.02	16.72	0.00
R²	0.67				0.87			

Table G.4. Regression results for the Rabbit Ears (06j09s) temperature station.

Independent Variable	T _{MAX}				T _{MIN}			
	Value	Std. Error	t value	Pr(> t)	Value	Std. Error	t value	Pr(> t)
Intercept	-0.30	0.30	-1.00	0.32	0.67	0.14	4.93	0.00
Dry Lake	0.25	0.02	14.26	0.00	0.20	0.02	10.06	0.00
Columbine	0.01	0.01	1.23	0.22	-	-	-	-
Lynx Pass	0.00	0.02	0.07	0.95	0.10	0.01	8.07	0.00
Elk River	0.04	0.01	3.37	0.00	0.21	0.02	11.70	0.00
Tower	0.11	0.02	7.57	0.00	0.12	0.01	8.32	0.00
Crosho	0.13	0.02	7.90	0.00	0.17	0.02	10.00	0.00
Ripple Creek	0.27	0.02	17.65	0.00	0.16	0.02	8.07	0.00
Burro Mountain	0.03	0.02	1.48	0.14	0.00	0.01	-0.05	0.96
Trapper Lake	0.15	0.02	6.44	0.00	0.02	0.01	1.32	0.19
R²	0.93				0.96			

Table G.5. Regression results for the Elk River (06j15s) temperature station.

Independent Variable	T _{MAX}				T _{MIN}			
	Value	Std. Error	t value	Pr(> t)	Value	Std. Error	t value	Pr(> t)
Intercept	-0.56	0.33	-1.70	0.09	1.96	0.11	18.47	0.00
Dry Lake	0.27	0.02	13.84	0.00	0.27	0.02	17.35	0.00
Columbine	-0.05	0.01	-6.32	0.00	0.02	0.01	3.13	0.00
Lynx Pass	0.09	0.02	5.22	0.00	-0.02	0.01	-1.95	0.05
Rabbit Ears	0.05	0.02	3.37	0.00	0.13	0.01	11.55	0.00
Tower	0.20	0.02	11.89	0.00	0.12	0.01	10.62	0.00
Crosho	0.16	0.02	8.47	0.00	0.17	0.01	12.53	0.00
Ripple Creek	0.15	0.02	8.34	0.00	0.28	0.02	17.58	0.00
Burro Mountain	0.07	0.02	2.81	0.01	0.05	0.01	6.75	0.00
Trapper Lake	0.11	0.03	4.12	0.00	-0.01	0.01	-1.21	0.23
R²	0.92				0.97			

Table G.6. Regression results for the Tower (06j29s) temperature station.

Independent Variable	T _{MAX}				T _{MIN}			
	Value	Std. Error	t value	Pr(> t)	Value	Std. Error	t value	Pr(> t)
Intercept	-9.43	0.25	-38.15	0	-2.95	0.13	-22.84	0.00
Dry Lake	0.25	0.02	14.69	0	0.39	0.02	20.47	0.00
Columbine	0.05	0.01	7.46	0	0.04	0.01	5.34	0.00
Lynx Pass	0.15	0.01	10.36	0	-0.18	0.01	-14.54	0.00
Rabbit Ears	0.10	0.01	7.57	0	0.12	0.01	8.08	0.00
Elk River	0.14	0.01	11.89	0	0.19	0.02	10.62	0.00
Crosho	0.07	0.02	4.58	0	-0.03	0.02	-1.76	0.08
Ripple Creek	0.00	0.02	0.30	0.76	0.67	0.02	38.16	0.00
Burro Mountain	-0.01	0.02	-0.71	0.48	-0.03	0.01	-3.15	0.00
Trapper Lake	0.26	0.02	11.95	0	-0.14	0.01	-9.42	0.00
R²	0.93				0.96			

Table G.7. Regression results for the Crosho (07j04s) temperature station.

Independent Variable	T _{MAX}				T _{MIN}			
	Value	Std. Error	t value	Pr(> t)	Value	Std. Error	t value	Pr(> t)
Intercept	-	-	-	-	1.17	0.12	10.05	0.00
Dry Lake	-	-	-	-	0.04	0.02	2.47	0.01
Columbine	-	-	-	-	0.00	0.01	0.20	0.84
Lynx Pass	-	-	-	-	0.27	0.01	25.94	0.00
Rabbit Ears	-	-	-	-	0.12	0.01	9.98	0.00
Elk River	-	-	-	-	0.20	0.02	12.73	0.00
Tower	-	-	-	-	-0.02	0.01	-1.83	0.07
Ripple Creek	-	-	-	-	0.17	0.02	9.89	0.00
Trapper Lake	-	-	-	-	0.24	0.01	19.47	0.00
R²	-				0.97			

Table G.8. Regression results for the Ripple Creek (07j05s) temperature station.

Independent Variable	T _{MAX}				T _{MIN}			
	Value	Std. Error	t value	Pr(> t)	Value	Std. Error	t value	Pr(> t)
Intercept	-2.54	0.27	-9.52	0.00	-0.87	0.10	-8.91	0.00
Dry Lake	0.18	0.02	10.91	0.00	0.04	0.01	2.71	0.01
Columbine	-0.07	0.01	-12.00	0.00	-0.01	0.01	-1.63	0.10
Lynx Pass	0.06	0.01	4.16	0.00	-0.14	0.01	-15.21	0.00
Rabbit Ears	0.22	0.01	17.65	0.00	0.08	0.01	8.12	0.00
Elk River	0.10	0.01	8.34	0.00	0.22	0.01	17.58	0.00
Tower	0.00	0.01	0.30	0.76	0.35	0.01	38.16	0.00
Crosho	0.01	0.01	0.88	0.38	0.11	0.01	9.23	0.00
Burro Mountain	0.28	0.02	15.37	0.00	0.12	0.01	17.73	0.00
Trapper Lake	0.22	0.02	10.83	0.00	0.20	0.01	19.64	0.00
R²	0.94				0.98			

Table G.9. Regression results for the Burro Mountain (07k02s) temperature station.

Independent Variable	T _{MAX}				T _{MIN}			
	Value	Std. Error	t value	Pr(> t)	Value	Std. Error	t value	Pr(> t)
Intercept	1.89	0.20	9.24	0.00	1.93	0.21	9.37	0.00
Dry Lake	0.09	0.01	7.43	0.00	0.00	0.03	0.00	1.00
Columbine	0.02	0.00	4.93	0.00	-0.05	0.01	-3.48	0.00
Lynx Pass	0.13	0.01	12.27	0.00	0.09	0.02	4.86	0.00
Rabbit Ears	0.01	0.01	1.48	0.14	0.01	0.02	0.27	0.79
Elk River	0.03	0.01	2.81	0.01	0.19	0.03	7.10	0.00
Tower	-0.01	0.01	-0.71	0.48	-0.07	0.02	-3.19	0.00
Crosho	0.17	0.01	15.39	0.00	-	-	-	-
Ripple Creek	0.17	0.01	15.37	0.00	0.54	0.03	18.10	0.00
Trapper Lake	0.33	0.02	21.39	0.00	0.29	0.02	13.32	0.00
R²	0.96				0.91			

Table G.10. Regression results for the Trapper Lake (07k13s) temperature station.

Independent Variable	T _{MAX}				T _{MIN}			
	Value	Std. Error	t value	Pr(> t)	Value	Std. Error	t value	Pr(> t)
Intercept	0.09	0.18	0.50	0.62	-3.34	0.12	-26.96	0.00
Dry Lake	0.10	0.01	9.38	0.00	0.08	0.02	4.02	0.00
Columbine	0.05	0.00	10.84	0.00	0.13	0.01	16.68	0.00
Lynx Pass	0.12	0.01	12.19	0.00	0.18	0.01	15.17	0.00
Rabbit Ears	0.06	0.01	6.44	0.00	0.01	0.01	0.68	0.50
Elk River	0.03	0.01	4.12	0.00	-0.02	0.02	-1.21	0.23
Tower	0.11	0.01	11.95	0.00	-0.13	0.01	-9.42	0.00
Crosho	0.14	0.01	14.49	0.00	0.30	0.02	18.87	0.00
Ripple Creek	0.11	0.01	10.83	0.00	0.37	0.02	19.64	0.00
Burro Mountain	0.26	0.01	21.39	0.00	0.11	0.01	12.46	0.00
R²	0.97				0.96			

Table G.11. Regression results for the Craig (CO-1932) temperature station.

Independent Variable	T _{MAX}				T _{MIN}			
	Value	Std. Error	t value	Pr(> t)	Value	Std. Error	t value	Pr(> t)
Intercept	3.70	0.24	15.70	0.00	3.68	0.14	26.19	0.00
Hayden	0.26	0.01	19.69	0.00	0.31	0.02	19.46	0.00
Maybell	0.05	0.01	10.35	0.00	0.31	0.01	26.14	0.00
Steamboat Springs	0.54	0.02	33.85	0.00	0.17	0.01	13.11	0.00
Yampa	0.11	0.02	6.36	0.00	0.18	0.01	13.82	0.00
R²	0.94				0.93			

Table G.12. Regression results for the Maybell (CO-5446) temperature station.

Independent Variable	T _{MAX}				T _{MIN}			
	Value	Std. Error	t value	Pr(> t)	Value	Std. Error	t value	Pr(> t)
Intercept	6.17	0.67	9.15	0.00	-3.95	0.16	-24.14	0.00
Craig	0.41	0.04	10.35	0.00	0.41	0.02	26.14	0.00
Hayden	0.06	0.04	1.44	0.15	0.25	0.02	13.38	0.00
Steamboat Springs	0.45	0.05	8.98	0.00	0.31	0.01	21.07	0.00
Yampa	0.01	0.05	0.18	0.86	0.09	0.02	5.72	0.00
R²	0.64				0.92			

Table G.13. Regression results for the Steamboat Springs (CO-7936) temperature station.

Independent Variable	T _{MAX}				T _{MIN}			
	Value	Std. Error	t value	Pr(> t)	Value	Std. Error	t value	Pr(> t)
Intercept	-4.36	0.19	-23.53	0.00	-3.44	0.16	-21.94	0.00
Craig	0.35	0.01	33.85	0.00	0.21	0.02	13.11	0.00
Hayden	0.20	0.01	18.67	0.00	0.40	0.02	22.97	0.00
Maybell	0.04	0.00	8.98	0.00	0.28	0.01	21.07	0.00
Yampa	0.49	0.01	40.82	0.00	0.10	0.01	6.67	0.00
R²	0.96				0.92			

Table G.14. Regression results for the Yampa (CO-9265) temperature station.

Independent Variable	T _{MAX}				T _{MIN}			
	Value	Std. Error	t value	Pr(> t)	Value	Std. Error	t value	Pr(> t)
Intercept	4.09	0.19	21.13	0.00	-0.54	0.16	-3.27	0.00
Craig	0.08	0.01	6.36	0.00	0.22	0.02	13.82	0.00
Hayden	0.26	0.01	23.87	0.00	0.55	0.02	33.92	0.00
Maybell	0.00	0.00	0.18	0.86	0.08	0.01	5.72	0.00
Steamboat Springs	0.52	0.01	40.82	0.00	0.10	0.01	6.67	0.00
R²	0.95				0.92			

APPENDIX H: MODELED ANNUAL WATER BALANCE SUMMARY FOR EACH OF THE PRMS RUNS

Table H.1. Modeled annual water balance summary expressed in inches using the MVM to derive the spatial parameters.

Year	Precip	ET	Storage	P- Runoff	O- Runoff	P – O	Mean Absolute Error (MAE) (%)
1987	14.7	10.9	1.0	6.8	4.5	2.3	51.1
1988	14.1	8.9	1.6	4.7	5.1	-0.4	7.8
1989	13.4	9.6	1.3	4.1	3.6	0.5	13.9
1990	14.2	10.2	1.3	4.0	3.9	0.1	2.6
1991	16.3	10.8	1.5	5.4	4.8	0.6	12.5
1992	15.4	11.9	1.3	3.6	3.4	0.2	5.9
1993	14.9	8.2	2.1	5.9	7.2	-1.3	18.1
1994	13.3	8.9	1.5	5.0	3.6	1.4	38.9
1995	19.0	10.6	3.7	6.3	8.2	-1.9	23.2
1996	16.6	9.7	2.8	7.8	8.7	-0.9	10.3
1997	24.6	12.9	5.1	9.4	10.3	-0.9	8.7
1998	15.6	10.7	2.2	7.8	8.6	-0.8	9.3
1999	18.0	11.6	2.5	6.3	6.0	0.3	5.0
2000	14.9	9.9	2.6	4.9	5.1	-0.2	3.9
2001	12.9	9.5	1.8	4.3	4.0	0.3	7.5
Total	247.3	161.3	1.6	88.9	88.9	0	14.6

Table H.2. Modeled annual water balance summary expressed in inches using the NLCD map to derive the spatial parameters.

Year	Precip	ET	Storage	P- Runoff	O- Runoff	P – O	Mean Absolute Error (MAE) (%)
1987	14.7	11.0	1.0	6.6	4.5	2.1	46.7
1988	14.1	9.1	1.6	4.5	5.1	-0.6	11.8
1989	13.4	9.9	1.3	3.8	3.6	0.2	5.6
1990	14.2	10.3	1.4	3.8	3.9	-0.1	2.6
1991	16.3	10.9	1.5	5.2	4.8	0.4	8.3
1992	15.4	12.0	1.3	3.5	3.4	0.1	2.9
1993	14.9	8.5	2.2	5.6	7.2	-1.6	22.2
1994	13.3	9.1	1.6	4.8	3.6	1.2	33.3
1995	19.0	10.7	3.9	6.0	8.2	-2.2	26.8
1996	16.6	10.0	3.1	7.5	8.7	-1.2	13.8
1997	24.6	13.1	5.5	9.1	10.3	-1.2	11.7
1998	15.6	10.9	2.6	7.6	8.6	-1.0	11.6
1999	18.0	11.7	2.9	6.1	6.0	0.1	1.7
2000	14.9	10.1	3.0	4.8	5.1	-0.3	5.9
2001	12.9	9.6	2.2	4.2	4.0	0.2	5.0
Total	247.3	164.3	1.9	85.6	88.9	-3.3	14.0

Table H.3. Modeled annual water balance summary expressed in inches using the CVM map to derive the spatial parameters.

Year	Precip	ET	Storage	P- Runoff	O- Runoff	P – O	Mean Absolute Error (MAE) (%)
1987	14.7	11.6	1.2	5.9	4.5	1.4	31.1
1988	14.1	9.7	1.6	4.0	5.1	-1.1	21.6
1989	13.4	10.4	1.4	3.3	3.6	-0.3	8.3
1990	14.2	10.8	1.5	3.3	3.9	-0.6	15.4
1991	16.3	11.5	1.7	4.6	4.8	-0.2	4.2
1992	15.4	12.5	1.5	3.1	3.4	-0.3	8.8
1993	14.9	9.0	2.3	5.1	7.2	-2.1	29.2
1994	13.3	9.7	1.7	4.2	3.6	0.6	16.7
1995	19.0	11.3	4.1	5.5	8.2	-2.7	32.9
1996	16.6	10.5	3.3	6.9	8.7	-1.8	20.7
1997	24.6	13.7	6.1	8.1	10.3	-2.2	21.4
1998	15.6	11.5	2.9	7.2	8.6	-1.4	16.3
1999	18.0	12.2	3.2	5.6	6.0	-0.4	6.7
2000	14.9	10.7	3.2	4.2	5.1	-0.9	17.6
2001	12.9	10.2	2.4	3.6	4.0	-0.4	10.0
Total	247.3	173.0	2.1	76.7	88.9	-12.2	17.4

Table H.4. Modeled annual water balance summary expressed in inches using the IGBP (MODIS) map to derive the spatial parameters.

Year	Precip	ET	Storage	P- Runoff	O- Runoff	P – O	Mean Absolute Error (MAE) (%)
1987	14.7	11.0	1.0	6.7	4.5	2.2	48.9
1988	14.1	9.0	1.6	4.6	5.1	-0.5	9.8
1989	13.4	9.7	1.3	4.0	3.6	0.4	11.1
1990	14.2	10.3	1.4	3.9	3.9	0.0	0.0
1991	16.3	10.9	1.5	5.2	4.8	0.4	8.3
1992	15.4	12.0	1.4	3.5	3.4	0.1	2.9
1993	14.9	8.4	2.3	5.7	7.2	-1.5	20.8
1994	13.3	9.0	1.8	4.8	3.6	1.2	33.3
1995	19.0	10.6	4.1	6.1	8.2	-2.1	25.6
1996	16.6	9.9	3.3	7.5	8.7	-1.2	13.8
1997	24.6	13.0	5.8	9.2	10.3	-1.1	10.7
1998	15.6	10.8	2.9	7.6	8.6	-1.0	11.6
1999	18.0	11.7	3.2	6.1	6.0	0.1	1.7
2000	14.9	10.0	3.4	4.8	5.1	-0.3	5.9
2001	12.9	9.6	2.5	4.2	4.0	0.2	5.0
Total	247.3	162.9	2.3	86.6	88.9	-2.3	14.0

Table H.5. Modeled annual water balance summary expressed in inches using the UMD map to derive the spatial parameters.

Year	Precip	ET	Storage	P- Runoff	O- Runoff	P - O	Mean Absolute Error (MAE) (%)
1987	14.7	11.0	1.0	6.7	4.5	2.2	48.9
1988	14.1	9.0	1.6	4.6	5.1	-0.5	9.8
1989	13.4	9.7	1.3	4.0	3.6	0.4	11.1
1990	14.2	10.3	1.4	3.9	3.9	0.0	0.0
1991	16.3	10.9	1.5	5.2	4.8	0.4	8.3
1992	15.4	12.0	1.4	3.5	3.4	0.1	2.9
1993	14.9	8.4	2.3	5.7	7.2	-1.5	20.8
1994	13.3	9.0	1.8	4.8	3.6	1.2	33.3
1995	19.0	10.6	4.1	6.1	8.2	-2.1	25.6
1996	16.6	9.9	3.3	7.5	8.7	-1.2	13.8
1997	24.6	13.0	5.8	9.2	10.3	-1.1	10.7
1998	15.6	10.8	2.9	7.6	8.6	-1.0	11.6
1999	18.0	11.7	3.2	6.1	6.0	0.1	1.7
2000	14.9	10.0	3.4	4.8	5.1	-0.3	5.9
2001	12.9	9.6	2.5	4.2	4.0	0.2	5.0
Total	247.3	162.9	2.3	86.6	88.9	-2.3	14.0

Table H.6. Modeled annual water balance summary expressed in inches using the LAI/fPAR map to derive the spatial parameters.

Year	Precip	ET	Storage	P- Runoff	O- Runoff	P - O	Mean Absolute Error (MAE) (%)
1987	14.7	10.7	1.0	7.0	4.5	2.5	55.6
1988	14.1	8.7	1.5	4.9	5.1	-0.2	3.9
1989	13.4	9.4	1.2	4.3	3.6	0.7	19.4
1990	14.2	10.0	1.2	4.1	3.9	0.2	5.1
1991	16.3	10.6	1.4	5.5	4.8	0.7	14.6
1992	15.4	11.9	1.2	3.7	3.4	0.3	8.8
1993	14.9	8.1	1.7	6.3	7.2	-0.9	12.5
1994	13.3	8.6	1.2	5.1	3.6	1.5	41.7
1995	19.0	10.5	3.3	6.5	8.2	-1.7	20.7
1996	16.6	9.5	2.2	8.2	8.7	-0.5	5.7
1997	24.6	12.8	4.2	9.8	10.3	-0.5	4.9
1998	15.6	10.5	1.4	8.0	8.6	-0.6	7.0
1999	18.0	11.4	1.6	6.4	6.0	0.4	6.7
2000	14.9	9.7	1.8	5.1	5.1	0.0	0.0
2001	12.9	9.3	1.1	4.4	4.0	0.4	10.0
Total	247.3	158.6	0.9	92.2	88.9	3.3	14.4

Table H.7. Modeled annual water balance summary expressed in inches using the USFS/USGS map to derive the spatial parameters.

Year	Precip	ET	Storage	P- Runoff	O- Runoff	P - O	Mean Absolute Error (MAE) (%)
1987	14.7	11.7	1.3	5.7	4.5	1.2	26.7
1988	14.1	9.8	1.7	3.9	5.1	-1.2	23.5
1989	13.4	10.4	1.6	3.1	3.6	-0.5	13.9
1990	14.2	10.9	1.7	3.2	3.9	-0.7	17.9
1991	16.3	11.6	2.0	4.4	4.8	-0.4	8.3
1992	15.4	12.6	1.9	2.9	3.4	-0.5	14.7
1993	14.9	9.1	2.8	4.9	7.2	-2.3	31.9
1994	13.3	9.7	2.4	4.0	3.6	0.4	11.1
1995	19.0	11.4	4.7	5.3	8.2	-2.9	35.4
1996	16.6	10.7	3.9	6.8	8.7	-1.9	21.8
1997	24.6	13.7	6.9	7.8	10.3	-2.5	24.3
1998	15.6	11.6	3.8	7.1	8.6	-1.5	17.4
1999	18.0	12.3	4.3	5.4	6.0	-0.6	10.0
2000	14.9	10.8	4.4	4.1	5.1	-1.0	19.6
2001	12.9	10.2	3.7	3.4	4.0	-0.6	15.0
Total	247.3	174.4	3.5	73.9	88.9	-15.0	19.4

Table H.8. Modeled annual water balance summary expressed in inches using the IGBP (AVHRR) map to derive the spatial parameters.

Year	Precip	ET	Storage	P- Runoff	O- Runoff	P - O	Mean Absolute Error (MAE) (%)
1987	14.7	10.9	1.1	6.7	4.5	2.2	48.9
1988	14.1	9.0	1.7	4.5	5.1	-0.6	11.8
1989	13.4	9.7	1.5	3.9	3.6	0.3	8.3
1990	14.2	10.3	1.6	3.8	3.9	-0.1	2.6
1991	16.3	10.9	1.8	5.2	4.8	0.4	8.3
1992	15.4	11.9	1.8	3.5	3.4	0.1	2.9
1993	14.9	8.3	2.8	5.6	7.2	-1.6	22.2
1994	13.3	8.9	2.4	4.8	3.6	1.2	33.3
1995	19.0	10.6	4.7	6.1	8.2	-2.1	25.6
1996	16.6	9.8	3.9	7.6	8.7	-1.1	12.6
1997	24.6	13.0	6.5	9.1	10.3	-1.2	11.7
1998	15.6	10.7	3.8	7.5	8.6	-1.1	12.8
1999	18.0	11.6	4.3	6.1	6.0	0.1	1.7
2000	14.9	9.9	4.5	4.8	5.1	-0.3	5.9
2001	12.9	9.4	3.9	4.2	4.0	0.2	5.0
Total	247.3	162.1	3.7	86.0	88.9	-2.9	14.2

Table H.9. Modeled annual water balance summary expressed in inches using the SLCR map to derive the spatial parameters.

Year	Precip	ET	Storage	P- Runoff	O- Runoff	P - O	Mean Absolute Error (MAE) (%)
1987	14.7	11.7	1.3	5.7	4.5	-1.2	26.7
1988	14.1	9.9	1.8	3.8	5.1	-1.3	25.5
1989	13.4	10.6	1.6	3.0	3.6	-0.6	16.7
1990	14.2	11.0	1.7	3.1	3.9	-0.8	20.5
1991	16.3	11.6	2.1	4.4	4.8	-0.4	8.3
1992	15.4	12.5	2.0	2.9	3.4	-0.5	14.7
1993	14.9	9.2	3.0	4.7	7.2	-2.5	34.7
1994	13.3	9.8	2.6	3.9	3.6	0.3	8.3
1995	19.0	11.4	5.1	5.1	8.2	-3.1	37.8
1996	16.6	10.8	4.4	6.6	8.7	-2.1	24.1
1997	24.6	13.8	7.4	7.7	10.3	-2.5	24.3
1998	15.6	11.7	4.3	7.0	8.6	-1.6	18.6
1999	18.0	12.3	4.7	5.4	6.0	-0.6	10.0
2000	14.9	10.8	4.9	4.0	5.1	-1.1	21.6
2001	12.9	10.3	4.2	3.4	4.0	-0.6	15.0
Total	247.3	175.4	4.0	72.4	88.9	-16.5	20.5

Table H.10. Modeled annual water balance summary expressed in inches using the SiB map to derive the spatial parameters.

Year	Precip	ET	Storage	P- Runoff	O- Runoff	P - O	Mean Absolute Error (MAE) (%)
1987	14.7	10.9	1.1	6.7	4.5	2.2	48.9
1988	14.1	9.0	1.7	4.6	5.1	-0.5	9.8
1989	13.4	9.6	1.4	4.0	3.6	0.4	11.1
1990	14.2	10.2	1.6	3.9	3.9	0.0	0.0
1991	16.3	10.8	1.8	5.2	4.8	0.4	8.3
1992	15.4	11.9	1.8	3.5	3.4	0.1	2.9
1993	14.9	8.3	2.7	5.7	7.2	-1.5	20.8
1994	13.3	8.9	2.4	4.8	3.6	1.2	33.3
1995	19.0	10.6	4.6	6.2	8.2	-2.0	24.4
1996	16.6	9.8	3.8	7.6	8.7	-1.1	12.6
1997	24.6	12.9	6.4	9.1	10.3	-1.2	11.7
1998	15.6	10.7	3.7	7.6	8.6	-1.0	11.6
1999	18.0	11.6	4.1	6.1	6.0	0.1	1.7
2000	14.9	9.9	4.4	4.8	5.1	-0.3	5.9
2001	12.9	9.4	3.7	4.2	4.0	0.2	5.0
Total	247.3	161.7	3.6	86.5	88.9	-2.4	13.9

Table H.11. Modeled annual water balance summary expressed in inches using the SiB2 map to derive the spatial parameters.

Year	Precip	ET	Storage	P- Runoff	O- Runoff	P - O	Mean Absolute Error (MAE) (%)
1987	14.7	10.9	1.1	6.7	4.5	2.2	48.9
1988	14.1	9.0	1.7	4.6	5.1	-0.5	9.8
1989	13.4	9.6	1.4	4.0	3.6	0.4	11.1
1990	14.2	10.2	1.6	3.9	3.9	0.0	0.0
1991	16.3	10.8	1.8	5.2	4.8	0.4	8.3
1992	15.4	11.9	1.8	3.5	3.4	0.1	2.9
1993	14.9	8.3	2.7	5.7	7.2	-1.5	20.8
1994	13.3	8.9	2.4	4.8	3.6	1.2	33.3
1995	19.0	10.6	4.6	6.2	8.2	-2.0	24.4
1996	16.6	9.8	3.8	7.6	8.7	-1.1	12.6
1997	24.6	12.9	6.4	9.1	10.3	-1.2	11.7
1998	15.6	10.7	3.7	7.6	8.6	-1.0	11.6
1999	18.0	11.6	4.1	6.1	6.0	0.1	1.7
2000	14.9	9.9	4.4	4.8	5.1	-0.3	5.9
2001	12.9	9.4	3.7	4.2	4.0	0.2	5.0
Total	247.3	161.7	3.6	86.5	88.9	-2.4	13.9

Table H.12. Modeled annual water balance summary expressed in inches using the OGE map to derive the spatial parameters.

Year	Precip	ET	Storage	P- Runoff	O- Runoff	P - O	Mean Absolute Error (MAE) (%)
1987	14.7	10.9	1.1	6.7	4.5	2.2	48.9
1988	14.1	9.0	1.7	4.5	5.1	-0.6	11.8
1989	13.4	9.7	1.5	3.9	3.6	0.3	8.3
1990	14.2	10.3	1.6	3.8	3.9	-0.1	2.6
1991	16.3	10.9	1.8	5.2	4.8	0.4	8.3
1992	15.4	11.9	1.8	3.5	3.4	0.1	2.9
1993	14.9	8.3	2.8	5.6	7.2	-1.6	22.2
1994	13.3	8.9	2.4	4.7	3.6	1.1	30.6
1995	19.0	10.6	4.7	6.1	8.2	-2.1	25.6
1996	16.6	9.8	4.0	7.6	8.7	-1.1	12.6
1997	24.6	13.0	6.5	9.1	10.3	-1.2	11.7
1998	15.6	10.7	3.9	7.5	8.6	-1.1	12.8
1999	18.0	11.6	4.3	6.1	6.0	0.1	1.7
2000	14.9	9.9	4.6	4.8	5.1	-0.3	5.9
2001	12.9	9.4	3.9	4.2	4.0	0.2	5.0
Total	247.3	162.1	3.8	85.9	88.9	-3.0	14.1

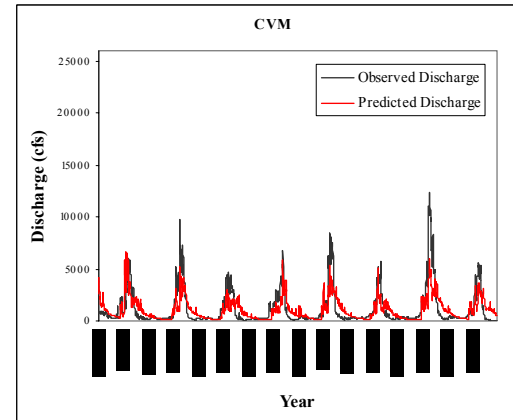
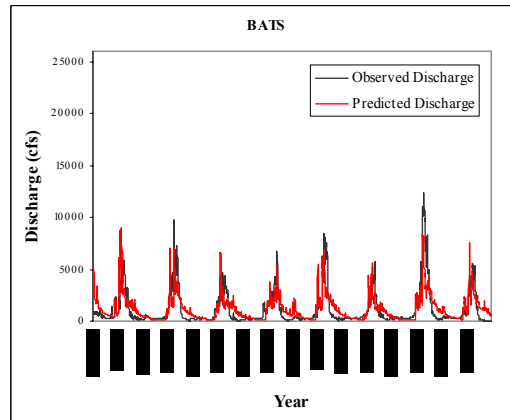
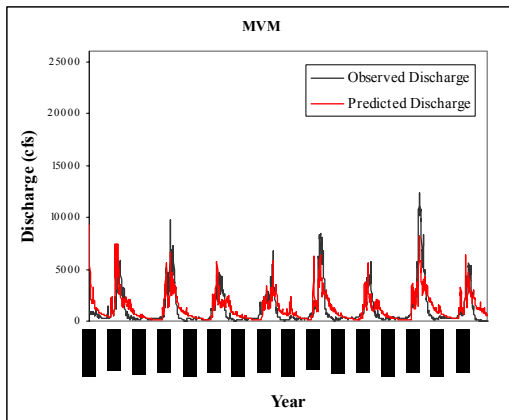
Table H.13. Modeled annual water balance summary expressed in inches using the BATS map to derive the spatial parameters.

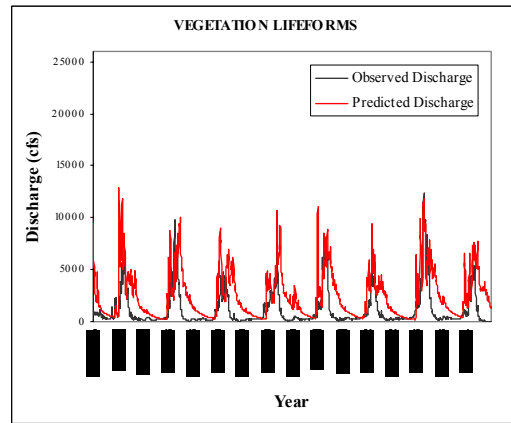
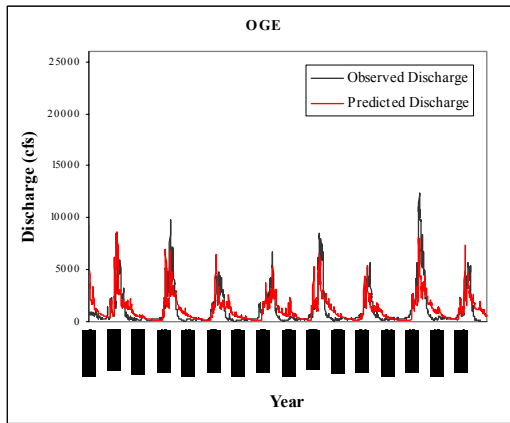
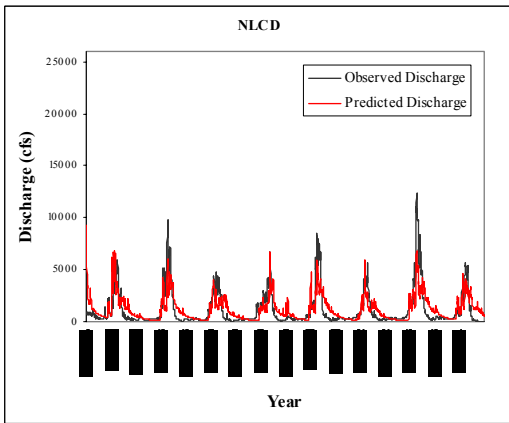
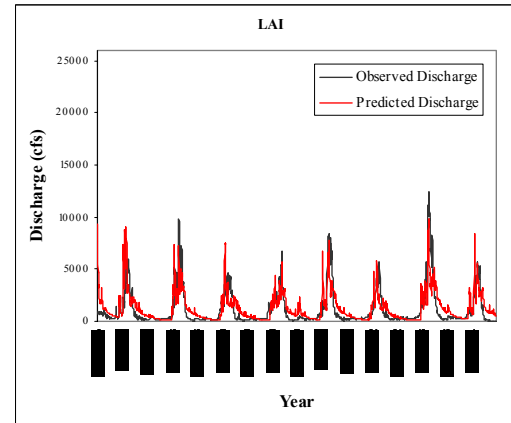
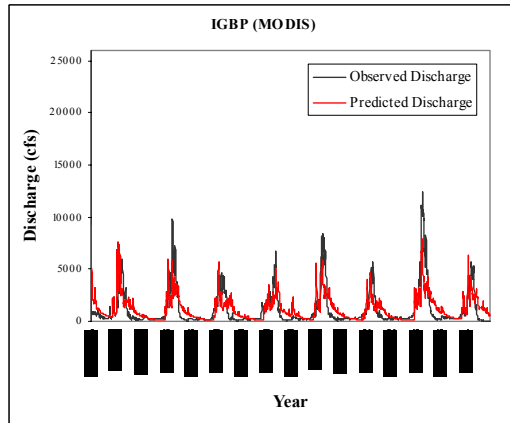
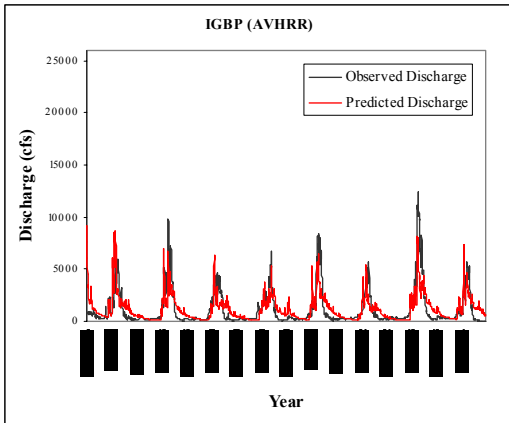
Year	Precip	ET	Storage	P- Runoff	O- Runoff	P - O	Mean Absolute Error (MAE) (%)
1987	14.7	10.9	1.1	6.7	4.5	2.2	48.9
1988	14.1	9.0	1.7	4.6	5.1	-0.5	9.8
1989	13.4	9.6	1.4	4.0	3.6	0.4	11.1
1990	14.2	10.2	1.6	3.9	3.9	0.0	0.0
1991	16.3	10.8	1.8	5.2	4.8	0.4	8.3
1992	15.4	11.9	1.8	3.5	3.4	0.1	2.9
1993	14.9	8.3	2.7	5.7	7.2	-1.5	20.8
1994	13.3	8.9	2.4	4.8	3.6	1.2	33.3
1995	19.0	10.6	4.6	6.2	8.2	-2.0	24.4
1996	16.6	9.8	3.9	7.6	8.7	-1.1	12.6
1997	24.6	12.9	6.4	9.1	10.3	-1.2	11.7
1998	15.6	10.7	3.8	7.5	8.6	-1.1	12.8
1999	18.0	11.6	4.2	6.1	6.0	0.1	1.7
2000	14.9	9.9	4.5	4.8	5.1	-0.3	5.9
2001	12.9	9.4	3.8	4.3	4.0	0.3	7.5
Total	247.3	161.6	3.6	86.5	88.9	-2.4	14.1

Table H.14. Modeled annual water balance summary expressed in inches using the VEGETATION LIFEFORMS map to derive the spatial parameters.

Year	Precip	ET	Storage	P- Runoff	O- Runoff	P - O	Mean Absolute Error (MAE) (%)
1987	14.7	11.1	1.1	6.5	4.5	2.0	44.4
1988	14.1	9.3	1.7	4.3	5.1	-0.8	15.7
1989	13.4	9.9	1.5	3.7	3.6	0.1	2.8
1990	14.2	10.4	1.7	3.7	3.9	-0.2	5.1
1991	16.3	11.0	2.0	5.0	4.8	0.2	4.2
1992	15.4	12.0	2.0	3.4	3.4	0.0	0.0
1993	14.9	8.5	3.1	5.2	7.2	-2.0	27.8
1994	13.3	9.1	2.8	4.5	3.6	0.9	25.0
1995	19.0	10.8	5.3	5.7	8.2	-2.5	30.5
1996	16.6	10.1	4.7	7.2	8.7	-1.5	17.2
1997	24.6	13.1	7.4	8.7	10.3	-1.6	15.5
1998	15.6	10.9	4.8	7.3	8.6	-1.3	15.1
1999	18.0	11.8	5.3	5.8	6.0	-0.2	3.3
2000	14.9	10.1	5.6	4.6	5.1	-0.5	9.8
2001	12.9	9.6	4.9	4.0	4.0	0.0	0.0
Total	247.3	165.1	4.7	81.9	88.9	-7.0	14.4

*APPENDIX I: PREDICTED VERSUS OBSERVED DISCHARGE FOR THE YAMPA RIVER BASIN
AT MAYBELL FROM WATER YEARS 1987 TO 2002 USING PRMS*





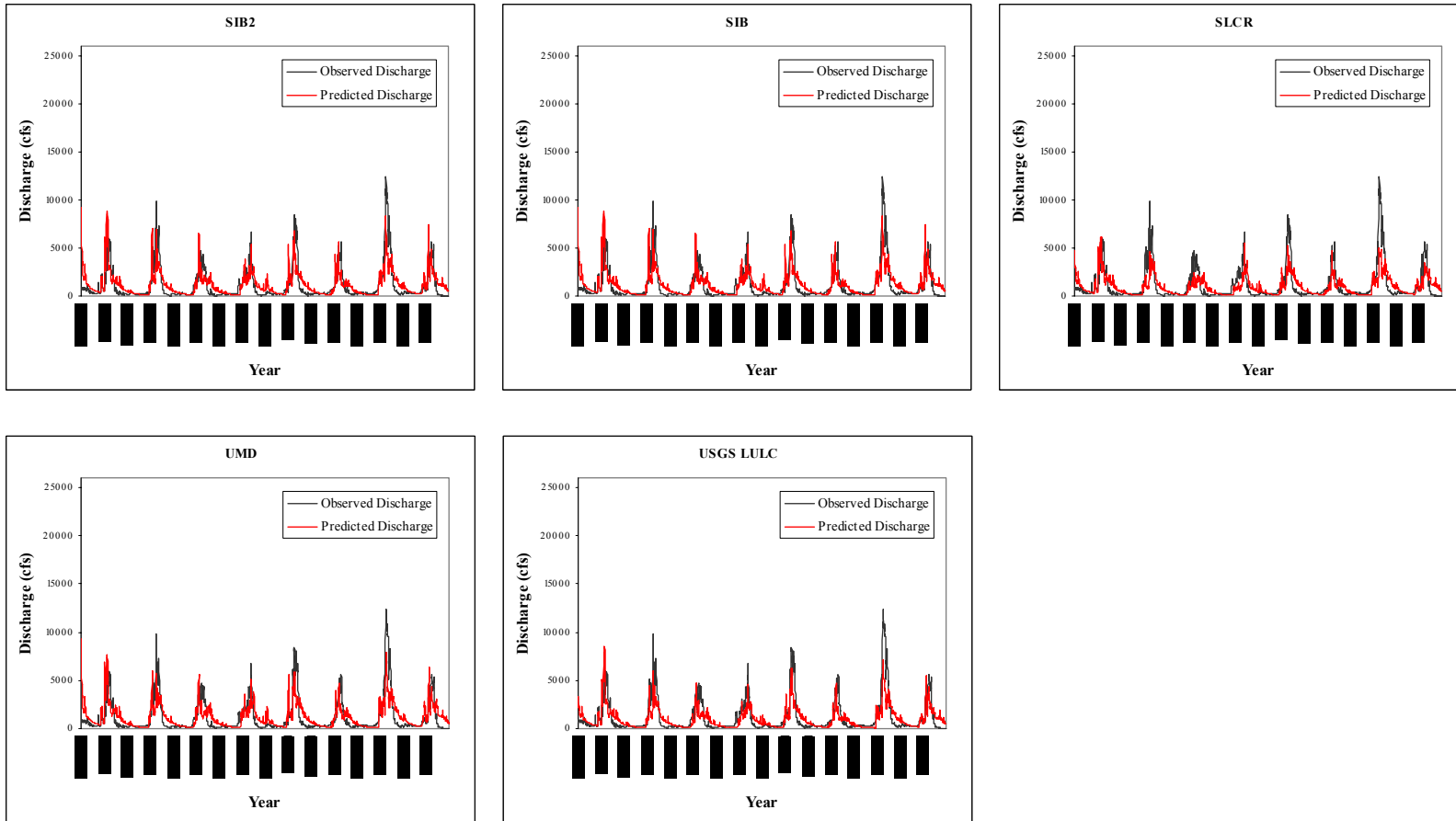
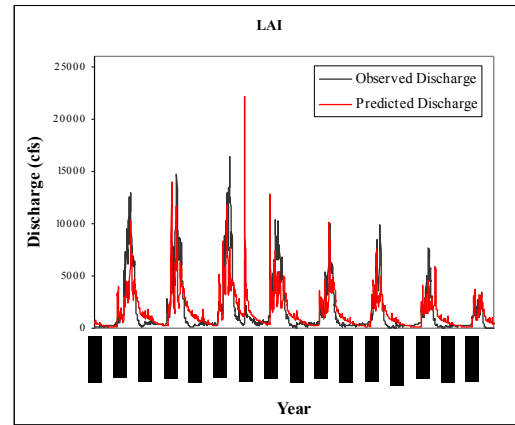
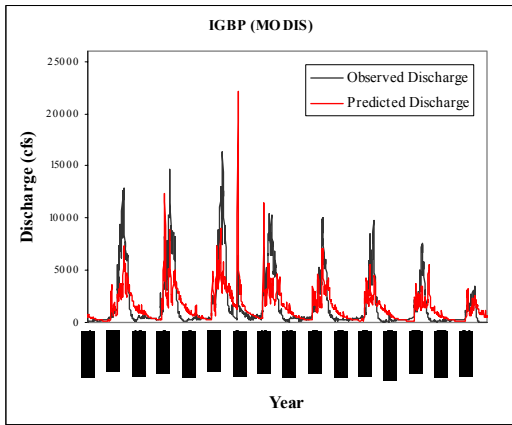
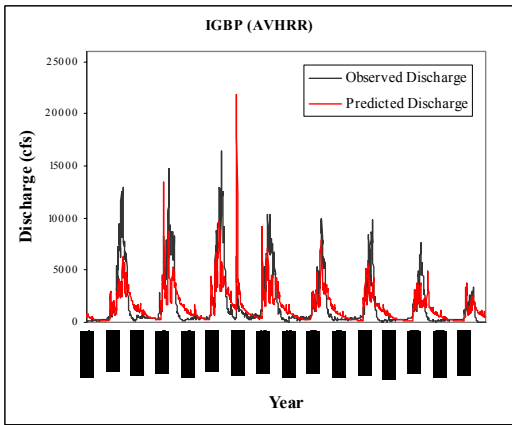
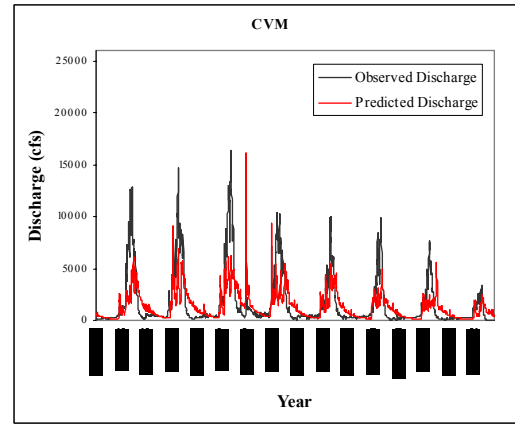
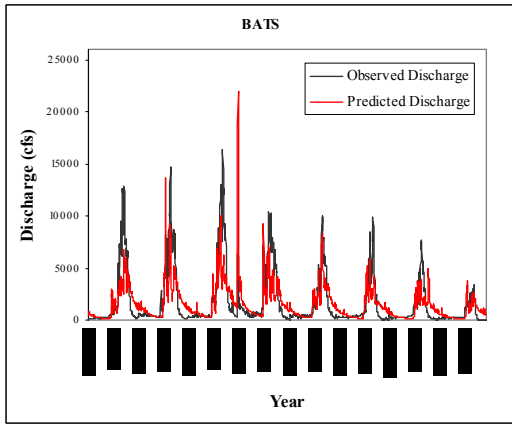
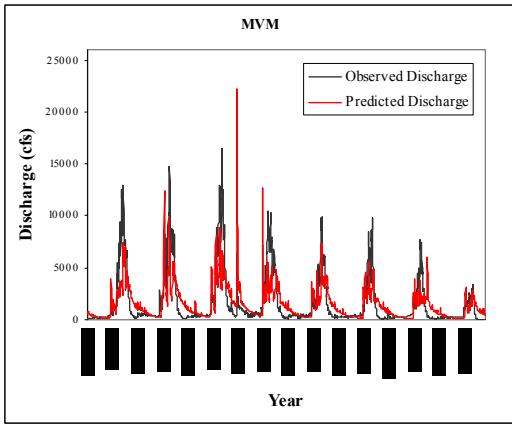
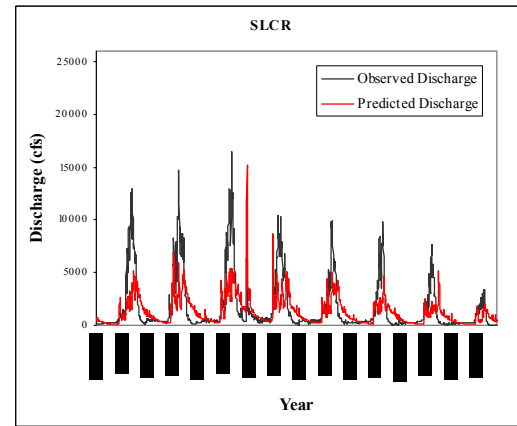
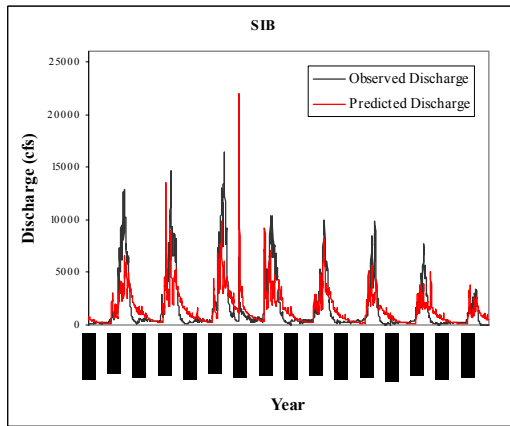
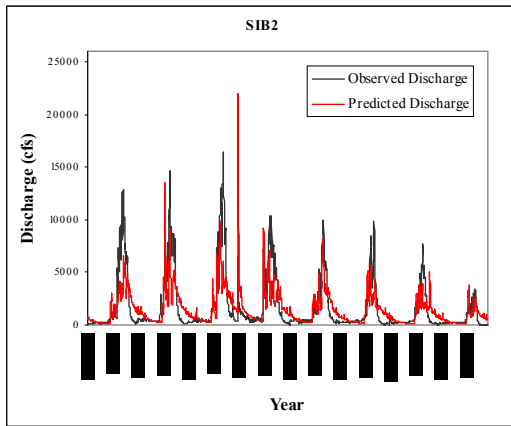
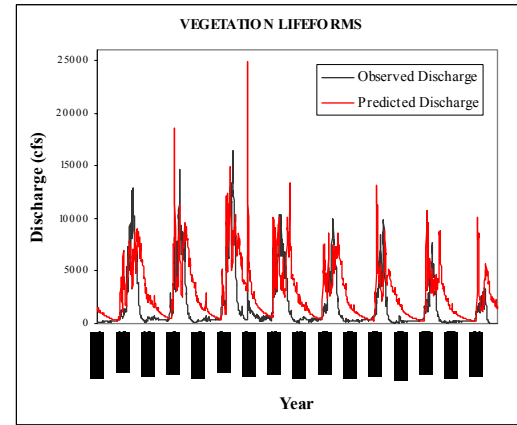
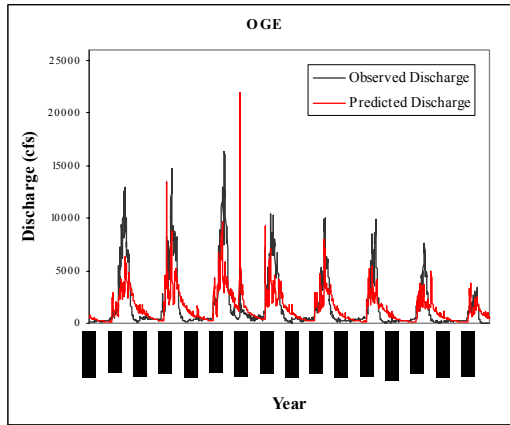
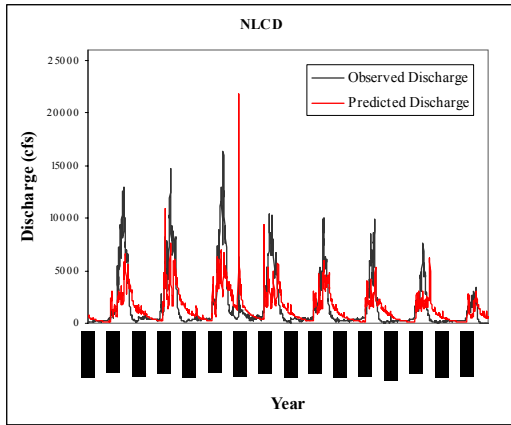


Figure I.1. Predicted discharge versus observed discharge for the Yampa River Basin at Maybell from October 1986 to September 1994.





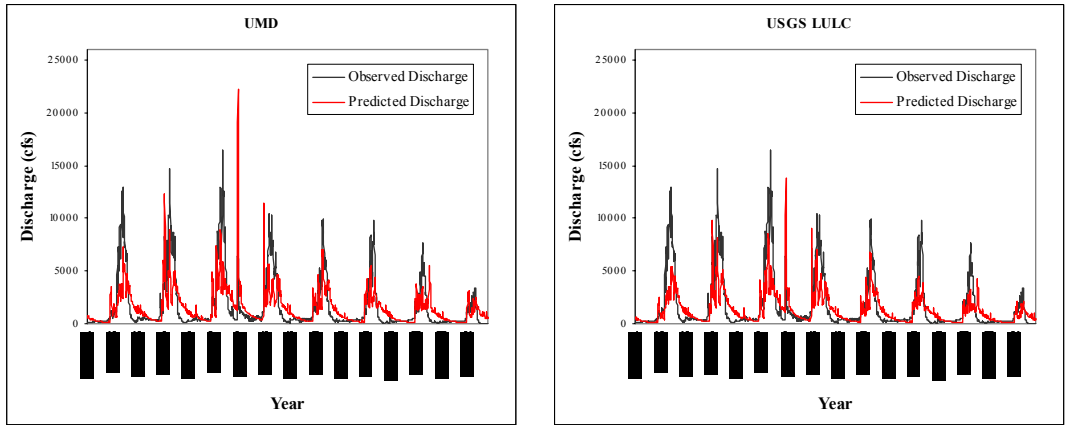


Figure I.2. Predicted discharge versus observed discharge for the Yampa River Basin at Maybell from October 1995 to August 2002.